ADVISORY REPORT 11

AGARD

ADVISORY GROUP FOR AEROSPACE RESEARCH & DEVELOPMENT

64 RUE DE VARENNE PARIS 7e FRANCE

Residual Strength in the Presence of Fatigue Cracks

by P. Kuhn

★

1967

NORTH ATLANTIC TREATY ORGANIZATION

ADVISORY REPORT 11

NORTH ATLANTIC TREATY ORGANIZATION

ADVISORY GROUP FOR AEROSPACE RESEARCH AND DEVELOPMENT

(ORGANISATION DU TRAITE DE L'ATLANTIQUE NORD)

RESIDUAL STRENGTH IN THE PRESENCE OF FATIGUE CRACKS

by

Paul Kuhn

NASA Langley Research Center,
Langley Station, Hampton, Virginia, USA

This Report was presented to the Structures and Materials Panel of AGARD. Sections 1-4 at Turin, Italy, on April 17, 1967 and Sections 5-7 at Ottawa, Canada, on September 25, 1967

SUMMARY

This report is the result of a survey, including visits to aeronautical organizations, undertaken as a project approved by the Structures and Materials Panel of AGARD. The appointed task was "To review the existing state of knowledge with respect to the residual strength of material specimens containing fatigue crack failure initiation of known proportions. Also to ascertain the present knowledge existing with respect to the residual strength of typical structures using various types of materials". Rather than presenting a comprehensive summary, the report concentrates instead on the presentation and critical analysis of methods of calculation, with usefulness to the structural engineer always kept in mind as the prime objective.

RESUME

Le présent Rapport donne les résultats d'une étude entreprise en taut que projet approuvé par la Commission des Structures et des Matériaux de l'AGARD et comportant des visites d'organismes aéronautiques. On avait pour mandat de "passer en revue l'état actuel des connaissances en ce qui concerne la résistance résiduelle d'éprouvettes caractérisées par l'amorçage de rupture due aux fissures en fatigue de proportions connues; de déterminer, en plus, l'état actuel des connaissances concernant la résistance résiduelle de structures types utilisant des matériaux de type différent". Au lieu de donner une synthèse des résultats obtenus on porte toute son attention à la présentation et à l'analyse critique de méthodes de calcul, en se fixant toujours comme but primordial la nécessité de tenir compte des intérêts de l'ingénieur de l'aéronautique.

539.43

CONTENTS

FOREWORD

In February 1966 the Structures and Materials Panel of AGARD approved a project described as follows:

Task A

To review the existing state of knowledge with respect to the residual strength of material specimens containing fatigue crack failure initiation of known proportions. Also to ascertain the present knowledge existing with respect to the residual strength of typical structures using various types of materials.

The National Aeronautics and Space Administration authorized the writer to accept this task. A survey trip covering especially aeronautical organizations was undertaken, as indicated in Appendix A. For the help given to him in the survey the writer is greatly indebted to all the organizations visited and more specifically to a number of individuals, as acknowledged in Appendix A.

At a symposium on "brittle fracture" 14 years ago, the chairman remarked in his opening talk: "So much has been written on this problem that one is now in the position of writing summaries of summaries." Since then, symposia and papers have proliferated at an increasing rate, with the overwhelming majority of papers being written from the viewpoint of the materials man. This writer holds two deep-rooted convictions: that materials are a means to an end, the end being a structure, and that a structural designer cannot work effectively with a large catalogue of undigested and unrelatable data - he needs methods of calculation as simple, but as general, as possible. The report, therefore, represents an effort to break away from the past trend of summaries by eschewing comprehensiveness in the sense of offering large collections of data or observations; it concentrates instead on the presentation and critical analysis of methods of calculation, with usefulness to the structural engineer always kept in mind as the prime objective.

As part of the survey work, the development of methods was furthered for parts with through-the-thickness cracks. However, no satisfactory solution was found for the problem of surface cracks, and the stress analysis of complex structures also poses unsolved problems. The residual strength of structures is therefore discussed only in a cursory manner.

Residual strength is important in several branches of engineering, but the extent to which it is given explicit consideration in design varies greatly. Aerospace engineering is characterized by the necessity of designing closely in order to achieve minimum structural weight. In the case of civil aircraft, there is the added consideration of public safety, which has led to government regulation. Thus, the development of more accurate methods for assessing residual strength has been undertaken primarily in response to the needs of civil aircraft design. However, the basic methods are sufficiently general and sufficiently simple to be applicable not only in aerospace engineering, but in other branches of engineering as well.

LIST OF TABLES

LIST OF FIGURES

NOTATION

Symbols Repeatedly Used

a	length of edge crack, or half-length of central crack, measured before loading begins; in. or mm
a_c	"critical" length of edge crack, or half-length of central crack, measured at instant when crack becomes "fast-running"; in. or mm
C_m	materials constant, $\text{in.}^{-\frac{1}{2}}$ (unless specified as $\text{mm}^{-\frac{1}{2}}$), used in basic CSA method, Equation (12)
C_m'	value of C_m as used in modified CSA method, Equation (14)
E	Young's modulus, ksi
E_N	secant modulus corresponding to stress equal to S_N, ksi
E_1; E_2	secant moduli as defined for Equation (4)
E_u	secant modulus corresponding to σ_u (see Figure 4), ksi
e	elongation on "standard" gage length (usually 2 in.), in./in.
k_w	width-effect coefficient of Dixon, defined by Equations (9a) and (9b)
K_c	notch-toughness constant of Irwin, defined by Equation (26), ksi $\sqrt{\text{(in.)}}$
$\bar{K}_c$	as K_c, but using a instead of a_c
K_T	theoretical (elastic) factor of stress concentration
K_N	factor of stress concentration in elastic range, corrected for size effect by (modified) Neuber formula, Equation (2)
K_p	factor of stress concentration corrected for size effect and for plasticity effect by Equation (4)
K_u	factor of stress concentration valid at instant of failure (maximum load)
P	maximum load carried (kips)
S_G	stress at failure, based on gross area (= wt), ksi or kg/mm^2
S_N	stress at failure, based on net area $t(w - 2a)$, ksi or kg/mm^2
S_{Nc}	stress at failure, based on "critical" net area $t(w - 2a_c)$, ksi or kg/mm^2
t	thickness, in. or mm

w	width, in. or mm
ρ	notch radius, in.
ρ'	Neuber constant as used in Equation (2), in.
σ_{max}	local stress at notch root, ksi
σ_{PL}	stress at proportional limit, ksi
σ_y	yield stress (0.2% off-set), ksi
σ_u	ultimate tensile stress, ksi
ω	flank angle of Vee-notch, radians
ω_e	effective flank angle in Equation (2), radians

Abbreviations

ksi	kips per square inch (1000 lb/in^2)
mil	one mil = 0.001 inch
typ	typical value of material property (e.g., σ_u) as given by handbook of materials manufacturer

RESIDUAL STRENGTH IN THE PRESENCE OF FATIGUE CRACKS

Paul Kuhn

1. RESIDUAL STRENGTH IN DESIGN

The initial design of a structure of any type is generally based on considerations of static strength under high but infrequent loads. The initial design is checked and modified to take care of

(a) smaller but frequently recurring loads (fatigue),

(b) deflections (aero-elastic effects, in the case of aircraft),

(c) vibration, steady or transient.

In the primitive stages of development, the design for static strength incorporates large "safety factors", and specific attention to Items (a) to (c) is not necessary. As the procedures for static strength design are refined, and the "safety factors" are reduced, increasing attention must be given to these ancillary design conditions.

In aircraft design, the ancillary design conditions listed entered into the picture roughly three decades ago. About one decade ago, it became clear that another ancillary design consideration should be used: design for residual strength in the presence of damage incurred in service. In principle, this consideration was not new: it had been standard practice on military airplanes with wire-braced structures to make calculations on the effects of battle damage. However, with the introduction of shell-type structures, the methods of calculation previously used became more or less inapplicable, and the calculations were partially replaced by gun-fire tests. For civil aircraft, rather extensive tests are currently required; the main impetus was furnished by the Comet accidents, but a strong sustaining impetus came from a number of accidents and groundings of civil as well as military aircraft which received little newspaper publicity.

With regard to the definition of "damage incurred in service", two lines of thought developed originally. One line was to consider damage as consisting of fatigue cracks; this line developed into the "safe-life" school of thought, which considers the service life as terminating when fatigue cracks begin to appear. The other line of thought, developed in the "fail-safe" approach, was that a certain amount of fatigue cracking and other service damage is unavoidable and can be tolerated, provided that inspection and repair can eliminate catastrophic failures.

The "safe-life" approach, in its pure form, is open to the objection that it makes no allowance for damage other than fatigue cracking; moreover, the laboratory simulation of service load experience and environment is imperfect. The "fail-safe" approach, in its pure form, is open to the objection that inspection and repair cost money, and perhaps to a prohibitive amount. As a result, there is more or less universal agreement

in civil design that some mixture of the safe-life and the fail-safe approach should be used. There is a wide divergence of opinion on what this mixture should be, and also on the question of how much testing or calculation should be required (i.e., mandatory) to demonstrate that the design goal (or requirements) have been achieved.

In military design, there appears to be a strong tendency to place reliance more less entirely on the safe-life approach. This tendency stems probably in the main from two factors. One is that military designers tend to disbelieve the claims made by some civil designers that a fail-safe approach need not result in weight penalties (and consequently performance penalties). The other factor is that battle damage takes a vastly greater variety of forms than the accidental damage likely to occur in a civil airplane; as a result, the proof of compliance with official design requirements might become a well-nigh prohibitive task.

In safe-life design in its pure form, the question of residual strength does not arise. However, knowledge of residual-strength characteristics may be used qualitatively for ranking materials, for quality control, and for choosing a new material if the material originally chosen proves unsatisfactory in service.

In fail-safe design, in its simplest form, cracks are assumed to exist in various locations, and the structure is designed such that, in the presence of any one of these cracks (or possibly some combinations), it can carry a stipulated percentage of the design load ("fail-safe load"). The length of any one crack to be used in design is arrived at by considerations of efficacy of inspection. In a more advanced form of fail-safe design, the consideration is introduced that a crack should not be able to grow to catastrophic proportions in one inspection period (or two periods). Thus, inspection - which is an integral part of the fail-safe concept - is introduced quantitatively in the design procedure, and together with it the rate of crack propagation.

Figure 1 (from Reference 1) shows schematically the location and size of the cracks that must be introduced in the fail-safe demonstration test of a pressurized fuselage. Such a drawing is prepared in the early design phase of a new type and results from a series of conferences between members of the design staff and of the regulatory agency. If the test shows inadequate strength, redesign and a new test becomes necessary. This may mean doubling the cost of the test (which is of the order of a million dollars on a large fuselage), some loss of prestige, and a slippage in the production schedule which, in turn, might lead to a serious loss of sales. Thus, it is obviously well worth while to expend some effort on calculations before the test in order to obtain reasonable assurance that the test will meet the requirements. Ultimately, calculations may largely replace the test.

Methods for calculating the residual strength of complex structures such as fuselages or wings are at present in the embryonic stage. Obviously, such methods cannot be developed very well until methods for simple specimens have proven adequate scope and accuracy. This stage of development for simple specimens is just being approached, as a study of the report will show. However, the discriminating application of proven methods to simple problems will serve to build up the foundation of experience and confidence necessary for further development.

The choice of the locations and length of the cracks shown in Figure 1 is, in effect, an attempt to predict the results of service. Records of service experience could

obviously be more conclusive than predictions if they are sufficiently extensive and sufficiently applicable. Thus, extensive service experience may be as reliable, or more reliable, than residual strength calculations for chosing between two materials. However, this simple answer may become questionable if one considers the details of the structure. Even in "conventional" structures, details often change in the course of time, and design details frequently are the source of serious trouble. In view of these considerations, it is not surprising that designers of "conventional" structures differ considerably in the relative importance they attach to service experience as compared with explicit attention to residual strength in design.

There is agreement, however, on the principle that explicit attention to residual strength is prudent for unconventional designs, for which no significant service experience exists. This is a common situation, for instance, for missiles and boosters. Another specific example that may be quoted is that residual strength played a decisive role in the choice of material for a set of hydrofoils.

It should be mentioned that the techniques of residual strength testing have been used to assess the effects of stress corrosion, which is often a controlling factor in the choice of material.

Finally, it should be noted that the problem of how to apply knowledge of residual strength in design is reasonably clear-cut, in principle, only if the over-riding objective is the avoidance of catastrophic failure. If the expected failure is non-catastrophic, the problem often becomes rather nebulous, because the designer may have no quantitative data on the economic considerations which now become dominant.

2. MATERIAL PROPERTIES AND STRUCTURAL DESIGN

Material properties are used by structural design engineers as indispensable basic information; the determination of these properties is in the hands of materials engineers. In spite of this close connection, conflicts of interests and attitude arise which merit discussion; the development of knowledge regarding residual strength has been significantly hampered by failure to properly recognize the existence of such conflicts.

The aerospace structural engineer must be able to predict the strength of structural elements with controlling dimensions varying from less than one inch to several hundred inches. The materials engineer would like to confine his work (for sound economic reasons) to specimens with controlling dimensions of the order of 1 in. (width of sheet specimens, for instance). Reluctantly, he may agree to test 3-in. specimens; anything much beyond this, he tends to consider as the responsibility of the structural engineer. But the structural engineer tends to consider simple specimens as being outside of his proper domain of interest. Thus, a large part of the work necessary to substantiate methods falls into a domain which, in practice, often turns out to be a no-mans-land.

If the materials engineer finds that tests on 1-in. specimens and on 3-in. specimens do not result in the same number, due to weakness of the formula used, he often adopts one of two attitudes. He may decide that the specimen configuration must be standardized - a single standard width must be used in all tests. Alternatively, he may devise a procedure which correlates the tests in the range of interest to him - say one to three inches of width. But certainly in the first case, and very likely in the second

case, the method is now a "ranking method", not a method for determining a materials property that can be applied in design calculations to structural elements of any size encountered in practice.

"Ranking methods" are adequate in some branches of structural engineering - where failures are unlikely to be catastrophic, where large safety factors are used, or where cost of material or other considerations are of overwhelming importance. However, it should be noted that a ranking method is inherently more or less vague, and it may be misleading in a case where the service problem is reasonably well defined. This situation may be illustrated by a simple example.

Figure 2 shows the net-section stress at failure for sheet specimens of a given width, plotted against crack length. The alloys represented by the two curves are both aluminum alloys; they have thus the same specific weight, and consequently the net-section stress affords a direct comparison of structural efficiency for a given crack length. It is evident that the two materials have the same structural efficiency (crack strength) if the crack length is l_0 ; if the crack length is greater than l_0 , alloy A is more efficient, if the crack length is less than l_0 , alloy B is more efficient. A ranking method would be based on tests with one fixed crack length; if this length is greater than l_0 , application of the ranking method would obviously be misleading if the specific problem on hand is the occurrence of short cracks (e.g., welding cracks).

Another very prevalent line of conflict of interest arises from the fact that the structural designer deals with the material "before the fact", the materials test engineer deals with it "after the fact". The designer makes strength calculations before the material is manufactured; the materials engineer begins his studies after a test has been made. As a result, the materials engineer can (and very often does) obtain and use information which is not available to the designer (e.g., percent of shear fracture, "critical" length of crack at instant where crack begins to "run fast"). This type of information may be of interest to the research metallurgist who wishes to improve the material, to the physicist who wishes to delve into the more fundamental aspects of fracture, or to the accident investigator. However, as long as the information is distinctly in the "non-predictable" category, it is of no use to the structural designer.

Communications between structural engineers and materials engineers have been poor in the past. They have improved, but there is still much room for further improvement. Structural engineers often make unrealistic demands of materials engineers, and materials engineers often display a lack of understanding of the process of structural design. An effort on both sides to broaden their basis of knowledge would be very helpful in any problem which, like residual strength, falls between the two traditional chairs of materials and structures.

3. THE NSA AND CSA METHODS FOR SIMPLE SHEET SPECIMENS

3.1 General Discussion

Figure 3 shows simple sheet specimens subjected to uniaxial loading and containing either notches or transverse through-cracks. In the present report, attention is focused primarily on cracks. It is possible to discuss cracks without discussing

notches, and this is the predominant practice; here, however, notches will be discussed first for two reasons. One reason is that the method of "crack-strength-analysis" (CSA method) presented in Section 3.3 is derived by considering the crack as the limiting case of a notch, with the notch radius $\rho \to 0$; thus, the basic assumptions and considerations involved in the notch strength analysis (NSA) are pertinent. The second reason is that the literature contains test results on notched specimens representing an investment of millions of dollars; if this investment is to bear full fruit; it is necessary to establish and maintain contact between "notch strength" and "crack strength".

The strength of a notched sheet specimen depends obviously on the material as well as on the geometry of the specimen. By definition, a "materials property" is independent of specimen geometry (at least in first approximation). Attempts to define notch strength by one (or two) "materials constants" are therefore unlikely to be satisfactory. Crack strength, on the other hand, is a somewhat simpler problem because the parameter "notch radius" has disappeared; thus, it is not too surprising that the definition of crack strength by one (or two) materials constants has turned out to be feasible.

For a given material and plan geometry (as defined by Figure 3), the strength of a specimen depends on grain direction, thickness, temperature, loading rate, and possibly environment. Materials constants derived by any method thus must be regarded as functions of these parameters. In parallel with the conventional treatment of tensile strength, it is assumed that failure occurs as soon as a certain load level is reached, that is, "delayed" failures at a fixed load level are considered to be a separate problem area.

In the discussions to be presented, it will be assumed that the length of each specimen is sufficient to make "length effects" negligible. Theoretical treatments of this problem are scanty, but this lack does not appear to be highly important in practice.

3.2 The Notch-Strength-Analysis (NSA) Method

When a notched specimen such as shown in Figure 3(a) or 3(b) is stressed in the elastic range, the maximum stress at the root of the notch is given theoretically by the expression

$$\sigma_{max} = S_N K_T \quad . \tag{1}$$

The factor K_T as derived by the theory of elasticity is valid only for the mathematical "model" material assumed in the theory; this mathematical material is generally isotropic, and always homogeneous and continuous. Many real materials, such as metal alloys, exhibit a granular structure when viewed on a sufficiently small scale; all materials, when viewed on a very small scale, consist of discrete molecules. Thus, the basic assumptions of the conventional theory of elasticity become questionable and finally untenable as the scale of viewing is reduced. These considerations become increasingly important as the key dimension of a notch - the notch radius - decreases, and they are vital in the limiting case of cracks, where the tip radius is immeasurably small.

The break-down of the conventional theory of elasticity is exhibited clearly by a comparison of the experimental factors of stress concentration for a series of geometrically similar specimens: as the size decreases, the stress-concentration factor

decreases. This decrease was first noted and studied for fatigue specimens at long lives, where the peak stress σ_{max} is well below the elastic limit, so that questions of yielding do not enter into the picture.

In order to make the well-developed elastic theory of stress concentration generally applicable to engineering problems, H. Neuber[2] assumed that the material consists of "building blocks" suggested by, but not identifiable with, the grains of metal alloys. Postulating that each block reacts only to the average stress across its face (that is, obliterating the stress gradient within the block), Neuber considered a number of cases and arrived at a general formula for converting the theoretical factor K_T into a "practical" factor, which is herein designated K_N (with the subscript N denoting Neuber). In slightly modified form and symbolism (see Notation), the formula is

$$K_N = 1 + \frac{K_T - 1}{1 + \frac{\pi}{\pi - \omega_e}\sqrt{\left(\frac{\rho'}{\rho}\right)}} \qquad (2)$$

where the quantity ρ' is considered to be a materials constant, herein designated "Neuber constant". The value of ρ' varies from zero for ideally notch-sensitive or "perfectly brittle" material to infinite for completely notch-insensitive material (some cast alloys, for instance). Equation (1) is now replaced by

$$\text{"effective"}\ \sigma_{max} = S_n K_N \ . \qquad (3)$$

Neuber did not use the term "effective" σ_{max}. The term is used here to denote that the stress σ_{max} computed with Equations (2) and (3) is useable for certain engineering applications (as discussed later), but that it may not be "real" in the sense of being measurable, even in concept. Obviously, however, as $K_N \to K_T$, the effective stress becomes identical with the real stress. In all further discussions, the term "effective" will not be used explicitly, but should be understood.

Neuber proposed to use his formula as basis for calculating fatigue notch factors for long endurance. The practicality of this proposal was established by the systematic determination of values of ρ' for low-alloy steels[3] and aluminum alloys[4]. The failure criterion used was

$$\sigma_{max} (\equiv S_N K_N) = \text{fatigue limit} \ .$$

Equation (2) is considered to be valid only as long as σ_{max} is in the elastic range; when σ_{max} is in the plastic range, an additional correction must be applied. For this purpose, the NSA method uses the "secant modulus formula" derived by E. Z. Stowell and generalized by Hardrath and Ohmann[5]

$$K_p = 1 + (K_N - 1)\frac{E_1}{E_2} \ , \qquad (4)$$

where E_1 is the secant modulus of elasticity pertaining to σ_{max} and E_2 is the secant modulus pertaining to the "average stress at a large distance from the notch".

In this paper, attention will be confined to the problem of ultimate strength under monotonically increasing load. If the failure criterion is assumed to be $\sigma_{max} = \sigma_u$, then $E_1 = E_u$, where E_u is the secant modulus defined in Figure 4. Attention will also be confined, in general, to cases in which the net-section stress at failure $S_N < \sigma_y$. Under this condition, the "average stress at a large distance from the notch" is less then σ_y, and consequently $E_2 = E$. For these conditions, Equation (4) takes the form

$$K_u = 1 + (K_N - 1)\frac{E_u}{E}, \qquad (S_N < \sigma_y) \quad . \tag{5}$$

In the literature, there is a very large volume of test data on notch strength which could be utilized to verify the applicability (or reliability) of Equation (5). Unfortunately, the data almost never include the stress-strain curve of the material, which is necessary to establish the ratio E_u/E. In order to make use of these data on notch strength, the ratio E_u/E has been estimated[4, 5] from the elongation e by the expression

$$\frac{E_u}{E} \simeq \frac{1}{1 + \dfrac{0.8eE}{\sigma_u}} \quad . \tag{6}$$

The factor 0.8 in Equation (6) is intended to reduce the measured total elongation e to the uniform elongation, which does not include the effect of necking; it is an average value which may be seriously in error for some materials.

Very few useful data exist from tests in which $S_N > \sigma_y$; they have been fitted best (so far) by using the expression

$$K_u = 1 + (K_N - 1)\frac{E_u}{\sqrt{(EE_N)}} \quad , \tag{7}$$

where E_N is the secant modulus pertaining to S_N. The solution of Equation (7) is effected conveniently by assuming a series of values of $S_N > \sigma_y$ (more precisely, $> \sigma_{PL}$) and computing a curve of K_u versus K_N. Sample curves are shown in Figure 5. A number of materials exhibit the phenomenon of "notch strengthening" evidenced by values of $S_N > \sigma_u$. Under such circumstances, the uni-axial stress-strain curve is no longer applicable, and a drastic modification of the method is necessary. No general method has been developed for this problem, insofar as known to the writer.

Finally, an important note of warning must be given. The NSA method is obviously a highly simplified theory for a physically very complex problem. It should also be noted that, for aluminum alloys, the method can be classed as a "theory" in the sense of the physicist, because no tensile strength tests on notched specimens were used originally to determine any of the constants involved. (The values of ρ' were determined by notch fatigue tests at the fatigue limit.) For a "theory" of this type, no amount of experimental verification constitutes a guaranty that continued testing may not uncover cases of poor agreement. For the tests originally available[4, 6], the agreement was generally at least fair, but later tests[7] showed some cases of very poor agreement for some newer alloys, and also for some older alloys at cryogenic or at elevated temperatures. Consequently, if an important engineering decision hinges on the result of a NSA calculation, a check should be made against published tests or new tests to ensure that the method gives adequate accuracy for the particular material and temperature in question.

3.3 The Crack-Strength-Analysis (CSA) Method

The analysis of sheet specimens containing through-cracks (Fig.3(c) and 3(d)) begins by idealizing the cracks into elliptical (or semi-elliptical) holes. The theoretical factor for such holes is given with adequate accuracy by the expression

$$K_T = 1 + 2k_w \sqrt{\left(\frac{a}{\rho}\right)} \quad . \tag{8}$$

with

$$k_w = \sqrt{\left(\frac{1 - \frac{2a}{w}}{1 + \frac{2a}{w}}\right)} \quad \text{for central cracks} \tag{9a}$$

$$k_w = 1 - \frac{2a}{w} \quad \text{for edge cracks} \quad . \tag{9b}$$

The function k_w is based on photo-elastic tests by Dixon[8], but is used in a somewhat different manner (see discussion of this item in Section 4.4).

Application of Equations (2), (5) and (8), and transition to the limit $\rho \to 0$ to represent cracks gives the formula

$$K_u = 1 + 2k_w \sqrt{\left(\frac{a}{\rho'}\right)} \frac{E_u}{E} \quad , \qquad (S_N < \sigma_y) \quad . \tag{10}$$

This formula is the (basic) NSA formula for cracks. Inspection of this formula shows that the materials constants involved (ρ' and E_u/E) appear in a simple combination, which may be replaced by a single constant. For convenience, the numerical constant 2 is included in this new constant

$$C_m = \frac{2}{\sqrt{(\rho')}} \frac{E_u}{E} \tag{11}$$

and Equation (10) then takes the form

$$K_u = 1 + C_m k_w \sqrt{a} \quad , \qquad (S_N < \sigma_y) \quad . \tag{12}$$

The net section stress at failure is given by the expression

$$S_N = \frac{\sigma_u}{K_u} \tag{13}$$

on the assumption that the failure criterion is $\sigma_{max} = \sigma_u$, that is, assuming that there is no notch strengthening, consonant with the assumptions made in deriving Equation (5). Equations (9), (12) and (13) constitute the "CSA method" for the "elastic range" ($S_N < \sigma_y$). For orientation purposes, Table I lists test values of the new constant C_m for a number of materials.

In the very large amount of test data available for cracked specimens, no direct evidence has been found so far that notch strengthening is exhibited by such specimens. Nevertheless, the formal assumption that it exists has been found useful for some materials because it improves the correlation of test results obtained from specimens of different widths, as will be shown in the following section. Equations (12) and (13) are then written in the form

$$K_u' = 1 + C_m' k_w \sqrt{a} \quad (S_N < \sigma_y) \tag{14}$$

$$S_N = \frac{\sigma_u'}{K_u'} . \tag{15}$$

Equations (12) and (13) constitute the "basic" form of the CSA method, while (14) and (15) constitute the "modified" form.

When the "basic" form is used, the tensile strength σ_u is determined by a conventional standard test. Thus, only the constant C_m needs to be determined from tests on cracked specimens, and a single test is sufficient for this purpose, in principle. When the "modified" form is used, the strength $\sigma_u'(> \sigma_u)$ must be determined together with C_m' ; thus, in principle, at least two tests on cracked specimens are needed, and these tests should be made with specimen widths as different as practicable.

If Equation (12) gives a $K_u < \sigma_u/\sigma_y$, the K_u/K_N curve (Fig. 5) of the material should be used to obtain a corrected value. (The calculated value is located on the straight line, and the corrected value is read directly above it from the curve.) It should be noted that the calculation of K_u from a known value of C_m is quite insensitive to errors; however, the solution of the inverse problem – the determination of C_m from an experimental value of K_u – is so sensitive to errors when $S_N > \sigma_y$ that it should not be attempted. In strength predictions with a given C_m , the limitation $S_N < \sigma_y$ can often be disregarded (see discussion on Figure 10).

In tests intended to determine crack strength as a "materials property", adequate attention must be given to the problem of "lip-buckling" discussed in the following Section 3.4.

3.4 Buckling of the Crack Lips

In a specimen containing a central crack (Fig. 3(d)), application of the longitudinal tension load produces compressive stresses parallel to the crack lips in the region near the lips. These stresses cause buckling of the lips and reduce the strength of the specimen below the strength that can be developed if the buckling is prevented by "anti-buckling guides". A rough approximation formula for the strength reduction in sheet specimens of aluminum alloy is[4]

$$\left(1 - 0.001 \frac{2a}{t}\right) . \tag{16}$$

For steel, the reduction is apparently much larger.

Since the lip-buckling effect is dependent on geometry, it seems advisable to eliminate it in tests intended to evaluate crack strength as a materials property.

Flat plates almost touching the specimen (sometimes greased) are used for this purpose. In the Langley Laboratory of the NASA, the platens used to heat the specimens for elevated temperature tests serve also as anti-buckling guides. Similarly, for standard tests at -109°F, blocks of dry ice serve the double purpose of controlling temperature and preventing buckling. If the guide contains an opening to permit observation of the crack, the width of the opening must be kept to a minimum in order to provide effective support close to the lips.

Although the principle of using anti-buckling guides for materials tests has been described by a number of investigators, many experimenters have not used them. Careful attention should be paid to this fact in the evaluation of published tests, where the strength reduction in some cases is estimated to be 30% and more.

3.5 Remarks on Relation Between NSA and CSA Methods

From the derivations given in Section 3.4, it is clear that the analysis of cracks is simply a limiting case of the analysis of notches; the transformation of the NSA Equation (10) into the CSA Equation (12) is purely formal and involves no new assumptions. Nevertheless, there are important practical differences between the two methods in the determination of the material constants.

In the CSA method, the material constants (C_m , or C'_m and the ratio σ'_u/σ_u) must be determined for each material from crack strength tests. A strength calculation for an untested configuration thus is not a true prediction, but simply an interpolation between, or extrapolation from, tests of the same type.

The NSA method, on the other hand, has been developed for aluminum alloys (and, to a lesser extent, for titanium alloys) to the point when only conventional stress-strain data are needed as basis for making crack strength calculations. These calculations, then, may be classified as "predictions", at least from the engineering view point. The elimination of the relatively cumbersome crack strength tests is a substantial practical gain, particularly considering tests at other than room temperature. Moreover, the possibility of making direct comparisons between crack strength tests and notch strength tests permits extracting new information from a vast body of published tests and correlating hitherto uncorrelated data. On the other side of the ledger is the unfortunate fact that the accuracy of prediction appears to be roughly on a par with the accuracy of weather prediction: good to fair in the majority of cases, and thus definitely useful, but with no guaranty against a significant percentage of very poor predictions.

In view of these considerations, it appears advisable for the time being to use the CSA method when dealing with cracks, either for making strength predictions or for determining material constants. However, it is desirable that crack strength tests be accompanied by coupon tests giving the stress-strain curve to maximum load (or alternatively, that at least σ_u ; σ_y ; and e be measured) in order to furnish data for the further development of notch analysis.

3.6 Sample Applications of NSA Method

3.6.1 Introduction

Sample applications of the NSA method will be given here for three materials. The first one is a very high-strength steel, but with good elongation. The second one is

a titanium alloy, which was heat-treated for research purposes to obtain maximum "brittleness" (no measurable elongation). The third one is a ceramic (stone), a class of material commonly used as classical example of a "completely brittle" material.

For the first two materials, tests included cracked as well as Vee-notch specimens; thus, the direct connection between notch analysis and crack analysis is demonstrated. The test results on the second and the third material, which have zero elongation, demonstrate the gross fallacy of the contention, made to this day by some authors, that "for brittle materials, $K_u \simeq K_T$".

3.6.2 High-Strength Steel

The test data shown on Figure 6 were taken from Reference 9; the material was H-11 (modified) tool steel. The elongation was estimated from information in Reference 10 on the basis of heat-treatment data. From the given data, by Equation (6),

$$E_u/E = 0.130 \quad .$$

The first step is the determination of ρ' from the strength tests on the six specimens with edge cracks. For these specimens $w = 1$ in, and $2a/w = 0.377$ (average). Thus, by Equation (9b),

$$k_w = 0.623$$

and $a = 0.1885$ in. From the test data

$$S_N/\sigma_u = 0.154 , \quad \text{thus} \quad K_u = 6.50 \quad .$$

Now, solving Equation (10) for $\sqrt{\rho'}$

$$\sqrt{\rho'} = 0.0128 \text{ in}^{\frac{1}{2}} \quad .$$

With ρ' known, factors can now be calculated for the Vee-notch specimens. For these specimens, $w = 1$ in , $2a/w = 0.32$. Equation (8) may be used for Vee-notches if $\rho < 0.01w$ and $w < 70^\circ$, which is true for the specimens considered. Thus, taking the specimen with $\rho = 0.004$ in. as example, Equation (8) gives $K_T = 9.60$; next, Equation (2) gives $K_N = 7.91$, and finally, Equation (5) gives $K_u = 1.895$, or $S_N/\sigma_u = 0.528$, as plotted in Figure 6.

The agreement between the test data and the computed curve is good for the four notch radii from 1 to 4 mils. At the smallest radius (0.6 mil), the agreement is very poor, but the machining appears to be "out of control". Considering the difficulty of machining such small radii in such high-strength steel, and the difficulty of measuring such small radii, it is considered plausible to attribute the discrepancy chiefly to experimental difficulties.

3.6.3 Titanium Alloy

Figure 7 shows results of tests on Vee-notch and cracked specimens made from a titanium alloy, heat-treated as mentioned to produce the maximum "brittleness" obtainable[11]. Two series of tests are shown; in one series, the width of the specimens was kept constant, in the other series, the specimen dimensions were chosen such that the stress gradient was constant.

Since the material has zero elongation, $E_u/E = 1$, and thus $K_u = K_N$. Therefore, only two materials constants are needed: σ_u and ρ'. The tensile strength σ_u was not measured directly because the investigator believes that tensile strength tests on brittle materials are unreliable[11]; he recommends that σ_u be obtained by extrapolating series of tests such as shown in Figure 7 to $K_T = 1$. To obtain the calculated curves shown, the equivalent of an extrapolation procedure was used: values of σ_u and ρ' were chosen and modified by trial-and-error until a reasonably good fit was obtained for all the data in both tests series, notched as well as cracked specimens.

The original investigator determined σ_u by plotting S_N versus K_T on a log-log plot and using straight-line extrapolation to $K_T = 1$; in this manner, he obtained $\sigma_u = 200$ ksi. Figures 7(a) and 7(b) show that values of S_N calculated from the expression $S_N = \sigma_u/K_T = 200/K_T$ are in excellent agreement with the test results when the notch radius is not small, say, $\rho > 0.008$ in. However, as ρ decreases below this value, the results obtained by using K_T directly deteriorate rapidly, and of course no useful answer is obtained for cracks ($S_N \simeq 0$). This is a good example for the observation that even an excellent straight-line fit for one set of data on a log-log plot does not constitute proof that the formula corresponding to the straight-line is valid over the entire range of interest, a subject discussed again in Section 4.7.

3.6.4 Ceramic

Figure 8 shows results obtained on a ceramic (stone); the test data were taken from Reference 11. It will be noted that this is the same reference as for the tests on the titanium alloy; thus, the test procedure was the same in that experimenter did not determine the tensile strength. The analysis was therefore made in the same manner as for the titanium alloy, that is, modifying assumed values of σ_u and ρ' until a satisfactory fit was obtained.

The curves of σ_u/K_T in Figure 8 demonstrate strikingly the fallacy of the notion that $K_u \simeq K_T$ for brittle materials. It may be noted that for the unfired material, the net-section stress is almost constant as K_T varies from about 3 to 13.

The values of ρ' shown can be converted into values of C_m by Equation (11) since $E_u/E = 1$ for this material; for the unfired material $C_m = 2$, and for the firedmaterial, $C_m = 5$. A value of $C_m = 2$ is roughly characteristic of a structural aluminum alloy with an elongation of about 6%; in such a material, the difference between K_u and K_T is conventionally attributed to yielding, or "plastic redistribution of stress at the notch root". The tests of the Lava specimens demonstrate that very large differences between K_u and K_T can be caused by size-effect alone, without any benefit from yielding.

3.7 Applications of the CSA Method

3.7.1 Introduction

In order to demonstrate applications of the CSA method, one set of test data has been selected for each of three types of material: an aluminum alloy, a steel, and a titanium alloy. The selection was guided chiefly by the desire to obtain as large a range of specimen widths as possible, because difficulties with "width effect" had been a troublesome problem with most other methods. Secondary considerations affecting

the selection have been adequate variation of the crack length and finally the use of anti-buckling guides, which eliminate a major source of error (or at least difficulty of interpretation) for the long cracks that are possible in wide specimens.

The test data on the aluminum alloy and the steel were obtained from the Boeing Aircraft Company, and grateful acknowledgement is hereby made to this company for granting the use of their data.

In addition to the three main sets of data, two other sets of data are shown. These data are quite old, having been obtained when crack strength work was in the exploratory stage; however, they are still of interest because they represent widely used materials.

3.7.2 Aluminum Alloy

The test results for the aluminum alloy are shown in Figure 9(a) together with curves calculated by Equations (12) and (13), the "basic" CSA method (no notch-strengthening).

The test stress for the specimen with the longest crack in the widest specimen ($2a/w = 0.855$; $w = 48$ in.) falls about 30% below the calculated curve; it is surmised that the anti-buckling guide was not sufficiently stiff to be fully effective in this extreme case. Presumably, the other test points at $2a/w \geq 0.75$ suffer from the same difficulty, although to a much smaller degree. For this reason, and because such extreme crack length ratios are of no practical interest, the following discussions will deal chiefly with those tests in which $2a/w < 0.75$.

At the large widths, a number of tests were made with varying crack lengths; at the smaller widths, only single tests were made. In line with this test pattern, the value of $C_m = 0.64$ was chosen to give the best fit at the largest width. The prediction error is therefore negligible at the large widths and increases as the width decreases; at the smallest width ($w = 3.5$ in), it amounts to 11%, the calculated stress being low (conservative) in all cases.

By choosing a somewhat lower value of C_m ($= 0.56$), the maximum prediction errors can be made to vary from 7% conservative at the smallest width to 7% unconservative at the largest width. The choice of the "best" value of C_m thus involves a conflict. The materials test engineer might consider as "best" that value of C_m which holds the maximum prediction error to the lowest possible value. The designer, on the other hand, would probably consider as "best" that value of C_m which gives maximum confidence that strength predictions for large structures are not unconservative.

Figure 9(b) shows the same test results accompanied by curves calculated by Equations (14) and (15), that is, taking notch strengthening into account. The constants $C'_m = 0.92$; $\sigma'_u = 85.5$ ksi are determined by trial-and-error. It will be seen that the systematic variation of prediction error with specimen width has been eliminated; the remaining errors are clearly random (if the tests at $2a/w \geq 0.75$ are disregarded as before).

3.7.3 Steel

Figure 10 shows the results from a test series on steel sheet, with the width varying from 3 to 48 in. In this case, the test engineer chose to investigate the effect of

varying the crack length at a small width (w = 5 in.). The value of C_n chosen in this case is a compromise, given about equal weight to the narrow and to the wide specimens. The maximum prediction errors are about ±6%, using an average line through the scatter band for the tests at w = 5 in.

The curve for w = 5 in. was calculated using Equation (12), disregarding the limitation $S_N < \sigma_y$. If the limitation were observed, the curve would be modified slightly at the left-hand end (say 2a/w < 0.02); an estimate based on an assumed stress-strain curve indicated a maximum modification of less than 3%, which may be regarded as insignificant considering the test scatter and considering that coupon values of σ_u also showed a range of 3%. This example then, illustrates that the limitation on Equation (12) can often be disregarded for practical purposes.

It may be noted that the prediction errors change from unconservative to conservative as the width changes from 40 to 12 in. Moreover, the two test points for w = 3 in. lie within the scatter band for w = 5 in. As a result, the prediction accuracy for this set of tests cannot be improved by assuming notch strengthening to exist.

3.7.4 Titanium Alloy

For titanium alloy, the most extensive set of tests available covers only a range of widths from w = 2 to w = 20 in. Figure 11(a) shows the test results and curves fitted on the assumption of no notch strengthening ($C_n = 0.75$). The maximum prediction errors are about ±12%. Figure 11(b) shows the results with curves fitted on the assumption that there is notch strengthening ($C_n' = 1.1$; $\sigma_u' = 1.19\sigma_u = 180$ ksi). There are now three points with prediction errors of 7%, and one with an error of 10%; the average prediction error is reduced substantially below that shown in Figure 11(a).

The trend of the experimental points for the two intermediate widths (w = 4 and 8 in.) differs noticeably from the computed curves, and for w = 2 in. , there is a sudden drop of S_N between 2a/w = 0.4 and 2a/w = 0.5 . There appears to be little hope of further improving the prediction accuracy for this material with any reasonably simple method.

3.7.5 Old Test Data

Reference 12 presented test results (and a first analysis) from the first extensive investigation of crack strength conducted at the Langley Laboratory of the NASA. Tests on 2024-T3 and 7075-T6 aluminum alloy were conducted at widths ranging from 2.25 to 35 in. and are presented in Figures 12 and 13.

The thicknesses of the specimens differed somewhat, and coupon data are incomplete. Calculations shown are therefore based on typical values of tensile strength, taken from the handbook of the materials manufacturer.

The importance of lip buckling was recognized as the tests were nearly completed. Check tests were run with anti-buckling guides for the longest cracks on the widest specimen for each material. For plotting on the two figures, test results were corrected to the "guided" condition using Equation (16); the largest correction was 10%.

Figure 12 shows the results for the 2024-T3 aluminum alloy. The calculations based on $C_n = 0.54$ (full-line curve) fit w = 35 in. and are about 5% unconservative for

w = 2.25 in. However, the calculated values for w = 2.25 in. are well above σ_y (50 ksi), and consequently the curve should be replaced by a curve based on the use of the K_u/K_N curve as described in Section 3.3. The corrected curve (dashed line) is about 5% conservative.

Figure 13 shows the results for the 7075-T6 aluminum alloy. The curves calculated with $C_m = 1.30$ (no notch-strengthening, full-line curves) give a good fit at w = 35 in. and for the majority of points at w = 12.; however, at variance from the results for the 2024-T3 sheet, the curve is conservative for w = 2.25 in., being about 10% lower than the low edge of the scatter band. (Note that, for the computed curve, $S_N < \sigma_y$ (73 ksi) throughout). Computations based on the assumption that notch-strengthening exists ($\sigma_u' = 1.33\sigma_u$; $C_m' = 2.0$; dash-dot curves) leave the curves for w = 35 in. and w = 12 essentially unchanged, but raise the curve for w = 2.25 in. so that it lies slightly above the lower edge of the scatter band.

3.7.6 Short Cracks in High-Strength Steels

Since short cracks in high-strength steels are a problem area of high interest, results from a pertinent investigation are presented here. The investigation[13] dealt with H-11 steel at four strength levels and with 4340 steel at one strength level. The test data are shown in Figure 14, together with curves fitted by the CSA (C_m) method. At strength levels of 200 to 260 ksi, the curves remain in good agreement (within 5%) with the tests down to the shortest cracks, except for the shortest crack at $\sigma_u = 240$ ksi, which is under-estimated about 10% by the curve. At the highest strength level (σ_u = 300 ksi), the agreement is still good at 2a = 0.06 in., but at 2a = 0.025 in., the curve grossly underestimates the strength. At the strength level of 270 ksi, there is similar gross disagreement for the shortest cracks, and substantial disagreement (about 20%) at 2a = 0.13 in. Thus, for very short cracks in materials at very high strength levels, the C_m-method can be unduly conservative.

Fair agreement could be achieved at the highest strength levels by using the C_m' method. However, the ratio σ_u'/σ_u required to achieve agreement is about three. While the theory of plasticity suggests that a ratio approaching three is possible, the ratio is far above any value that may be regarded as reasonably well established experimentally. It is suggested, therefore, that the analysis of such cases be deferred until more data become available.

3.8 Slow Crack Growth

It is well known that many materials exhibit the phenomenon of "slow crack growth", that is, under a slowly applied load, the crack begins to grow at a load sometimes significantly lower than the maximum load. The rate of "slow" crack growth is typically of the order of several hundred feet per second, while the final fracture is typically at the rate of several thousand feet per second. In the "Fracture Mechanics" developed by G. Irwin, which will be discussed later, the length of the crack at the instant when final rupture begins is called the "critical crack length". Irwin argues that the critical crack length is physically more significant for fracture than the initial crack length, and advocates therefore the use of this length as basis for the calculation of his "notch toughness" constant K_c.

Irwin's argument is unquestionably sound, from the theoretical point of view. However, it leads to severe practical difficulties. The measurement of the critical crack

length is not easy even at room temperature, and consequently often omitted in exploratory work, even by people who use the formulas of Fracture Mechanics to evaluate and report their tests. At test temperatures other than room temperature, where access to the specimen is severely limited, there appears to be universal agreement (at least until now) that the difficulties of measuring the critical crack length are prohibitive. In other words, even adherents of Fracture Mechanics use the initial crack length often at room temperature, and always (up to now) at other temperatures.

A logical question then is: What is the practical consequence of using the initial rather than the critical crack length? A partial answer to this question can be given as follows. A number of investigators have concluded that the relation

$$\text{(critical crack length)} = \text{(initial crack length)} \times \text{constant}$$

holds either with good accuracy, or at least with acceptable accuracy. Under these circumstances, the difference between using either the critical or the initial length is essentially a constant numerical factor attached to the "notch toughness" number, and such a difference is immaterial. The question remains open, of course, when the relation between initial and critical length is more complex.

From a practical point of view, the following consideration is pertinent. The use of "fail-safe" calculations is based on the concept that cracks may develop in service, but would be found by an inspector. On the basis of the calculations, the inspector must decide whether the structure can stay in service for the time being, or must be taken out of service to be repaired. Any crack length measured by an inspector can hardly be anything other than an "initial" length. To be consistent with this concept, the calculations must also begin with the initial length as base datum.

In principle, of course, a calculation might use the initial length as base datum and still use a fracture strength criterion based on critical crack length. Such a procedure, however, would require that a reliable procedure exists for *predicting* the critical length corresponding to a known initial length. At present, no such procedure exists (Appendix B).

The foregoing consideration as well as the difficulties in measuring the critical crack length were responsible for the decision to base the CSA (and NSA) method on the use of the initial crack length. It is suggested, however, that information on slow crack growth be collected and analyzed, in order to be available to the designer as auxiliary information, to be used in situations where it may be useful (situations where "leak-before-burst" can give useful warning).

Finally, another consideration should be mentioned that appears to have escaped notice. Two nominally identical specimens (with the same initial crack length) are subjected to test. Specimen B fails at a lower load than specimen A, but exhibits a much larger amount of slow cracking and consequently achieves a higher notch-toughness number ($S\sqrt{a}$). The metallurgist would consider B as being "better material", but the structural engineer would probably disagree.

The calculation of the stress for initial cracking can be handled by Equations (12) and (13), with the subscript i used to denote stresses or constants pertinent to initial cracking ($K_i = 1 + C_{mi}k_w\sqrt{a}$ and $S_{Ni} = S_i/K_i$). Two examples based on test data from

Reference 14 are given in Figure 15. The figure also shows the failing stresses; it is evident that the stress for initial cracking approaches the failing stress more and more as the crack length decreases. The calculations indicate that the initial cracking stress would be equal to the failing stress at initial crack lengths of about 10 mm for both materials, but there are no data for such short cracks. It should be noted that very few calculations of this nature have been made so far.

3.9 The Simulation of Cracks, Especially by Saw Cuts

For practical reasons, it is often desired to simulate fatigue cracks either by sharp notches or by saw cuts. The question arises: When is the simulation close enough to be acceptable?

For the simulation by means of sharp notches, an example was given in Figure 6 for a very high-strength steel (σ_u = 311 ksi). The figure shows that with a notch radius of 0.001 in., the smallest one that was successfully machined, the strength was between two and three times as high as for cracks. Direct simulation of a crack by a machined Vee-notch is therefore not feasible for this material.

Figure 6 also shows that the curve which gives the relation between crack strength and notch can be computed. To obtain the data for this computation, it is necessary to make a standard tension test (to obtain σ_u and E_u/E, by Equation (6)), and (at least) one test on either a crack specimen or a Vee-notch specimen to obtain a first estimate of ρ'.

Under other conditions, saw cuts have been widely used to simulate cracks. As a rule, a rather wide cut is first made with a saw or a milling cutter, and this cut is then extended by cutting with a jeweller's saw, which is about 0.01 in. thick.

The shape of the end of a saw cut, particularly in thin sheet, is rather indefinite. The calculation of the stress concentration factor can therefore only produce two limits. The upper limit is obtained on the assumption that the ends of the saw cut are ideally square; the cut then acts like a crack, and K_u is calculated by Equation (12) (or (14), if necessary). The lower limit is obtained by assuming that the end of the saw cut is semi-circular, with a radius ρ equal to one-half the thickness of the saw. The factor K_u is then obtained by Equations (8), (2) and (5) (and a K_u/K_N curve like Figure 5 is used if necessary). This part of the procedure is the same as for Vee-notches.

Figure 16 shows applications to two aluminum alloys; the test data for the crack specimens are taken from Figures 12 and 13, and data points for saw-cut specimens have been added. The values of C_m given in Figure 12 and C_m' given in Figure 13 were used as base data. Values of ρ' were taken from the "master curves" published in References 4 and 6.

(A problem arises when notch strengthening is prominent, as for the 7075-T6 alloy. The fact that use is made of a $\sigma_u'(> \sigma_u)$ indicates that the uni-axial stress-strain curve is not applicable, and consequently Equation (6) cannot be used to compute E_u/E. For this case, it was assumed that Equation (11) is also valid for C_m', and the ratio E_u/E was computed from C_m' and ρ' by this formula.)

Figure 16 shows, for each material, one curve computed for cracks, and one curve computed for slots with semi-circular ends. The results for cracked specimens are expected to cluster around the first curve, while the results for saw-cut specimens are expected to lie between the two curves.

For the 2024-T3 alloy, both calculated curves in Figure 14 (lower part) are somewhat low. If both curves are raised 6%, the lower curve fits the crack data, and the upper curve fits the saw-cut data quite well. The difference in strength between the two types of specimens is thus about 6%.

For the 7075-T6 alloy (Figure 16, upper part), the calculated curve for cracks is in reasonable agreement with the test data. The validity of the method of calculation used for the upper curve (slots) is questionable for the right-hand half, because S_N is well above σ_y and finally even above σ_u. The left-hand half, however, should be reasonably good, and as expected, the test points for saw cuts fall between the two curves. The difference in strength between cracked and saw-cut specimens (as computed) is about 20%. For this material, then, a saw cut cannot be regarded as a good simulation of a crack.

Figure 17 shows test data and computations for a high-strength steel[14]. The material is quite crack-sensitive ($C_s \simeq 5$), and the difference between cracks and saw cuts is so large ($\simeq$ 70%) that the term "simulation" is obviously inappropriate.

The data shown suggest that the difference between "saw-cut strength" and crack strength can be estimated fairly well if the necessary materials data are available. Together with other scattered data, they suggest that the direct simulation of cracks by saw cuts (with maximum errors less than, say, 10%) is probably possible in materials which give no concern about service behavior (2024-T3). However, when the service behavior is considered as marginal, the useability of saw cuts becomes very marginal, also. The use of correction factors might be considered, but the indeterminate nature of the saw cut must be borne in mind. Finally, it should be noted that the ratio of saw-cut strength to crack strength is size-dependent. For instance, for the PH15-7Mo steel, and a fixed value of $2a/w = 0.2$, the ratio is calculated as 1.46 for $w = 1$ in., 1.68 for $w = 4$ in., and 2.00 for $w = 50$ in.

Significantly different results were reported in Reference 15. Tests were made on 2024-T3 and 7075-T6, with two crack lengths. In each test group, there were four specimens with fatigue cracks and two with saw cuts. The scatter range for the specimens with cracks was quite small, and the strengths of the specimens with saw cuts fell within this range. It would appear, therefore, that all saw cuts achieved essentially square corners, a success apparently not achieved previously in any other laboratory. Since the problem of simulating cracks is sometimes of very great importance in fail-safe demonstration tests, it would seem worth-while to study the technique of sawing used for the tests in Reference 14.

3.10 Notch Strength and Notch-Strength Ratios

The notch strength S_N as measured on a standard specimen has been used widely for various purposes. The test is strictly a "ranking" test, and as pointed out already in Section 2, a ranking test can be misleading. However, it is very simple, and if used with proper caution, it can be useful. If a suitable specimen configuration is

chosen, it should be adequate for such purposes as studying the effects of varying heat treatment, chemical composition, etc., on a given material. Some doubts may arise when the test is used to compare different materials. However, as a result of economic necessity, it has been widely used as a screening test; in the initial work on materials for a supersonic transport, for instance, tests of this type were vital in reducing an initial list of about 70 candidate materials to less than ten.

For a general comparison of materials, the notch strength itself is generally considered to be less useful than a notch strength ratio. Two such ratios are in use: the ratio of notch strength to tensile strength, and the ratio of notch strength to yield strength. The former is preferred by almost all aircraft designers, because the strength design of aircraft is universally based on ultimate strength. The latter is preferred by most designers of stationary structures, because they generally consider yielding rather than ultimate failure as the basic design criterion. Missile designers may follow either practice. (The abbreviated term "notch strength ratio" usually refers to the first ratio mentioned.)

When materials are being compared for a specific application, two situations may exist. If the structure is being designed to operate essentially at one temperature, the notch strength ratio may still be used. However, a subsonic aircraft, for instance, is designed initially for a "normal" temperature, and the strength is then checked for a low temperature. Now, as the temperature decreases, the notch strength ratio may decrease, but the notch strength itself may increase, because the tensile strength increases in some materials. Obviously, the relevant quantity is the notch strength itself, not the notch strength ratio.

In general, when design has reached the stage where such comparisons are being made, conclusive answers can be obtained only by making specific calculations in accordance with the design requirements. Since a ranking method cannot be used for such calculations, the choice between notch strength and notch strength ratio becomes an academic question at this stage.

4. OTHER METHODS FOR SIMPLE SHEET SPECIMENS

4.1 Comparison Plots

A widely used method for comparing materials is to make plots of S_0/σ_u versus $2a/w$, as shown in Figure 18. The sloping straight line represents material completely insensitive to cracks ($C_m = 0$, $S_N = \sigma_y = \sigma_u$).

This method of comparison is simple, but suffers from the defect that any one plot is valid only for one fixed width of specimen. Although this limitation has often been pointed out, it is still disregarded by some authors. For instance, in a paper presented less than three years ago before the ASM Western Metal Congress, a plot of this type for aluminum alloys showed curves for specimen widths of 1.5, 12 and 20 in. Such a plot is devoid of meaning if interpreted as a comparison of materials, a fact which should be evident if one notes the effect of width (at a fixed value of $2a/w$) on such plots as Figure 9.

To a much lesser extent, plots of S_N/σ_u versus $2a/w$ have been used in a similar way. Some of the early investigators elaborated on such plots by drawing straight

lines through the test points and deriving constants from these straight lines. In the light of current knowledge, such procedures lack generality and are no longer of interest.

4.2 Crichlow's Method

The method of Crichlow, which has been used by a number of aircraft companies, and is still used by some, was presented in Reference 16. It utilized the concept of "effective width", a concept originally developed and widely used for buckled skin panels. Crichlow postulated that the effective width of a cracked sheet follows an assumed empirical law and determined the constants empirically.

In a recent paper, Crichlow[17] no longer used this method, but uses the NSA Equation (10); a discussion of his original effective-width formula therefore appears unnecessary.

4.3 The Method of Christensen and Denke

In Reference 18, Christensen and Denke presented three formulas. All three are based on the concept of effective width, but efforts had been made to improve on the formula of Crichlow. The authors point out that their third formula (which appears in the last Appendix of their report) has a sounder physical basis than their first two formulas, and later reports by these authors use this third formula. Therefore, only this (third) formula will be discussed here.

The distribution of stress over the net section in an infinitely wide sheet is postulated to be as follows: in the region of the effective width w_e, the stress is equal to the tensile ultimate σ_u; beyond this region, the stress follows the law of distribution derived theoretically by Westergaard. Integration leads to a formula for the failing stress in an infinitely wide sheet. In order to account for finite width, a factor (1 - 2a/w) is introduced, leading to the final formula

$$\frac{S_G}{\sigma_u} = \frac{1 - 2a/w}{\sqrt{\left(1 + 3\,\frac{2a}{R_p'}\right)}} \,, \tag{17}$$

where $R_p' = 3w_e$ is considered to be the materials constant, to be determined by tests.

Equation (17) is in terms of gross-area stress. If the concept of a stress concentration factor based on net-area stress is used, it follows immediately that

$$K_u = \sqrt{\left(1 + 3\,\frac{2a}{R_p'}\right)} \,. \tag{18}$$

According to this formula, the factor K_u is independent of specimen width; it is a function of the crack length (2a) and of the constant R_p'.

As example, the formula has been applied to the 2219-T87 material for which test data were shown in Figure 9. Figure 19 shows, in the lower part, a plot of K_u as calculated by the above formula, with R_p' taken as 10 in. (dashed-line curve). Also

shown as full-line curves are values of K_u calculated by the CSA method (which, in turn lead to the S_N-values shown in Figure 9(a)). It is evident that the single curve given by the Christensen-Denke Equation (18) is only a very rough "average" representation of the family of curves given the CSA method. More specifically, it is evident that, once a value of R_D' has been chosen, the Christensen-Denke formula can fit correctly only one single crack length at any given width. This point is brought out by the two plots in the upper part of Figure 19, which show the ratios of calculated to experimental strength for $w = 48$ and $w = 24$ in. When the calculations are made by the CSA method, the ratio is within ±5% of unity until the cracks become very long ($2a/w = 0.75$). When the calculations are made by the Christensen-Denke formula, the ratio is unity only for one crack length at each width and departs rapidly from unity as the crack length departs from the point of fit in either direction.

4.4 Welbourne's Method

The method of Welbourne[19] is the basis of the Royal Aeronautical Society Data Sheets for crack strength. In basic purpose, it parallels the NSA method (which was developed at about the same time): it provides a procedure for predicting the crack strength from a knowledge of readily available materials properties (in principle, the stress-strain curve) plus one novel "materials property", which Welbourne calls "effective radius of the fatigue crack (tip)".

A brief comparison of fundamental assumptions and formulas of Welbourne's method and of the NSA method will be given below. A number of numerical comparisons have also been made for aluminum alloys, including cases in the elastic range ($S_N < \sigma_y$) as well as a few cases in the "plastic" range ($S_N > \sigma_y$). No significant differences in the prediction accuracy of the two methods have been found for materials on which information existed at the time when the methods were under development.

Tests performed since that time on newer aluminum alloys have disclosed some cases of very bad predictions, indicating that the "class relationships" assumed by either Welbourne or Kuhn are not as general as hoped for. Figure 20 shows test data and predictions for 2020-T6, representing the worst case of mis-prediction so far encountered with the NSA method. It is interesting to note that the Welbourne prediction agrees much better with the NSA prediction than with the test data. Figure 21 represents another case of poor prediction, with the predictions conservative (as against unconservative for the 2020 alloy) for the Welbourne method as well as for the NSA method.

With regard to the more detailed comparison between the Welbourne method and the NSA method, the following remarks may be made.

Welbourne assumes that the failure criterion is the attainment of a limiting strain, while the NSA method assumes the attainment of a limiting stress. However, as long as notch strengthening is assumed to be absent (or is neglected), the two failure criteria are interchangeable, because both methods assume that the strain and the stress at failure are taken from the stress-strain curve of the material at the top point.

Welbourne assumes that the elastic concentration factor (K_T) can be used as strain concentration factor up to failure, while the NSA method uses the generalized Stowell secant-modulus Equation (4). This is a sharp difference, in principle. The secant-modulus formula has been partially verified in direct tests[20], while other tests (for instance, Reference 21) have shown that the strain concentration factor for a circular

hole increases by a factor of 2 to 3. Since the final results obtained by the Welbourne method are generally good, it can only be surmised that other assumptions involved in the method counteract errors that would be expected from the assumption of a constant factor of strain concentration.

In the elastic range ($S_N < \sigma_y$, or more precisely, $S_N < \sigma_{PL}$), Welbourne's formulas lead to a factor

$$\text{(Welbourne)} \quad K_u = \frac{\left(1 + 2\sqrt{\left(\frac{a}{r}\right)}\right) k_w}{1 + \frac{eE}{\sigma_u}} \quad (S_N < \sigma_y) \quad , \tag{19}$$

while the corresponding NSA formula is

$$\text{(NSA)} \quad K_u = 1 + \frac{2k_w\sqrt{\left(\frac{a}{\rho'}\right)}}{1 + \frac{0.8eE}{\sigma_u}} \quad (S_N < \sigma_y) \quad . \tag{20}$$

Obviously, the "effective radius" (r) of Welbourne can be identified with the Neuber constant ρ' of the NSA formula.

The elongation e is multiplied by a factor 0.8 in the NSA formula, which is intended as a first approximation to convert from total strain at fracture to the uniform strain which exists before necking begins. Welbourne does not use such a factor, but obtains automatically a (qualitatively) similar effect on K_u in that his values of r are larger than the values of ρ' . At the present state of knowledge, these differences can only be regarded as insignificant.

The Dixon function k_w is used by Welbourne in the manner suggested by Dixon (outside of the bracket). In the NSA (and CSA) method, the function k_w is placed inside of the bracket. Direct checks against the Dixon photoelastic results show about the same accuracy of fit. The NSA-CSA formulation was chosen to avoid the possibility of obtaining stress concentration factors less than unity, which are physically inadmissible but can be obtained for some proportions if the Dixon-Welbourne formulation is used. However, the difficulty appears only in rather rare cases.

Welbourne uses a single value of the effective tip radius r , while in the NSA method, ρ' is considered to be a function of σ_u , and can vary by a factor of two between high strength and low strength alloys. This difference might be expected to have significant consequences, but none have been disclosed by numerical checks. The explanation is probably that the low-strength alloys have also very high elongation, as a rule; for such materials, the value of S_N at failure is between σ_y and σ_u for a wide range of specimen configurations, and consequently is not sensitive to changes in parameters.

In summary, then, significant differences in predictions by Welbourne's method and by the NSA method appear to be confined to cases where both methods give very poor predictions.

4.5 The Method of McEvily-Illg-Hardrath

The method of McEvily, Illg, and Hardrath[22] is the predecessor of the NSA method. As applied to notches only, the two methods are identical. In the application to cracks, the method of McEvily, Illg, and Hardrath does not make the limit transition ($\rho \to 0$) as proposed by Neuber and adopted in the NSA method; instead, it assumes that a crack behaves as though it had a finite radius at the tip, which is called "effective radius" ρ_e. For the two aluminum alloys investigated in Reference 22, it was found that the assumption $\rho_e = \rho'$ gave adequate accuracy. Thus, by Equation (8),

$$K_T = 1 + 2k_w\sqrt{\left(\frac{a}{\rho_e}\right)} ,$$

then, by Equation (2), with $\rho' = \rho_e$

$$K_N = 1 + k_w\sqrt{\left(\frac{a}{\rho_e}\right)} ,$$

and finally, by Equation (5)

$$K_u = 1 + k_w\sqrt{\left(\frac{a}{\rho_e}\right)\frac{E_u}{E}} .$$

This formula differs from (10) by having in it ρ_e instead of ρ', and by the factor 2 missing in front of the square root. Thus, if the constants are derived from the same test and other details are kept identical,

$$4\rho_e = \rho'$$

that is, the constants appearing in the two methods differ by a factor of four, but the results are identical as long as only cracks are analyzed.

The two methods give different results when factors K_u for a notch as well as for a crack are predicted for one material using a single material constant: the relation between the notch factor and the crack factor is not the same in the two methods. One consequence of this fact is that, in the NSA method, the stress concentration factor for a configuration of notch plus crack is always larger than for the notch alone; in the McEvily method, it is possible for the configuration notch plus crack to have a smaller stress concentration factor than the notch alone. This feature can be used to describe mathematically the phenomenon of non-propagating fatigue cracks, and this is the reason why the concept of the "effective radius" was introduced into the McEvily method.

It may be remarked that the concept of an "effective radius" has been used by some investigators to describe the size effect (stress-gradient effect), while others have used it to describe the plasticity effect. Since the McEvily method uses the constant ρ' to describe size effect, and the term E_u/E to describe plasticity effect, it is difficult to find any physical justification for an additional "effective radius" effect. Internal stresses might be considered, but it is difficult to believe that these would always be sufficiently similar to justify a single constant. The phrasing of Reference 22 might suggest that the "effective radius" is intended to be an estimate of the actual radius, arrived at by indirect means because direct measurement is

impossible. However, this explanation is not tenable because microscopic examinations clearly show that the physical radius at the tip of a crack is at least two to three orders of magnitude smaller than the value of ρ_e given by McEvily.

Basically, the McEvily method as well as the NSA method are, of course, empirical; consequently, the relative confidence that can be placed in them is roughly proportional to the amount of test evidence supporting each method. The NSA method was published for the first time several years later than the McEvily method and has been up-dated several times since then. Thus, it has been in a position to utilize a large amount of new test data on crack strength and on static strength of notch specimens; it has also utilized a large body of data on notch fatigue.

In view of the much larger scope of experimental backing, it would seem justified to consider the NSA method as having supplanted the McEvily-Illg-Hardrath method except for the special purpose of dealing with non-propagating fatigue cracks. This conclusion is supported by the observation that application of the McEvily method to other materials would require a separate decision for each material whether the relation $\rho_e = \rho'$ is applicable or not.

4.6 The Griffith-Irwin Method

4.6.1 General Discussion

As is well known, the pioneering work on the effect of cracks was done by Griffith[23, 24] on glass; he derived the expression

$$S\sqrt{a} = \text{constant} \quad , \tag{21}$$

which will be referred to hereafter as the "Griffith expression". This expression was later applied to other materials by Irwin and by Orowan, and Irwin and others have done a large amount of work to develop the formula into a basis for a body of knowledge known as Fracture Mechanics. A large body of literature exists dealing with principles and applications of Fracture Mechanics; a convenient guide in this field are the reports of the Fracture Committee of the ASTM[25].

For convenience of discussion, the Griffith expression will be derived here by the CSA method, that is, using Equations (12) and (13) as basis. For the infinitely wide sheet, $k_w = 1$, and $S_N = S_G = S$; thus

$$K_u = 1 + C_m\sqrt{a} \tag{22}$$

$$S = \frac{\sigma_u}{K_u} = \frac{\sigma_u}{1 + C_m\sqrt{a}} \quad . \tag{23}$$

Griffith noted that for cracks, the stress concentration factor was certain to be very much larger than unity; he therefore proposed to write

$$K_u \simeq \sqrt{a} \times \text{constant} \tag{24}$$

that is, to drop the quantity "one" in front of the expression for K_u. When this simplification is made, Equation (23) becomes

$$S = \frac{\sigma_u}{C_m\sqrt{a}} \quad . \tag{25}$$

At this stage, Griffith proposed to transfer the quantity $\sqrt{a}$ to the left-hand side of the equation, which would leave only constants on the right-hand side; the final result thus was the Griffith expression (21).

The expression (22) for K_u is based on the mathematically exact formula for an elliptical hole. The use of the simplified expression (24) therefore entails an error which is negligible for large values of K_u, but grows as K_u becomes smaller; the error is evidently about 1% if $K_u = 100$ and about 10% if $K_u = 10$. Of prime interest is the error introduced in the prediction of a failing stress S from the expression $S = (\text{constant})/\sqrt{a}$ after the constant has been determined by test; this error approaches infinity as $a \to 0$ and thus the (true) $K_u \to 1$.

It should be noted that the errors referred to are introduced solely by the use of the mathematically simplified expression for K_u. By virtue of being based on this simplified expression, the Griffith expression (21) must be regarded as an asymptotic expression which has good accuracy only when $K_u \gg 1$, that is to say, the failing stress is a very small fraction of the tensile strength of the material. *The presence or absence of ductility in the material has no bearing on the validity of this statement.*

In practical structural engineering, the designer aims at achieving reasonably high stress levels, certainly larger than, say 10% of the tensile strength. Under these circumstances, the quantity $S\sqrt{a}$ must be expected to be a variable rather than a constant, and this variability will be examined in the following Section 4.6.2. For reasons of greater practical usefulness, the examination will be made for sheet specimens of finite width rather than for specimens of infinite width.

For specimens of finite width with central cracks, Irwin utilized derivations by Westergaard and derived the formula

$$K_c = S_0\sqrt{\left(w \tan\frac{\pi a_c}{w}\right)} \quad . \tag{26}$$

which transforms into the Griffith expression as a/w becomes small (provided the difference between a_c and a is either negligible or disregarded). The quantity K_c is usually called "notch toughness" or "fracture toughness" (basic form, without corrections which will be discussed later).

The discussion in Sections 4.6.2 to 4.6.5 will be confined to specimens with central cracks; the differences between edge cracks and central cracks are not significant for the purposes of this discussion.

4.6.2 Variability of K_c

A study of the variability of K_c on the basis of test data alone is next to impossible, because test data of adequate scope do not exist. It was necessary, therefore, to generate "synthetic" test data by calculation, using the CSA method. This procedure involves a problem which requires some discussion.

Equation (26) contains the critical crack length a_c, while the CSA method employs the initial crack length a. However, as mentioned in Section 3.8, in actual practice K_c is often computed using a rather than a_c. In Fracture Mechanics, the resulting value is sometimes (but not always) designated "nominal K_c". In the present report, to avoid confusion, the symbol $\bar{K}_c$ will be used to designate any value of K_c based on the initial crack length a.

Any conclusions regarding the variation of $\bar{K}_c$ due to change of specimen configuration (width and crack length) evidently apply directly when there is no slow cracking. This condition holds for some materials even under rather slowly applied loads; it holds evidently under fast rates of loadings, which have been used extensively during the past three years on airframe materials to simulate loading rates experienced in service.

When slow cracking does occur, various investigators have found for a number of materials that the relation

$$a_c/a = \text{constant} \tag{27}$$

holds either quite well, or at least with a scatter such that the resulting scatter in K_c is difficult to distinguish from scatter in material strength (note that the crack length appears in Equation (26) under the square root sign). Under these conditions, $\bar{K}_c$ differs from K_c for a given material only by a constant multiplier, which does not affect any conclusions with regard to variability on a percentage basis. For materials in which slow cracking is very extensive and also does not follow the relation a_c/a = constant, the variability of K_c would have to be investigated directly.

The investigation then was made as follows. A series of values of C_m was chosen; by Equations (12) and (13), values of S_N/σ_u were calculated for a series of configurations in the range of practical interest, converted into S_Q/σ_u and finally converted into values of $\bar{K}_c/\sigma_u$ by Equation (26).

Figure 22 shows the results for the two most crack-sensitive materials considered. Curves are shown only for the minimum and the maximum crack length; near-vertical portions of the curves (for $2a/w \to 1$) are omitted. For $C_m = 104$, the two curves practically coincide and are practically horizontal, again confirming that the Griffith expression (21) is indeed very accurate for glass. For the brittle titanium ($C_m = 36$), the two curves are distinctly separated; however, a straight horizontal line would approximate all values lying between the two curves within ±5%, which might be considered as a tolerable error.

In Figure 23, for $C_m = 2$, a family of curves appears, covering a roughly "triangular" area. At the width of $w = 50$ in., the maximum value of $\bar{K}_c$ (obtained with $2a = 16$ in.) is 2.6 times the minimum value (obtained with $2a = 0.1$ in.). Finally, in Figure 24, for $C_m = 0.5$, it may be seen that $\bar{K}_c$ varies by a factor of about 5 as the crack length increases from 0.1 to 16 in. at a width $w = 50$ in.; this factor will be referred to as the "spread factor". (Disregard, for the moment, that some of the curves in Figure 24 are in dashed lines.)

4.6.3 Effect of the Validity Limitation $S_{Nc} < 0.8\sigma_y$

When complete curves are available, as in Figures 22 to 24, the nature of the configuration dependence of $\bar{K}_c$ is obvious. When only very limited test results are

available on any one material, possibly beset by material scatter, the nature of the dependence is, of course, difficult to discern. However, the fact that a configuration dependence exists had been recognized experimentally some years ago: one effort to reduce it resulted in the rule that tests should be considered as valid only if the test stress $S_{Nc} < 0.8\sigma_y$ (Ref. 25). Consequently, Figures 22 to 24 will be re-examined to determine how effective this validity limitation is.

The materials of concern in Figure 22 do not yield; consequently, this figure is not affected by the introduction of the validity limitation.

In order to show the effect of the limitation on the results shown in Figures 23 and 24, plausible ratios σ_y/σ_u were selected, and dashed lines were used to indicate the portions of the curves for which the criterion $S_N < 0.8\sigma_y$ is not fulfilled. (Since the calculation of $\bar{K}_c$ is based on a rather than a_c, S_N must be used rather than S_{Nc}.)

Inspection of Figure 23 shows that only the left-hand end of the curve for $2a = 0.1$ in. is invalidated (the area below this curve is the "invalid domain"). Thus, the spread factor for $\bar{K}_c$ is not changed.

In Figure 24, most of the curves are invalidated for the assumed ratio $\sigma_y/\sigma_u = 0.75$; only a small portion at the top of the figure is left valid. Thus, the spread of $\bar{K}_c$ is indeed reduced drastically, but at the expense of a drastic reduction in scope of validity: specimens must be at least 20 in. wide, and cracks must be about 4.5 in. long or longer. This reduction of scope affects materials testing as well as prediction (design) calculations.

A study of materials properties shows that materials with $C_n \simeq 0.5$ can have widely different ratios of σ_y/σ_u. Figure 24 shows therefore circles at the right-hand edge, pertaining to ratios of σ_y/σ_u from 0.75 to 0.99. A horizontal line through a circle, if drawn, would show approximately the lower boundary of the "valid domain". It is evident that an increase in the ratio σ_y/σ_u increases the range of widths and crack lengths over which the results are considered valid, but that it also increases the spread factor for $\bar{K}_c$.

4.6.4 *Effect of the Plastic-Zone Correction*

A second effort to reduce the spread in K_c resulted in the "plastic-zone correction"[25]. This correction is made by replacing the crack length a_c in expression (26) by the quantity

$$a_c + (K_c^2/2\pi\sigma_y^2) \ . \qquad (28)$$

The quantity added to a_c is the "radius" of the plastic zone surrounding the crack tip; more precisely, it is the distance from the crack tip to that point on the extended crack line at which the stress computed by the stress-intensity factor K is equal to the yield stress. This distance is usually a fraction of an inch and thus has a negligible effect on the value of K_c when the crack length is large.

Materials with very high values of C_n, such as those shown in Figure 22, exhibit typically no yielding before failure, and consequently there is no plastic-zone correction (nor is a correction needed, since K_c is already nearly constant).

For materials with an intermediate value of C_m , ($C_m = 2$) the material properties shown in Figure 23 were again chosen as example. Application of the plastic-zone correction would raise the curve for $2a = 0.1$ in. about 22%, but would leave the curve for $2a = 16$ in. practically unchanged. The spread factor for $\bar{K}_c$ would be reduced from 2.6 to 2.1. This is an improvement, but not enough to consider the corrected value of $\bar{K}_c$ as constant.

For materials with rather low values of $C_m (C_m \simeq 0.5)$, a specific example was chosen: the 4330M steel for which data and calculations were shown previously in Figure 10. In Figure 25, uncorrected values of $\bar{K}_c$ as defined by Equation (26) (except that a is used instead of a_c) are shown as full lines when $S_N < 0.8\sigma_y$, and as dashed lines when $S_N > 0.8\sigma_y$. Values of $\bar{K}_c$ incorporating the plastic-zone correction are shown as dash-dot lines where they are valid ($S_N < 0.8\sigma_y$). The plastic-zone correction reduces the spread factor from 1.70 to 1.53; again, this is an improvement, but not enough to consider the corrected value of $\bar{K}_c$ as constant.

4.6.5 *Specific Example*

As mentioned in Section 4.6.2, the general study of the variability of K_c is handicapped by the lack of extensive sets of test data. However, the set of data for 2219-T87 used previously is reasonably adequate to permit a direct comparison between calculations and tests. Calculated curves and test points are shown in Figure 26. The calculated curves for $\bar{K}_c$ are based on the calculated values of S_N shown in Figure 9(b).

Test results are shown in open symbols when the test is considered as "valid" in Fracture Mechanics ($S_{Nc} < 0.8\sigma_y$), and in solid symbols when the test is considered as "invalid". In Reference 25(e), a plot similar to Figure 26 is shown (using K_c instead of $\bar{K}_c$), exhibiting only the "valid" (open) points. The test data are correlated in the reference by a curve corresponding to the dashed-line curve in Figure 26. (The dashed-line curve was obtained by multiplying the ordinates of the curve given in Reference 25(e) by 0.87, which is the average ratio of $\bar{K}_c/K_c$ as computed directly from the test data, the maximum dispersion being ±6%.)

Two observations may be made directly: the dashed line is a rather rough representation of the data (note high points at $w = 48$ in.), and the validity limitation rule imposes a very severe restriction on the scope of the method: cracks must be well over 2 in. long, and specimens must be at least 18 inches wide to obtain "valid" results.

Much more important in the long run, however, is the observation that most of the test points rejected as "invalid" by Fracture Mechanics fall very close to the computed curves. The computations make no allowance for "gross yielding", which Fracture Mechanics advances as reason for obtaining "apparent" values of K_c lower than the "actual" value. The close agreement between tests and calculations thus may be interpreted as direct evidence that low values of K_c (or $\bar{K}_c$) are not caused by "gross yielding", but are simply the inevitable consequence of using a (slightly modified) Griffith expression ($S\sqrt{a}$) under conditions violating the Griffith limitation $K_u \gg 1$.

(The CSA method begins to make corrections for yielding when $S_N > \sigma_y$. This is a much less severe condition than $S_{Nc} > 0.8\sigma_y$ because the factor 0.8 is missing, and because, for this material, $S_N \simeq 1.23 S_{Nc}$. Figure 26 contains no points for which

$S_N > \sigma_y$. The disagreement for the two low points at w = 24 in. might suggest an effect of "gross yielding", but since the low point at the extreme left shows perfect agreement, it is considered more likely that the disagreement for these two points is due to material scatter.)

In conclusion, then, the validity limitation and the plastic-zone correction are not only inadequate quantitatively to produce a constant K_c , but they are also based on an erroneous belief: the belief that "gross yielding" is the prime factor responsible for failure to obtain a constant value of K_c .

4.6.6 Recent Developments

Sections 4.6.1 through 4.6.5 were written in the fall of 1966. Since then, an important development has taken place.

The Griffith-Irwin method was very actively sponsored by the Fracture Committee of the ASTM, as evidenced by the series of reports published[25]. As a result, the method has, in effect, the status of a "recommended procedure". However, in March 1967, a review article[27] by a member of this Committee appeared, which contains the following statement:

"It is now generally realized that mixed-mode (or K_c) fracture testing is more complicated than was first supposed, and that considerable additional thought and research are needed to define precisely just what quantities should be measured."

As a consequence of this realization, the Committee decided that the previously recommended procedure should not become an official standard; the recommended testing procedure is now drastically standardized and the K_c-concept is no longer used[28]. Quoting from this reference, "This recommended practice is restricted to one specimen width which is generally suitable for evaluation of high-strength materials . . The recommended practice provides a comparative measure ... It is not intended to provide an absolute measure of resistance to crack propagation which might be used in calculations of the strength of structures. However, it can serve the following purposes: In research and development of materials ... In service evaluation ... For specification of acceptance and manufacturing quality control ..."

The specimen width is specified as 3 in. The specimen may contain either a fatigue crack, 1.0 in. long, or symmetrical Vee-notches with a combined depth between 0.9 and 1.1 in. and with a root radius $\rho \leq 0.0007$ in. The test result is to be reported as "sharp-notch strength" (failing stress based on net section before test). The maximum specimen thickness is specified as 0.25 in., with the note that the notch strength may vary with thickness.

The "Proposed Recommended Practice" as given in Reference 28 is thus strictly a "ranking method", with applicability to strength calculations for structures specifically disclaimed. The problem of unsatisfactory compatibility of results obtained with different sizes of specimens exhibited by the K_c-method – as discussed in the preceding sections – has thus been eliminated, but at a high price from the designer's point of view: he is informed that the numbers obtained cannot be used to solve design problems such as those posed by Figure 1.

4.7 Log-Log Plot Methods

The use of log-log plots is a time-honored engineering device for facilitating the "fairing" of experimental curves by means of a straight edge. Some investigators have contended that a log-log plot of S_N versus crack length gives a straight line; others have contended that a plot of S_G versus crack length gives a straight line. For convenience, the two types of plot will be examined together.

To begin with, the data for the 2219-T87 aluminum alloy have been examined. In order to provide systematic coverage, computed curves have been used rather than test points. The method of computation is again that used for Figure 9(b), which shows that the curves fit all the test points quite accurately except for very large ratios of $2a/w$, which will not be considered here. The resulting log-log plots are shown in Figure 27 with all curves terminated at $2a/w = 0.6$.

Consider first the curve of S_N for $w = 48$ in. The left-hand part can obviously be approximated by a sloping straight line, but towards the right, the curve becomes horizontal and then rises again. Thus, if a single sloping straight line is to be used, it is evidently necessary to exclude from consideration the right-hand portion of the curve, that is, to confine attention to reasonably low values of $2a/w$. Tick marks indicate $2a/w = 0.33$ on each curve, and attention will be confined to configurations with $2a/w < 0.33$. This constitutes the first (and severe) limitation on a method of this type.

Let $w = 48$ in. be designated the "maximum acceptable" width of test specimen, and $2a/w = 0.33$ the "maximum acceptable" crack length ratio. From inspection of Figure 27, it is evident that (on either the S_N or the S_G-plot), all "acceptable" test points lie between the curve for $w = 48$ in. and the curve for $2a/w = 0.33$. In order to indicate trends, corresponding curves are shown in Figure 28 for two materials, one very insensitive to cracks ($C_m = 0.1$) and one very sensitive to cracks ($C_m = 20$).

For $C_m = 0.1$, all values of S_N fall practically on one line, which is nearly straight. The values of S_G, on the other hand, spread apart toward the left; the straight-line approximation for S_G (dashed line) thus entails maximum errors of about ±22% at $2a = 1$ in. For $C_m = 20$, the situation is reversed: the values of S_G fall into a fairly narrow band, (±5%), while the values of S_N spread apart ±13% Thus, the choice between S_N-and S_G-plot depends on the crack sensitivity of the material.

The dashed lines in Figure 28 suggest the straight lines that would be obtained if the test points were concentrated at $2a = 16$ in. and $2a = 1$ in. If the number of tests is small, the location of the straight line at its left end becomes very dependent on the choice of test configurations, for which no guiding considerations are given. In the limit, if a test engineer decides to run only two specimens, it is quite possible for him to choose the test configurations in such a way that the straight line connecting these two points slopes the wrong way (points A and B in S_G-plot for $C_m = 0.1$). This consideration indicates the crucial limitation of the log-log plots: the straight-line relation is a global relation which applies more or less accurately to the entire population of "acceptable" test points, but it may give grossly misleading results when applied to a small number of test configurations.

A detailed specific example of the short-comings of a log-log plot is given in the following Section 4.8.

4.8 Broek's Method

In the course of an extensive investigation of the residual strength properties of two light alloys, Broek[26] made tests on specimens of three widths, ranging up to 600 mm. He noted that the relation (27) a_c/a = constant holds quite well for the largest width, and concludes that it holds rigorously for the infinitely wide sheet. Starting with an elaboration of the energy-balance criterion pioneered by Griffith, and using Equation (27), he arrives at a formula for the residual strength which, in the symbols of the present report, is

$$S_G a_c = \text{constant} \qquad (29)$$

where c is a materials constant. This formula is of the type for which the log-log plots are used, as discussed in Section 4.7. Recognizing that relation (27) holds strictly only for the infinitely wide sheet, Broek makes the log-log plots only for the tests on the widest specimens, and his plots are reproduced here in Figure 29.

Broek notes explicitly that his fracture criterion cannot satisfactorily explain test results on small specimens and on specimens with large cracks. Consequently, when showing his test results for all widths and crack lengths, he fairs curves through the test points. Figure 30 reproduces the test plots shown by Broek, omitting the faired curves. Instead, curves are shown which are obtained by two methods. The full-line curves are computed by the CSA method, using C_m for the 2024-T3 alloy and C_m as well as C_m' for the 7075-T6. The dashed-line curves are derived by applying the Broeks failure criterion, that is, the straight lines from Figure 29, regardless of width. (Note that, according to Broek, this procedure is expected to give unsatisfactory results; however, other proponents of the log-log plot method use it, and no other method of utilizing the plots of Figure 29 is apparent.)

It may be seen that the CSA curves give good agreement throughout the test range for both materials with the exception of a single test point (longest crack in 7075-T6 at w = 600 mm). The dashed-line curves based on the log-log plots, on the other hand, badly over-estimate the strength of the narrower specimens. For the specimens with the largest width, the curve is, of course, simply a transfer of the straight lines in Figure 29 to Cartesian coordinates, but extended to longer cracks than shown in Figure 29. For the 7075-T6, the extended curve still fits the only test point available (which disagrees with the C_m-curve). For the 2024-T3, on the other hand, the extended portion of the Broek curve over-estimates the strength to an increasing extent as the crack length increases.

It might be noted that the crack-sensitivity constants C_m for 2024-T3 and C_m' for 7075-T6 derived from the Broek tests, which are on Alclad material, are each 10% lower than the corresponding constants for bare material derived from the old NASA tests shown in Figures 12 and 13.

5. EFFECTS OF THICKNESS ON SHEET AND PLATE WITH THROUGH-CRACKS

5.1 General Discussion

It is a matter of ancient experience that the tensile strength of a metal plate tends to increase as the plate is rolled down to thinner sheet; the change is due to

the beneficial effect of working the material, and an additional gain may accrue from the higher quenching rate possible in a thin sheet. Similarly, the residual strength tends to increase as the thickness decreases, but the change is often much more pronounced. The relatively poorer residual strength of a thick plate is also attributed in part to another factor: in a thick plate, the stress condition at the root of a notch approaches the plane-strain condition, rather than the plane-stress condition realized in a thin sheet. Because of the rapid increase in the number and size of large structures employing thick material, large efforts are being devoted to the problem of residual-strength testing of thick material. In fact, during the past three years, large-scale organized effort in the aerospace field has been devoted almost exclusively to the development of techniques for evaluating thick sections, while corresponding work on sheet has been dropped for the time being.

The planning of the organized effort is based on ideas developed out of the Fracture Mechanics (K_c) method discussed in Section 4.6. The main lines of effort are described in detail in Reference 29 and may be characterized as follows:

(a) Concentrate attention on the "thickness-invariant" quantity K_{Ic} (the plane-strain or "pop-in" value of K_c).

(b) Define (by extensive testing) ranges of proportions and size of test specimens that will give (essentially) a single value of K_{Ic} for a given material.

(c) Develop specimens that do not require excessive capacities of testing machines (notch-bend specimens instead of notch-tensile specimens).

The crack-toughness parameter K_c (defined by Equations (26) and (28)) which is the key-stone of Fracture Mechanics decreases markedly as the thickness increases and appears to approach a limiting value as the condition of plane strain is reached; this (assumed) limiting value is designated K_{Ic}.

In very thick specimens, the fracture tends to be sudden and complete (in materials at aerospace interest). However, at smaller thicknesses, the final fracture is generally preceded by discrete bursts of crack propagation, beginning at a load level sometimes very substantially below that of final fracture. If the plate (or sheet) is not very thin, the initial burst is often announced by a very audible "pop" and is therefore called the "pop-in". It was discovered that the stress-intensity factor K at pop-in, regardless of thickness, appeared to be the same as K_{Ic}, which designates "pop-in" as well as final fracture in very thick plate. Thus, the quantity K_{Ic} appears to be a "thickness-invariant" materials property, which can be measured on all but thin sheet, where the "pop-in" becomes too indistinct. In practice, the pop-in load is seldom determined acoustically, but generally from autographic records of crack opening versus load, as will be discussed later.

The foregoing statements summarize the historical development of the Fracture Mechanics school of thought; they do not necessarily reflect current thinking in all respects, since the plane-stress parameter K_c has lost its former standing (Section 4.6.6). Some additional discussion will be given in the following sections; it must be understood, however, that a comprehensive review of Fracture Mechanics is not feasible here, and the reader interested in more detail is referred to References 29 to 31.

It is evident, on very brief reflection, that the development effort outlined focuses attention on the needs of the materials engineer, but disregards the needs of the structural engineer, except for fields in which weight of the structure is of very minor

concern compared with cost or reliability. Structural engineering requirements in the aerospace field exist in terms of strength, that is, fracture; K_{Ic} provides no information on fracture, only on "pop-in", and there has been practically no discussion on how much the structural engineer should be concerned with this phenomenon. Moreover, the configuration-dependence of K_c discussed in Section 4.6.1 must be expected to exist also for K_{Ic}, although to a lesser degree. (The existence of a configuration-dependence is recognized at least implicitly, but the rules under investigation are expected to define a range of configurations within which K_{Ic} is essentially constant.)

In order to cater explicitly to the needs of the structural engineer, checks have been made to ascertain whether the CSA method (Section 3.3) is applicable to plate. Suitable test data are very limited, but they give favorable indications. The CSA method does not offer the convenience of a single "thickness-invariant" quantity, but it does offer the basic capability of making strength calculations for structures.

5.2 Treatment of Thickness Effects in the Fracture Mechanics Method

5.2.1 *Relation between* K_c *and* K_{Ic}

In Fracture Mechanics, the plane-stress or "mixed-mode" notch toughness (see Section 5.4.4) is defined by the formula resulting from the combination of Equations (26) and (28), that is,

$$K_c = S_G \sqrt{\left(w \tan\left[\frac{\pi}{w} \left(a_c + \frac{K_c^2}{2\pi\sigma_y^2} \right) \right] \right)} \quad . \tag{30}$$

where S_G denotes the gross section stress at fracture. Figure 31 shows a plot of this quantity against thickness (circle symbols). It may be seen that K_c decreases as the thickness increases and that it appears to approach a constant value.

The square symbols represent values of K_{Ic} or "pop-in" values characterizing plane-strain notch toughness. The "pop-in" during the test announces the first advance of the crack front (see sketch in Figure 31); the defining formula is generally given as

$$K_{Ic} = S_{GPI} \sqrt{\left(w \tan\left[\frac{\pi}{w} \left(a + \frac{K_{Ic}^2}{6\pi\sigma_y^2} \right) \right] \right)} \quad . \tag{31}$$

where S_{GPI} is the gross section stress at the pop-in load, a is the initial (half-) crack length, and the plastic-zone correction has a smaller value than for K_c (coefficient 1/6 instead of 1/2). (When load-displacement records are used, as discussed in the following section, the plastic-zone correction is usually omitted from the expression (31).)

5.2.2 *Measurement of* K_{Ic}

Originally, the pop-in load was determined acoustically, aided at times by rather elaborate instrumentation (microphone, tape and oscillograph recording). However, at present, the acoustical determination is used, if at all, only as auxiliary; the currently preferred method of primary determination is based on an autographic record of crack opening versus load. The crack opening is measured by a compliance gage which measures the relative displacement of two points located on opposite sides of the crack. Extensive details on instrumentation are given in References 29 and 30.

Figure 32 shows three classes of load-displacement records. In Case I, the pop-in coincides with fracture. In Case II, there is a clear-cut pop-in. In Case III, the record becomes non-linear, and the steps in the curve are very small. Obviously, it is quite possible to have cases where tremors of the recording stylus obscure the pop-in.

Records of Class III are quite common. In order to provide for unambiguous evaluation of records of this class (and of more complex shape), as well as of records of Classes I and II, a new "secant-offset" procedure has been proposed[32]. The explicit purpose is to define the plane-strain notch toughness by the load at which the original crack length is increased (effectively) by 2%, as determined by deviation of the load-displacement record from a straight line, somewhat analogous to the determination of the yield stress by the secant off-set method. Since such a deviation from the straight line may be caused in part by local yielding, a procedure for graphical analysis of the record is prescribed, intended to insure that the major part of the deviation is caused by lengthening of the crack rather than by local yielding.

5.2.3 *Choice of Specimen Configuration and Size*

Specimen configurations used are shown in Figure 33. The machined notch is deepened by fatigue cracking whenever feasible; when this is not feasible, due to size or configuration of the specimen, the root radius should be as small as feasible (and should be reported with the test results). The symmetrical types of tension specimen are preferred in principle because the fundamental stress analysis for them is more accurate than for the unsymmetrical types; however, considerations of validity of test often lead to specimen sizes that are beyond the capacities of the testing machines commonly available. Unsymmetrical (single-edge-notch) tension specimens afford some reduction in machine capacity required, and notch-bend specimens afford a large reduction; most of the current work is therefore devoted to notch-bend tests using one-point loading as shown in Figure 33 or two-point loading[29].

The validity of a test on a sheet specimen (plane-stress K_c) was governed by the validity limitation discussed in Section 4.6.3 ($S_{Nc} < 0.8\sigma_y$). A rule of this type is now considered as inadequate and, in part at least, as inconsistent with the rationale of linear elastic fracture mechanics (Ref. 29, pp. 18-19). The rationale now advanced is as follows (Ref. 29, p. 19 et seq.).

A plate specimen has three pertinent dimensions: crack length, thickness, and ligament (uncracked) length. Each of these dimensions must be reasonably large compared with the plastic-zone size if linear elastic fracture mechanics is to be applicable. The plastic-zone size is proportional to the quantity $(K_{Ic}/\sigma_y)^2$. Therefore, each of the pertinent dimensions must be more than a certain multiple of the quantity $(K_{Ic}/\sigma_y)^2$ as established by tests.

The tests are made in two stages. In the first stage, a number of preliminary tests are made to establish an approximate value of K_{Ic}. Next, series of tests are made in which the pertinent dimensions are varied systematically in order to establish the minimum permissible magnitude of each dimension. Tests of this nature are presented in References 29 and 32 (chiefly notch-bend tests, some single-edge-crack tensile tests, with specimen widths up to 4.5 in.). The results show sensibly constant values of K_{Ic} (with varying amounts of scatter) as long as the ratio $a/(K_{Ic}/\sigma_y)^2$ as well as the ratio $t/(K_{Ic}/\sigma_y)^2$ is above 2.5. (For at least one material, this rule is very conservative; K_{Ic} remains constant down to $t/(K_{Ic}/\sigma_y)^2$ about 0.5.) The tests include

maraging steel, 4340 steel, one titanium, and one aluminum alloy. The only set of tests on ligament length was inconclusive; at the smallest ligament length tested, there was still no change in K_{Ic}. A typical test plot is shown schematically in Figure 34.

In the tests available so far, the value of K_{Ic} is almost always too high if the crack length or the thickness is too small to give valid results. This is opposite to the situation for K_c-tests, where tests which are invalid (due to too small a width) give values that are too low.

At the present time (fall 1967), a number of laboratories are engaged in cooperative tests on various materials in order to firm up the tentative rules proposed. For aluminum alloys, it is stated that the procedures used give satisfactory consistency. However, great stress is placed on the warning that all the detailed rules about specimen size, acceptance (or rejection) of load-displacement records and interpretation of these records must be obeyed meticulously if out-of-line results are to be avoided.

5.3 Discussion of Fracture Mechanics Method

5.3.1 Relation of K_{Ic} to Design Requirements

Values of K_{Ic} when incorporated in standard handbooks, such as Reference 33, can evidently be used as "ranking numbers" for comparing materials. How can they be used in design strength calculation?

Explicit design requirements are exemplified by Figure 1; they stipulate that the structure must be able to carry a stipulated load (the "fail-safe load") in the presence of cracks of stipulated length. The designer can (in principle) compute the stress-intensity factor for any crack under an applied load equal to the fail-safe load. If this stress-intensity factor is equal to K_{Ic} for the material chosen, the designer knows that a *pop-in* will take place; however, he does not know when *fracture* will take place. But pop-in cannot be correlated with design requirements as they exist now; only fracture can be correlated.

Consider Figure 31, and assume for the moment that the curves (K_{Ic} and K_c) may indeed be regarded as showing material properties. Assume also that the structural components with cracks cover the range of thickness, from thin sheet to thick plate, and that the design has been adjusted so that the level of K_{Ic} is just reached for all components. The K_c curve, which pertains to fracture, then indicates that the designer will have margins of safety against *fracture* varying from zero for the thick pieces to over 100% for the thin pieces. But the designer would not have the K_c curve (under current proposals), and consequently the margins would be "hidden margins".

Extensive tests on a large number of aluminum alloys have recently been compared by Kaufman[34]. Of special relevance here is the closing paragraph of this paper, which reads:

"Obviously, only the large center-notched panels provided information on the critical instability of the alloys in terms of K_c for the thickness tested. This seems an important point, since at a thickness of 1 in., all of the aluminum alloys except 2020-T651 and 7001-T75 exhibited values of K_c considerably higher than K_{Ic}, in one direction at least, i.e., more crack toughness than indicated by the plane-strain values. As a result, the use of the K_{Ic} values in design would be quite conservative in situations where plane-strain conditions do not exist."

In order to illustrate Kaufman's statement, a representative load-displacement curve for 7075-T651 taken from his paper is reproduced in Figure 35. It may be seen that there is a very clear pop-in, but final fracture does not take place until the load has been increased 61% above the pop-in value.

Table II is an abbreviated version of Table II from Reference 34. It may be seen that K_c exceeds the "candidate" values of K_{Ic} (tentative values) by substantial margins in most cases. In other words, 1 in. thick plates tested in tension do not approach the plane-strain condition (as indicated by pop-in loads) at all closely except for two materials tested in the transverse direction.

It is very doubtful that an aerospace structures designer could afford to design with hidden (and variable) margins of the magnitude indicated. It appears, therefore, that either the design requirements would have to be rewritten in terms of pop-in (rather than fracture), or the use of K_{Ic} would have to be confined to the ranking of materials and quality control.

With regard to the use of the secant offset method of evaluating the records, Kaufman[34] remarks:

"The secant-offset concept is a useful concept in view of the large number of cases in which the clear plane-strain instabilities are not manifest, but it does lack the fundamental basis that could have been provided by requirements for "pop-in" behavior."

5.3.2 Relation of K_c to K_{Ic}

In the preceding section, it was assumed for the moment that the K_c-curve shown in Figure 31 might be regarded as a materials property. This assumption is not tenable, in general, because K_c varies with specimen width and crack length as discussed in Section 4.6.2. The effect of this variability is illustrated by Figure 36.

The values of K_c given by points A, B, C, and D, as well as the values of K_{Ic} are taken from Reference 35; all test specimens had a width $w = 4.0$ in. and slots ($\rho \leq 0.5$ mil) with $2a = 1.7$ in. The relation between the full-line curve for K_c and the horizontal line for K_{Ic} is in agreement with the schematic Figure 31.

For $t = 0.5$ in., three points have been added to the original data. Two points (E and F) are computed for specimen configurations selected on the basis of the variability study presented in Section 4.6.2. (The computations were made using a value of C_m derived from point D and assuming a ratio $a_c/a = 1.24$, on the basis of tests shown in Reference 36.) Point G is a test point.

Assume now that a materials engineer had available to him points A, B, C, and G or E. He would then draw the curve of K_c versus t as shown by the dashed line. This procedure would be legitimate because all the points are "valid". Specifically, for points D and G, the ratio S_{Nc}/σ_y is 0.45 and 0.30, respectively, far below the stipulated maximum of 0.8 necessary for validity. The engineer would then draw two conclusions:

(a) The state of plane strain is reached for a thickness $t \simeq 0.25$ in.

(b) The value of K_{Ic} should be about 45 ksi $\times$ in.$^{\frac{1}{2}}$.

As soon as point D is made available, however, it becomes obvious that both conclusions are substantially in error. The reason for the error is evident: a plot such as Figure 31 is not uniquely determined for a given material because it is determined also by specimen configuration.

Since K_{Ic} is calculated by essentially the same formula as K_c, it must be expected to show a dependence on configuration as discussed in Section 4.4.2. Quantitatively, the variability of K_{Ic} is less than that of K_c as measured on thin sheet of the same material because the pop-in takes place at a lower stress level than the fracture of thin sheet (often substantially lower); thus, the basic criterion $K_u >> 1$ for the applicability of a Griffith-type expression such as K_c is more nearly fulfilled (see discussion of Equation (25)). Direction experimental evidence can be quoted at present only in a fragmentary manner, because very few comparable K_{Ic}-tests on specimens of the same thickness but widely different widths are available.

5.3.3 Problem in Determination of K_{Ic}

A problem encountered in the determination of K_{Ic} is that very large thicknesses are required to achieve "valid" tests for reasonably tough materials, and the engineer is left in a quandary if a specific order of the material is not produced in a large thickness. For instance, for the tests on 7079 aluminum alloy shown in Figure 38, the material was furnished in a maximum thickness of 5/8 in., and tests were made at thicknesses down to 0.16 in. For the conventional heat treatment (-T6), all K_{Ic} tests were invalid except for the transverse tests at the largest thickness, and the (invalid) K_{Ic} numbers varied by a factor of over two from the largest thickness to the smallest thickness.

In Reference 29, p.87. R.H.Heyer (Armco Steel Corp.) comments: "If the proposed thickness requirements are confirmed, the range of application of valid K_{Ic} testing will be quite restrictive, and the need for mixed mode fracture toughness criteria remains.

"While parameters which are independent of thickness are highly desirable, they may be unattainable for materials not amenable to K_{Ic} testing, and serious considerations may have to be given to parameters applicable within limited thickness ranges."

Thus, a problem of obtaining valid tests is known to exist for aluminum alloys as well as steels, and it may be safely assumed that it exists for titanium alloys, also.

5.4 Treatment of Thickness Effects by the CSA Method

5.4.1 Application of CSA Method to Fracture

The CSA method is described in Section 3.3, and applications to thin sheet material are given in Section 3.7. The method of application to thicker sheet and plate is the same except that explicit attention is given to the fact that the constants involved are functions of the thickness as determined by tests.

Figure 37 shows test data on 7075-T6 (sheet) and -T651 (plate) evaluated by the CSA method (C_m-method). Although this is the largest set of data available for one material, it is evident that there are not enough points at intermediate thicknesses (say 0.3 to 0.9 in.) to establish curves with sufficient accuracy to justify extrapolation to

larger thicknesses than the maximum thickness tested; the curves shown are intended simply as guides to the eye. The general trend of the data is as expected – the crack sensitivity increases as the thickness increases. Also, as expected, the residual strength is lower (C_m is higher) in the transverse direction than in the longitudinal direction, although this trend is obscured by scatter for the thinnest sheet tested.

Note should be taken of the fact that at $t = 0.5$ in., close correlation is shown for a test point with $w = 4$ in. and one with $w = 15$ in. In Figure 36, the K_c values for these two points are shown as points D and G, with $K_c = 34.3$ and 46.4 ksi $\times$ in.$^{\frac{1}{2}}$, respectively.

Figure 38 shows C_m-plots for 7079 aluminum alloy with three different heat treatments; the "peak-aged" condition is the conventional-T6 heat treatment. Of main interest here is the fact that tests in the longitudinal direction were made on specimens with widths of 8, 12, and 36 in. It will be noted that the results obtained for different widths either agree very closely, or, if they do show differences, the differences exhibit no consistent pattern and may thus be attributed to scatter of material properties.

(The values of C_m derived from tests on 36-in. specimens with $t = 0.16$ in. for the under-aged and the over-aged material are accompanied by question marks. The values of S_N for these specimens were about 12% higher than for the corresponding 12-in. specimens (at the same ratio $2a/w$). This constitutes an abnormal relationship never observed before; consequently, these two values of C_m should be discounted unless verified by additional tests.)

Figure 39 shows data for 7079-T651 obtained by the Alcoa Research Laboratories. The relevant data from Figure 38 are also shown in simplified form and are seen to agree quite well.

5.4.2 *Notes on Evaluation of Test Data*

As noted previously, there is currently a large amount of testing for the purpose of producing K_{Ic} data on thick sections, utilizing almost exclusively notch-bend specimens and single-edge-notch specimens. Unfortunately, these data cannot be used to derive C_m values, partly because the necessary formulas have not been derived, partly because often only "derived data" are published (specimen dimensions, test loads or stresses, tensile strength of material are often not reported).

A significant amount of data potentially useful chiefly to derive K_c or C_m values is reported from tests on symmetrical Vee-notch specimens without or with fatigue-crack "tipping" of the notches. Comparisons of data derived from such tests with data derived from center-slotted or center-cracked specimens often showed a much larger scatter range, with the lower edge of the scatter band lying in the band for the center-slotted specimens. The difference is believed to be attributable, in the main, to cracking starting on one side first, and the resulting eccentricity being more deleterious for the edge-notch than for the center-slot specimens. Results from edge-notch specimens are therefore used sparingly in this report.

At the Aluminum Company of America, slots with a tip radius specified as $\rho \leq 0.5$ mil have been used for some time when it is impractical to provide fatigue cracking. Values of C_m derived from such tests have been increased by 10% (unless otherwise noted) as

an approximate correction to the fatigue-crack condition. Application of the NSA method indicates a larger correction variable with material, but a more elaborate correction procedure is not felt to be justifiable at present in view of two observations. The first one was that two micro-photographs indicate $\rho \simeq 0.3$ mil and $\rho \simeq 0.1$ mil, respectively, that is, only a fraction of the specified maximum of 0.5 mil. The second observations was that in a few cases, the average strength (for three specimens from one heat) of the radius specimens was actually less (by 1 to 2%) than the corresponding average of fatigue-cracked specimens, indicating that material scatter could over-shadow the difference between a slot (with $\rho \leq 0.5$ mil) and a crack for the average of a small sample. (For larger samples, three heats of material with three specimens each, this was no longer true.)

In a few cases, it was desired to utilize data from tests on sheet made without buckling guides (Section 3.4). The test loads were corrected by formula (16), but no tests were used if the correction was greater than 20%.

Occassionally, some published test series in which the crack length is varied show failing loads higher than expected for short cracks, and special or additional tests to trace the reason for the discrepancies are seldom feasible. When such discrepancies appeared to be of significant magnitude, the results obtained with short cracks ($2a/w < 0.15$) were not used, in order to maintain a conservative tendency in the derived constants.

5.4.3 *Application of CSA Method to Pop-in*

Test data on pop-in (stress at pop-in and crack length) can be evaluated in the form of C_m-values for pop-in, designated by the symbol C_m^{PI}. As example, data from Reference 37 for 7075-T651 aluminum alloy are shown in Figure 40(a), while Figure 40(b) shows the same data evaluated in the form of K_{Ic}. Figure 40(b) also shows some additional points for $t = 1.375$ in. obtained from notch-bend tests, which cannot be evaluated in the form of C_m, as noted before.

The plot of C_m^{PI} indicates some thickness effect, the values for the thick plate being somewhat higher than for the thin material. First inspection of the corresponding data in Figure 40(b) shows apparently no thickness effect. It must be noted, however, that the tests on the thin material were made on specimens 3 or 4 in. wide, while the (center-notched) specimens of the thick plate were 20 in. wide; thus, attention must be given to the width-effect on K_c discussed in Section 4.6.2.

Assuming that notch-strengthening has no significant effect, K_c-values obtained with $w = 20$ in. can be adjusted to $w = 3$ in. by using the CSA method. Considering center-cracked specimens of these two widths, with $2a/w = 0.33$, the CSA method gives the ratio

$$K_{Ic(w=3)}/K_{Ic(w=20)} = 0.39(1 + 1.30C_m)/(1 + 0.50C_m) \quad . \tag{32}$$

A plot of this ratio is given in Figure 41. The vertical bar shown in Figure 40(b) is the result of applying Equation (32) to the K_{Ic}-values for transverse-grain specimens 20 in. wide, thus "adjusting" them to $w = 3$ in. It may be noted that the bar is bracketed by two test points obtained on notch-bend specimens of somewhat greater thickness and a width $w = 3$ in. This experimental "corroboration" of the adjustment is, of course, of unknown quantitative value, because the width effect on notch-bend specimens has not been investigated; however, experience has suggested that such comparisons between tensile and bend specimens give useful indications.

5.5 Concept of Critical Thickness

In studies of the effect of thickness, much attention has been directed to the change of the fracture topography or "fracture mode". In very thick specimens, the fracture is essentially flat, with a "shear lip" occupying only a small part of the fracture surface (right-hand sketch, Figure 42). As the thickness decreases, the shear lip occupies an increasingly larger percentage of the fracture surface ("mixed-mode"). Finally, at and below a certain thickness, the fracture is entirely of the "slant" type.

Bluhm[39] has proposed a model which correlates fracture mode and residual strength, on the assumption (suggested by observations) that the width of the shear lip is a constant for a given material at a given temperature. This model exhibits increasing strength as the thickness decreases (Fig.42) until the thickness is just equal to the width of the two shear lips (which may combine into a single slant fracture). As the thickness is further decreased, the strength remains at the same level or decreases toward zero, depending on whether lip formation is a surface phenomenon or a volume phenomenon.

Bluhm was not able to produce direct experimental proof of the existence of a maximum of the residual strength or "notch toughness" curve (curves based on Charpy impact energy had shown a maximum). A few sketchy sets of older tear tests do show a decrease in strength with decrease in thickness, suggesting that the entire test range is to the left of the maximum; however, closer examination shows that much of the decrease can generally be attributed to two factors often overlooked. One is the lip-buckling effect (Section 3.4), which results in a decrease of strength for thinner sheet. The other effect is a "cladding effect", produced by the fact that the percentage of cladding is greater on thin sheet than on thick sheet.

More recently, several sets of data have been presented by Broek[36]. Figure 43 reproduced from this reference shows excellent agreement between the maximum on the strength curve and the percentage of shear.

An investigation made at the Lewis Laboratory of the NASA[40] is worth while quoting here, because it brings out two conclusions.

The material was B120VCA titanium alloy (13V-11Cr-3Al), which develops a tensile strength of 175 to 200 ksi when aged. The specimens were Vee-notch specimens ($\rho < 0.7$ mil), and the results are reported as notch tensile strength. The different thicknesses were produced in three ways:

(a) By rolling down from a single sheet with t = 0.13 in. (plus resolution treatment and ageing).

(b) By machining (grinding) down from the same single sheet.

(c) Each thickness was produced at the mill from a different heat of material.

The main results of interest here are shown in Figure 44. For the "Single Sheet Rolled" and the "Single Sheet Machined", the notch strength decreases monotonically, reaching a plateau in about the middle of the thickness range investigated. The two curves agree quite well, indicating that rolling plus reheat-treatment resulted in the same notch strength as that shown by the original sheet. (However, microstructural

changes were noted, and the reheat-treatment did lower the smooth tensile strength about 12%. Thus, the "Rolled" and the "Machined" specimens have a somewhat different notch-strength *ratio*, although the notch strength itself is the same.) The conclusion that thickness differences may be more important than metallurgical differences appears to be of rather wide applicability.

The most noteworthy result is the comparison between these two curves and the corresponding curve of notch strength for different thicknesses originating from different heats. For $t \simeq 0.06$ in., the results are about the same. However, for $t \simeq 0.025$ in., the notch strength for the "Different Heats" tests is very much higher than for the "Single Sheet" tests, while at $t \simeq 0.018$ in., the strength is much lower, in fact, as low as that for the thickest sheet. Thus, variation from heat to heat completely obscured the thickness effect in this series of tests and produced a spurious maximum.

Quantitatively, this conclusion should of course not be generalized. Qualitatively, however, it should be borne in mind when interpreting test data. (With respect to the specific material, it should be noted that the material was fabricated about 1959. The results may therefore not be typical of current material.)

6. PART-THROUGH CRACKS

6.1 Randall's Investigation

Cracks that do not extend through the entire thickness of the sheet or plate may be completely embedded flaws, or they may be surface cracks. A method for analyzing embedded elliptical flaws or semi-eliptical surface flaws due to G.R. Irwin may be found in Reference 25(e). For the surface crack the depth of the crack is used as controlling parameter, but is modified by a factor Q to make allowance for the shape of the crack.

An extensive study of surface cracks, sponsored by the US Air Force, has been made by Randall and is discussed by him in Reference 29 (pp. 88-126). Two materials were used: D6-AC steel, heat-treated to 290 and 230 ksi ultimate, and Ti-6Al-4V heat-treated to 174 and 162 ksi ultimate. The "low strength", in each material, represents a strength level conventionally used; the "high strength" represents a level high enough to permit the use of linear elastic fracture mechanics with some confidence.

Randall concludes his discussion as follows:

"As a result of the rather close scrutiny of the test results for crack size particularly, we do not recommend the writing of a specification or test standard for the general use of the surface-cracked specimen to measure fracture toughness. We believe that the correction factors suggested for K_{Ic} are proper, but no claim can be made that they will give a constant value of K_{Ic} for a given material, independent of crack size. Yet the basic reason for use of a K_{Ic} value to characterize fracture toughness is that it permits the correlation of stress to flaw size.

"The surface-cracked specimen can be used effectively in specific hardware programs where the flaw size can be estimated, where the flaw geometry resembles surface cracks, and where material thicknesses are known and can be used in the test specimen as well."

The authors of Reference 29 (Brown and Srawley) concur in the following words:

"The results he obtained illustrate the complexities associated with the stress analysis of this specimen and serve to emphasize that it is not suitable for general use in K_{Ic} testing. Further experimental work of the type described by Mr Randall should be encouraged."

The tests made by Randall were apparently well performed, and their scope is quite fair (two "high-strength" and two "low-strength" materials). This writer is therefore inclined to make a somewhat different recommendation, namely that a renewed analytical attack on the problem be encouraged, using Randall's data as first proof stone. Ultimately, of course, it would be highly desirable to have at least one set of data on surface cracks accompanied by a set of data on the same material obtained with center-crack specimens for conclusive correlation of the residual strength characteristic used.

6.2 Proposal by W. Barrois

Specimens with "through" cracks operate in one of the "principal" systems as defined in Appendix C; in a longitudinal specimen, for instance, the crack would propagate either in the width direction (RW specimen) or in the thickness direction (RT specimen). In a longitudinal specimen containing a transverse surface crack, however, the crack would propagate in the width direction, in the thickness direction, and in all intermediate directions at the same time. Several investigators have pointed out this fact and suggested that it may be the reason for poor correlation with the theory.

Related observations have been made by W. Barrois. He points out that the most common type of fatigue cracks encountered in service develops as shown in Figure 45(a). He proposes, therefore, to run notch-bend tests on specimens of square cross-section oriented as shown in Figure 45(b). In the system of Appendix C, a longitudinal specimen of this type would be designated a R-WT specimen. It would be the most logical basis for evaluating residual strength in the presence of cracks such as shown in Figure 45(a), and therefore, it deserves serious consideration, even when used simply as a ranking test. Its use for determining a materials constant, of course, would require an appropriate stress analysis.

7. OUTLOOK ON COMPLEX STRUCTURES

The strength analysis of a complex structure containing cracks obviously requires, as fundamental basis, the ability of analyzing the elementary problem of a simple rectangular specimen containing a crack. The discussion presented in this report makes it clear that the ability to handle the elementary problem has been developed only very recently, and that even this development is not complete, the problem of surface cracks, for instance, being unsolved. Thus, it is not surprising that methods for analyzing complex structures are at present in the embryonic stage.

The problems that must be tackled may be divided roughly into two categories: problems of stress-distribution analysis, and problems of crack-arrest.

The stress-distribution analysis of complex structures in the undamaged state has been greatly facilitated by the introduction of computing machines. The existence of automated stress analysis has made it feasible to re-introduce a feature which was

standard in an earlier era of aircraft design: computation of the strength of the structure with certain elements completely removed from the structure. The assumption that some selected element is missing can readily be fed into the computer, and the corresponding analysis is then obtained automatically. The assumption that an element is completely missing was quite realistic for strut-and-wire structures. However, for the present type of structure, the assumption is often quite unrealistic: the effect of a crack in a skin panel is quite different from the effect of removing the entire skin panel. Additions to the so-called "computer libraries" must be developed to represent damage such as cracks or holes reasonably realistically.

In the analysis of the undamaged structure, it is usually permissible to assume that concentrated members (stringers, rings, spar caps, and longerons) take only axial forces. In the presence of local damage, it may be desirable or even necessary to recognize that such members can take bending loads. Since a general provision for such action would overpower the computer capacity, it will often be necessary to make a special local analysis, to be coupled with the standard analysis for the whole structure.

The problem of crack arrest arises already in a simple tension panel consisting of sheet and longitudinal stringers. A transverse crack in such a panel will propagate suddenly at some load, but it may be arrested at a stringer and spread no further if the load is not increased. The question is: Under what conditions will arrest take place, rather than complete fracture? Published literature in this area is very scanty indeed, and all of it requires a searching re-appraisal in the light of current knowledge. Much additional work is needed; a very promising beginning is that described in the final section of the paper by Broek[36].

Tests on complete complex structures such as wings or fuselages containing cracks or other damage are too expensive to justify tests for research purposes alone. Thus, it is highly desirable that tests made for purposes of development or airworthiness demonstration be utilized as fully as possible. A number of attempts have been made in several countries during the past 30 years or so to improve the reliability of static strength analysis of airplanes by having a central staff analyze the results of all major strength tests. All these attempts have failed, because the geographical and organizational separation made the conduct of the work too inefficient. It appears, therefore, that the individual manufacturing firm is the most logical place for beginning the task of making damage analyses of complex structures. It will be an added burden for an already badly burdened industry, but the potential pay-off is visible and should be sufficient to justify a reasonable effort. Obviously, this is an area in which the gains would be multiplied by a pooling of the results.

REFERENCES

1. Dougherty, James E. — *FAA Fatigue Strength Criteria and Practices.* ICAF Symposium on Aeronautical Fatigue, Munich, Germany, June 1965.

2. Neuber, H. — *Theory of Notch Stresses: Principles for Exact Stress Calculation.* J.W.Edwards, Ann Arbor, Mich., 1946. (Kerbspannungslehre: Grundlagen fur genaue Spannungsberechnung, Julius Springer, Berlin, 1937.)

3. Kuhn, P. Hardrath, H.F. — *An Engineering Method for Estimating Notch-Size Effect in Fatigue Tests on Steel.* NACA TN 2805, 1952.

4. Kuhn, P. Figge, I.E. — *Unified Notch-Strength Analysis for Wrought Aluminum Alloys.* NASA TN D-1259, 1962.

5. Hardrath, H.F. Ohman, L. — *A Study of Elastic and Plastic Stress Concentration Factors due to Notches and Fillets in Flat Plates.* NASA (NACA) TR 1117, 1953.

6. Kuhn, P. — *Notch Effects on Fatigue and Static Strength.* ICAF-AGARD Symposium on Aeronautical Fatigue, 229-264, Rome, April 1963.

7. Figge, I.E. — *Residual Strength of Alloys Potentially Useful in Supersonic Aircraft.* NASA TN D-2613, 1965.

8. Dixon, J.R. — (a) *Stress Distribution Around a Central Crack in a Plate Loaded in Tension; Effect of Finite Width of Plate.* Journal of the Royal Aeronautical Society, 1960.
(b) *Stress Distribution Around Edge Slits in a Plate Loaded in Tension - The Effect of Finite Width of Plate.* Journal of the Royal Aeronautical Society, 1962.

9. - — Third Report of a Special ASTM Committee on Fracture Testing of High-Strength Sheet Materials, ASTM Materials Research and Standards, November 1961.

10. - — *Metals Handbook.* Vol.1, 8th Edition American Society for Metals, 499, 1961.

11. Weiss, V. et al. — *The Effect of Stress Gradient and Stress Biaxiality on the Behavior of Materials.* ASD Tecnical Report 61-725, October 1961.

12. McEvily, A.J., Jr et al. — *Static Strength of Aluminum-Alloy Specimens Containing Fatigue Cracks.* NASA (NACA) TN 3816, October 1956.

13. Manning, G.K. — *Effect of Small Cracks on the Load-Carrying Ability of High-Strength Steel.* ASTM STP No. 302, 1961.

14. Christensen, R.H. — *Cracking and Fracture in Metals and Structures.* Symposium on Crack Propagation, Cranfield, September 1961.

15. Broek, D. — *The Residual Strength of Light Alloy Sheets Containing Fatigue Cracks.* Paper presented at 5th Congress of ICAS, London, September 1966.

16. Crichlow, W.J. — *The Ultimate Strength of Damaged Structures - Analysis Methods with Correlating Test Data.* "Full-Scale Fatigue Testing of Aircraft Structures", edited by F.J.Plantema and J.Schijve. Pergamon Press, 1961.

17. Crichlow, W.J. Wells, R.H. — *Crack Propagation and Residual Static Strength of Fatigue Cracked Titanium and Steel Cylinders.* ASTM Fatigue Crack Propagation Symposium, June 1966.

18. Christensen, R.H. Denke, P.H. — *Crack Strength and Crack Propagation Characteristics of High-Strength Metals.* ASD-TR-61-207, January 1962.

19. Welbourne, E.R. — *The Correlation of Unstable Crack Length Data for Sheet Material.* Aeronautical Quarterly, November 1961.

20. Hardrath, H.F. Ohman, L. — *A Study of Elastic and Plastic Stress Concentration Factors due to Notches and Fillets in Flat Plates.* NASA (NACA) TR 1117, 1953.

21. Griffith, G.E. — *Experimental Investigation of the Effects of Plastic Flow in a Tension Panel with a Circular Hole.* NASA (NACA) TN 1705, September 1948.

22. McEvily, A.J., Jr et al. — *Static Strength of Aluminum-Alloy Specimens Containing Fatigue Cracks.* NASA (NACA) TN 3816, October 1956.

23. Griffith, A.A. — *The Phenomena of Rupture and Flow in Solids.* Royal Society of London, Philosophical Transactions, Series A, 163-198, October 1920.

24. Griffith, A.A. — *The Theory of Rupture.* Proceedings of the First International Congress for Applied Mechanics, 55-63, Delft, 1924.

25. - — *Reports of a Special ASTM Committee on Fracture Testing of High-Strength Sheet Materials.* ASTM Materials and Standards. (a) First Report, Chapter I, January 1960; Chapter II, February 1960, (b) Second Report, May 1961, (c) Third Report, November 1961, (d) Fourth Report, March 1962, (e) Fifth Report, March 1964.

26. Broek, D. — *The Residual Strength of Light Alloy Sheets Containing Fatigue Cracks.* Paper presented at 5th Congress of ICAS, London, September 1966.

27. Brown, W.F., Jr — *Fracture Testing and ASTM.* ASTM Materials Research and Standards, March 1967.

28. – — 1966 Book of ASTM Standards, Part 30, p.908. (Also 1967 Book of ASTM Standards, Part 31, p.945.)

29. Brown, William F., Jr; Srawley, John E. — *Plane Strain Crack Toughness Testing of High Strength Metallic Materials.* ASTM STP 410 (in cooperation with National Aeronautics and Space Administration), Philadelphia, Pennsylvania, 1967.

30. – — *Fracture Toughness Testing and its Applications.* (Symposium, Chicago, June 1964.) ASTM STP 381, Philadelphia, Pennsylvania.

31. – — *Reports of a Special ASTM Committee on Fracture Testing of High-Strength Sheet Materials.* ASTM Materials Research and Standards. (a) First Report, Chapter I, January 1960; Chapter II, February 1960, (b) Second Report, May 1961, (c) Third Report, November 1961, (d) Fourth Report, March 1962, (e) Fifth Report, March 1964.

32. Srawley, J.E. et al. — *Determination of Plane Strain Fracture Toughness.* ASTM Materials Research and Standards, June 1967.

33. – — Military Handbook-5A, Metallic Materials and Elements for Aerospace Vehicle Structures. Department of Defense, Washington, D.C.

34. Kaufman, J.G. et al. — *Fracture Toughness of Aluminum Alloy Plate Determined With Center-Notch Tension, Single-Edge-Notch Tension and Notch-Bend Tests.* Presented at National Symposium on Fracture Mechanics, Lehigh University, June 1967.

35. Kaufman, J.G. — *Fracture Toughness of 7075-T6 and -T651 Sheet, Plate, and Multi-Layered Adhesive-Bonded Panels.* Presented at ASME Metals Engineering Conference, Houston, Texas, April 1967.

36. Broek, D. — *The Residual Strength of Light Alloy Sheets Containing Fatigue Cracks.* Presented at 5th Congress of ICAS, London, September 1966.

37. Kaufman, J.G.; Holt, M. — *Fracture Characteristics of Aluminum Alloys.* Alcoa Research Laboratories Technical Paper No.18, 1965.

38. Kaufman, J.G. et al. — *Fracture Toughness, Fatigue and Corrosion Characteristics of 7075-T651, 7075-T7351 and 7079-T651 Aluminum Alloys.* Technical Report AFML-TR-65-170, May 1965.

39. Bluhm, J. I. *A Model for the Effect of Thickness on Fracture Toughness.* ASTM Proceedings, 1961.

40. Repko, A. J. et al. *Influence of Sheet Thickness on the Sharp Edge Notch Properties of a β Titanium Alloy at Room and Low Temperatures.* ASTM STP 302, 1962.

APPENDIX A

Visits made on AGARD Survey.

BAC = British Aircraft Corporation (Operating) Ltd
HS = Hawker-Siddeley Aviation Ltd.

England

August 22, 23	Royal Aircraft Establishment, Farnborough
24	BAC, Weybridge
25, 26	Royal Aeronautical Society, London
29	HS, Manchester
30	BAC, Preston
31	HS, Kingston
September 1	HS, Hatfield

Belgium

September 5	Brussels (Joint Meeting, government and universities)

Holland

September 6	Fokker, Amsterdam
7	National Aero- and Aeronautical Research Institute, Amsterdam
8	Technological University, Delft (Prof. Koiter)

France

September 12	Service Technique Aéronautique, Paris
13	AGARD, Paris
14	Sud Aviation, Paris
16	AGARD, Paris

Italy

September 19	Fiat, Turin

Germany

September 28	Darmstadt (Joint Meeting, government and aircraft industry)
29, 30	Laboratory for Service Strength, Darmstadt
October 1	Laboratory for Service Strength, Darmstadt

Canada

October 18	Committee for Aircraft Fatigue (Spec. Meeting), Ottawa
19	National Research Council, Structures Division, Ottawa
20	DeHavilland, Downsview
21	Canadair, Montreal.

Grateful acknowledgement is made to all the organizations visited for providing extensive information and fruitful discussions. In the great majority of cases, a number of individuals participated in the discussion; consequently, it is not practicable to express appropriate thanks to each individual. However, special thanks are given to the following, who served as main contacts in their respective countries or organized special meetings which greatly simplified the itinerary.

Belgium: Monsieur J. Van Laer

Canada: Mr A.H.Hall, Mr J.A.Dunsby

England: Mr R.J.Atkinson

France: Monsieur W.Barrois

Germany: Dr.-Ing. J.Kowalewski, Prof. Dr.-Ing. E.Gassner

Holland: Dr F.J.Plantema

Italy: Ing. G.Incarbone

In the United States, the author had been in essentially continuous contact with the airframe industry for a number of years. However, two special trips were made to the Aluminum Company of America, and the author is greatly indebted to Mr J.G.Kaufman for extensive discussions and for help in evaluating data.

APPENDIX B

Report of ASTM Fracture Committee, May 1961, p.390.

"On the other hand, it is not possible, at present, to relate the fracture stress to the original dimensions of the specimen."

APPENDIX C

Tensile tests on thin sheet (un-notched or notched) are usually made in the with-grain or longitudinal direction and in the cross-grain or transverse direction. For plate, a more elaborate system is necessary; a symbolism for such a system proposed in Reference 25(b) is shown in Figure 46. The principal directions of the plate are designated as R (rolling), W (width), and T (thickness, short transverse). Each type of specimen carries a two-letter symbol: the first letter designates the normal to the plane of the original crack, the second letter designates the direction of crack propagation.

TABLE I

Test Values of Crack Sensitivity C_m

(For orientation purposes only)

(Tests at room temperature)

Material	t *(in.)*	C_m $(in.^{-\frac{1}{2}})$	*Notes*
2014-T6	0.06	1.2	
X2020-T6	0.06	$\simeq$ 3	
2024-T3	0.04 - 0.10	0.5	
2024-T86	0.06	1.8	
2219-T87	0.10	0.6	
7075-T6	0.04 - 0.10	$\simeq$ 1.4	
4330M	0.08	0.5	σ_u = 223 ksi
4330M	0.14	0.9	σ_u = 222 ksi
AM350 (SCT 950)	0.05	0.4	
17-7PH (RH 1050)	0.04	0.9	
PH15-7Mo (TH 1050)	0.025	0.7	
PH15-7Mo (RH 950)	0.05	5-7	
H-11	0.06	19	Aged 1000°F (1 + 1 + 1 hr)
Vascojet 1000	0.06	24	Aged 1000°F (2 + 2 + 2 hr)
Ti 2.5Al-16V	0.08	36(?)	Aged 4 hr at 700°F to obtain maximum brittleness
Glass		104	Griffith tests

Note: In some materials, values of C_m for longitudinal and transverse directions differ substantially; values shown are averages. Most tests obtained for a single heat of material.

TABLE II

Tension Tests on Panels with Center Slots

w = 20 in.; t = 1.00 in.; 2a = 7.00 in.; $\rho \leq 0.0005$ in.

Material	*Longitudinal*		*Transverse*	
	K_Q	K_c	K_Q	K_c
2020-T651	22.3	29.0	19.1	19.1
2024-T851	28.6	46.1	23.8	32.3
2219-T851	49.7	82.5	44.2	63.1
7001-T75	26.8	34.3	23.1	25.5
7075-T651	32.9	70.8	27.7	33.8
7075-T7351	43.2	99.5	34.8	55.9
7079-T651	35.6	61.2	27.4	36.4

1. Data are averages from Table II, Reference 34.
2. All values are averages of three tests.
3. K_Q are "candidate" values for K_{Ic}, subject to final agreement on validity rules. Values are ksi x $in.^{\frac{1}{2}}$.

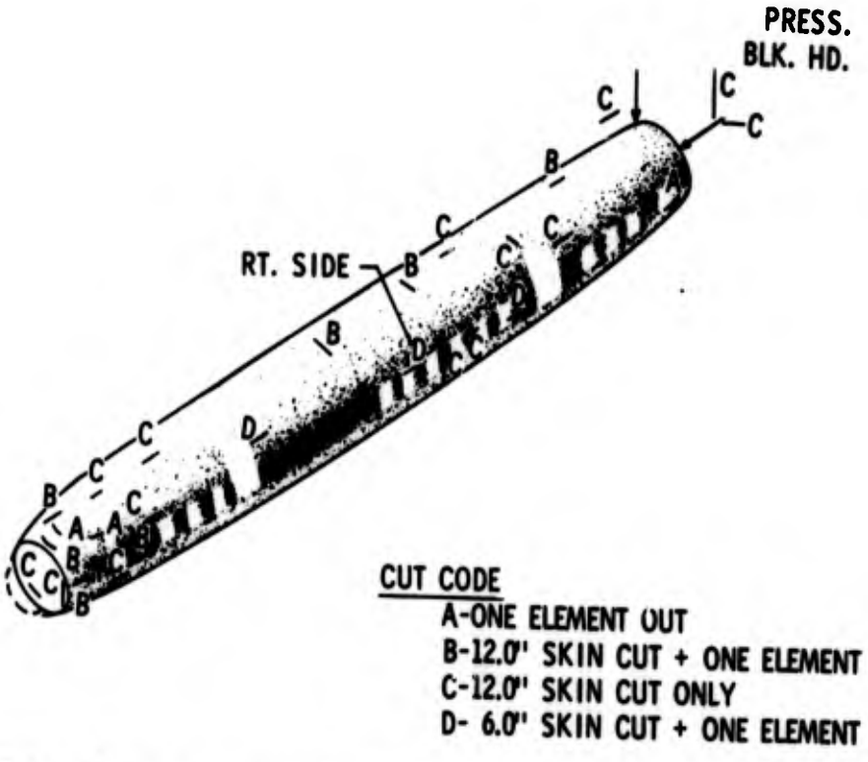

Fig. 1 Fuselage fail-safe demonstration test. From Reference 1

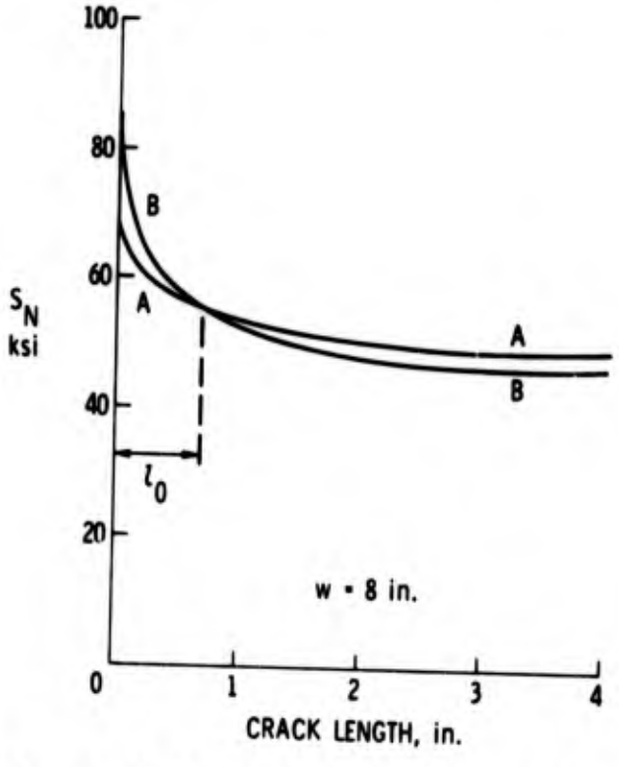

Fig. 2 Residual strength of two aluminum alloys

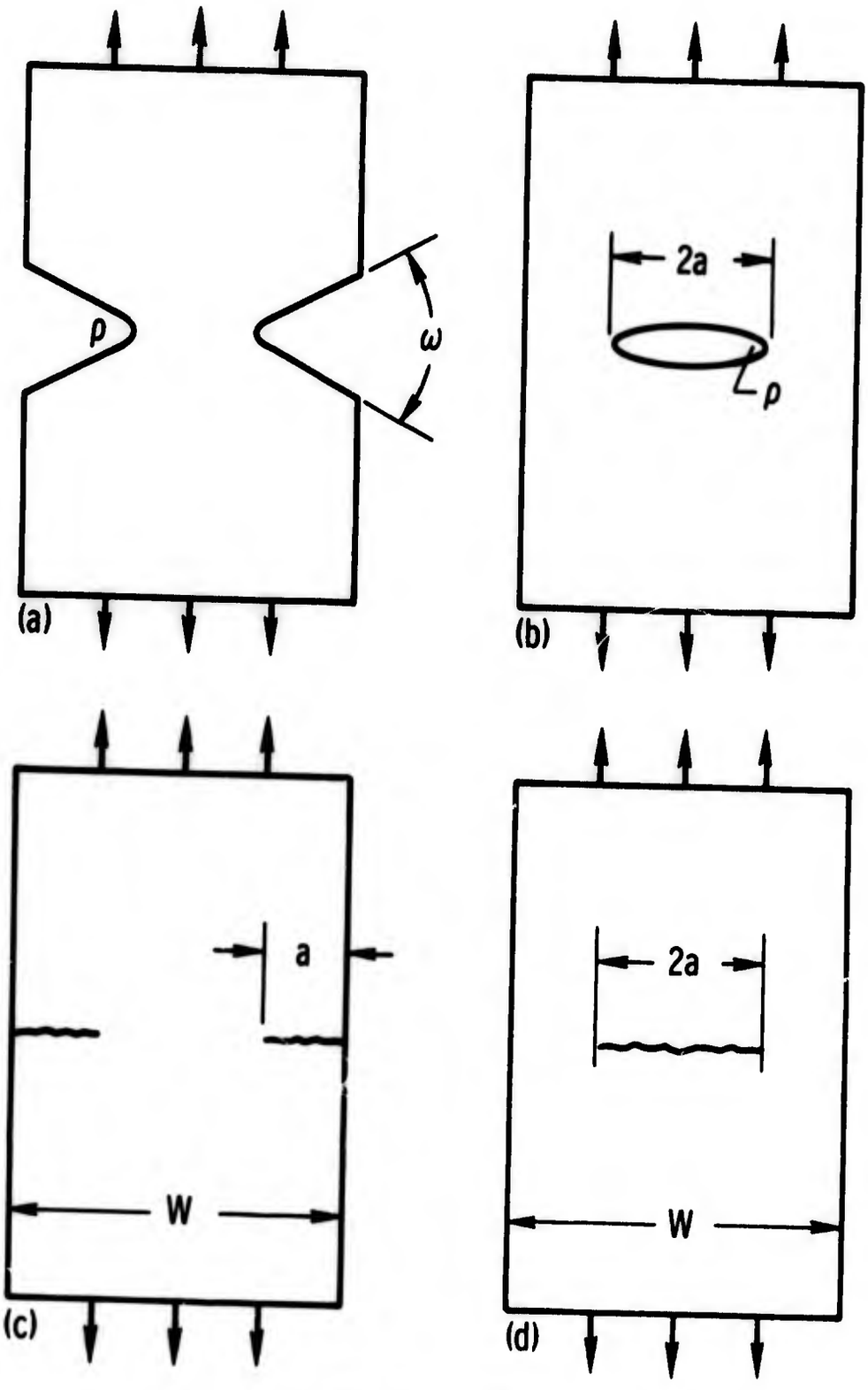

Fig. 3 Specimen configurations

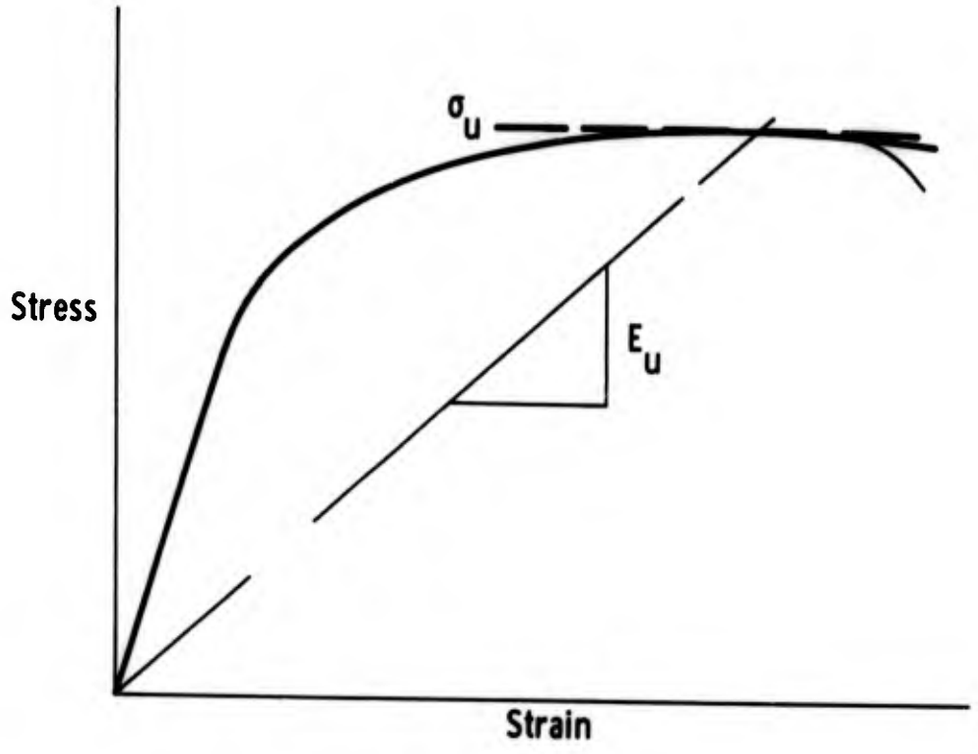

Fig. 4 Definition of E_u

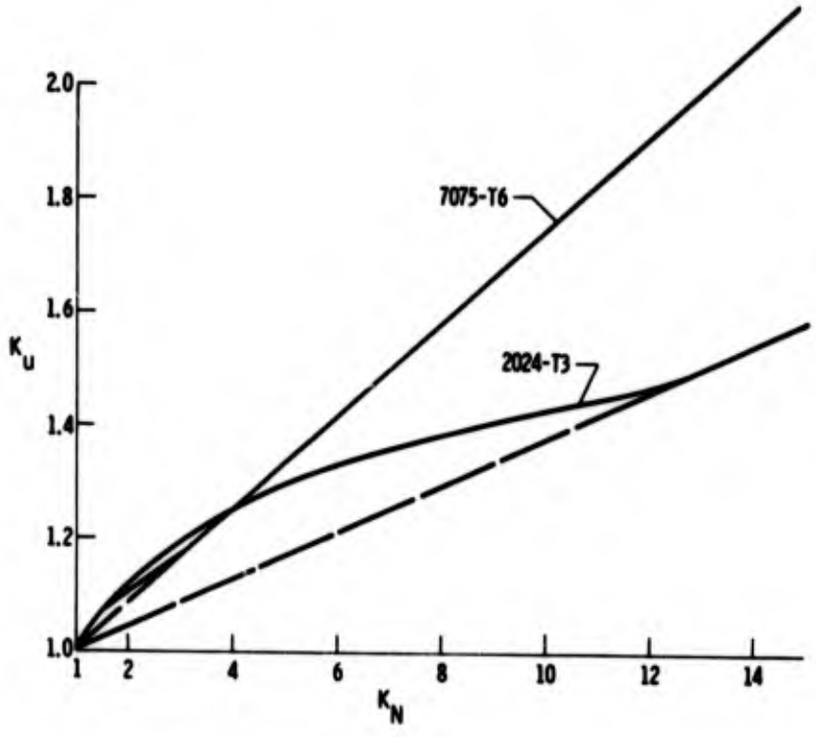

Fig. 5 Correction curves (K_u/K_N) for two aluminum alloys. Based on Equation (7)

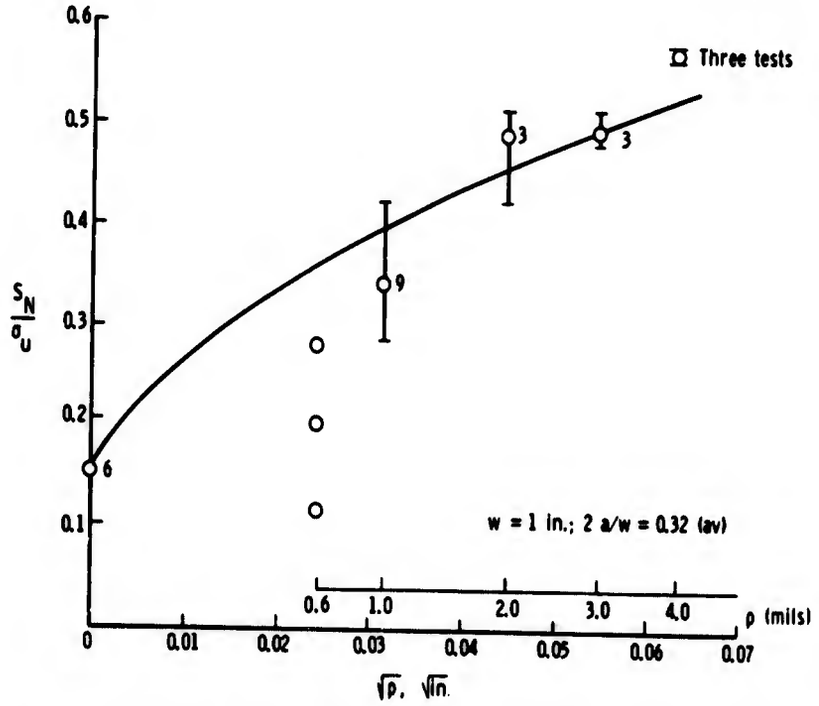

Fig. 6 Failing stresses on H-11 (mod) steel specimens with 60° Vee-notches or edge cracks. Test data from Reference 9(c). Curves calculated with σ_u = 311 ksi; e = 9%; ρ' = 1.61 x 10^{-4} in.

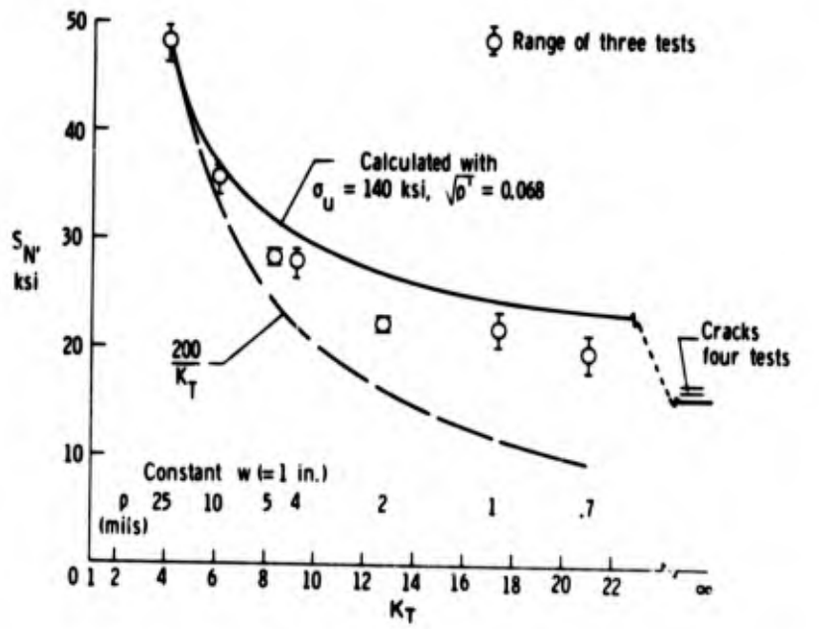

(a) Constant width series

Fig. 7 Failing stresses on Ti 2.5Al-16V specimens (t = 0.09 in.; 60° Vee-notches; 2a/w = 0.30; aged to give full brittle condition). Test data from Reference 11

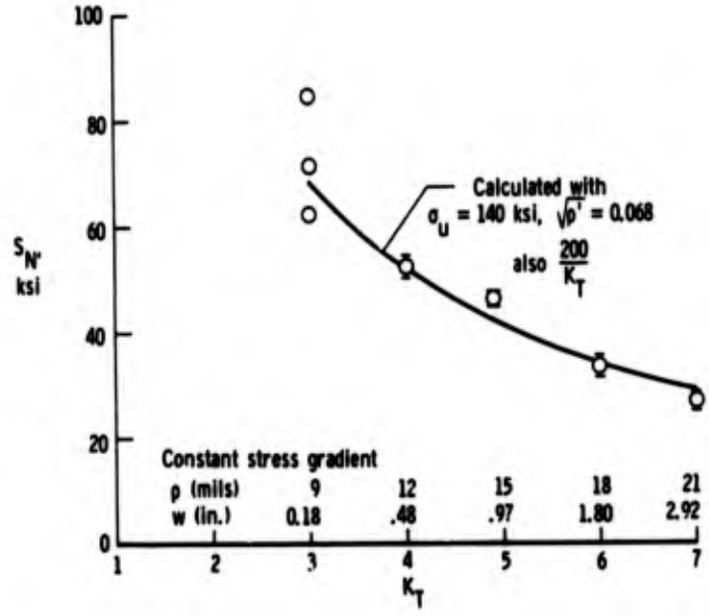

(b) Constant stress gradient series

Fig. 7 Concluded

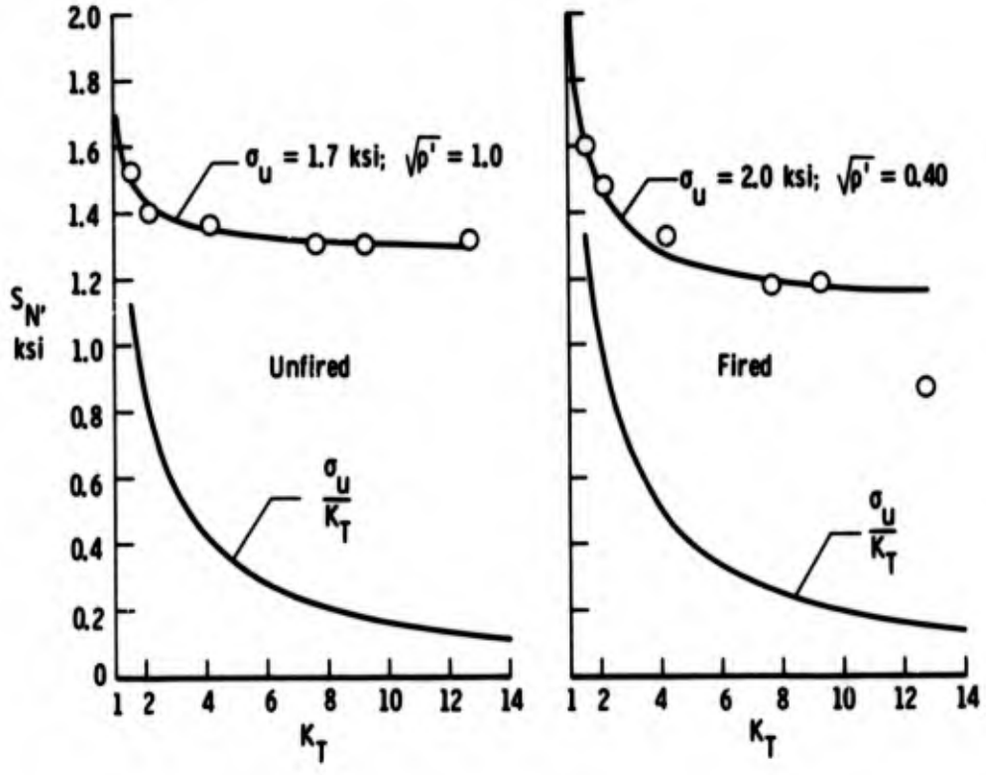

Fig. 8 Failing stresses on Lava Grade A specimens (t = 0.25 in.; w = 0.5 in.; 60° Vee-notches; 2a/w = 0.30). Test data from Reference 11

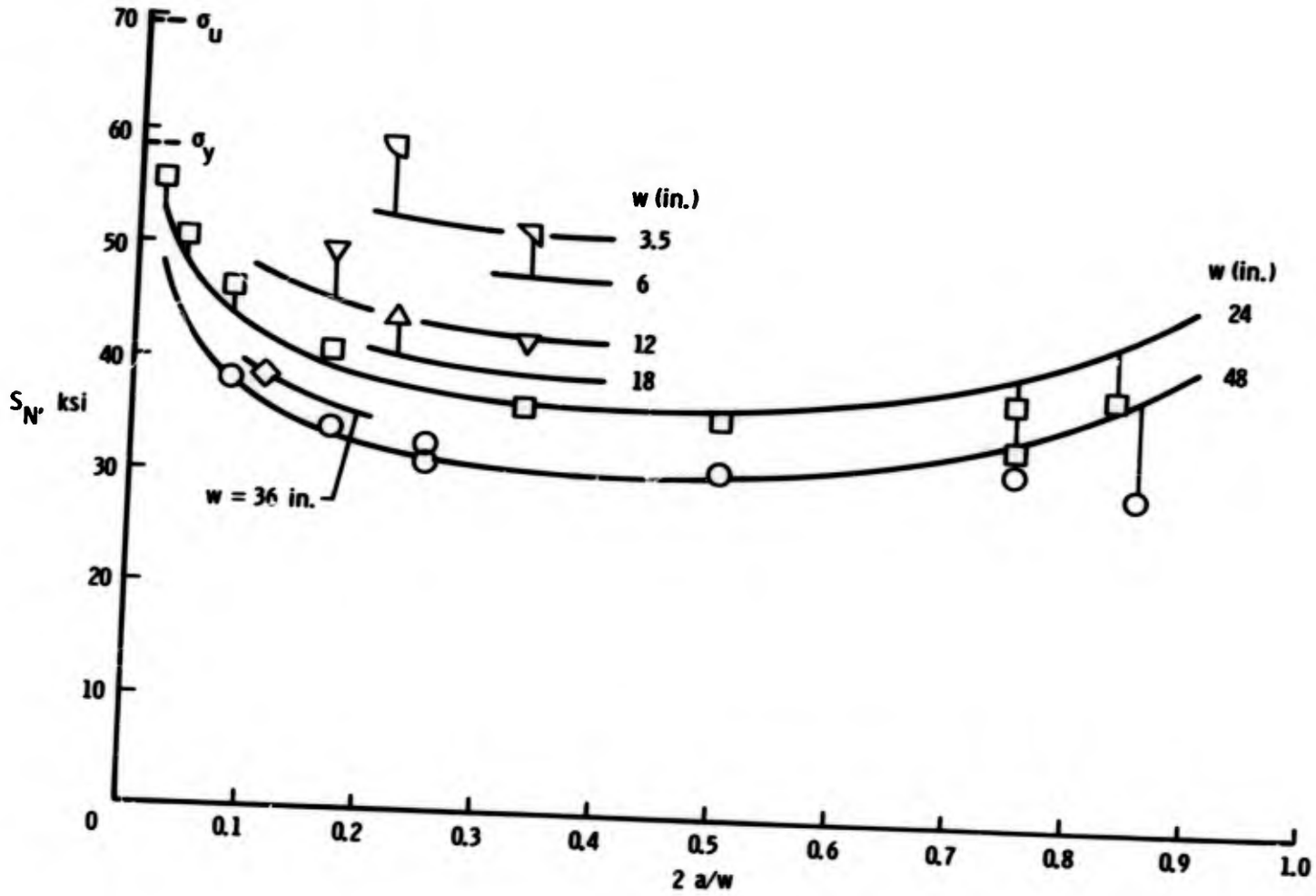

(a) Curves calculated with σ_u = 69.4 ksi; C_m = 0.64 in.$^{-\frac{1}{2}}$

Fig.9 Failing stresses on 2219-T87 aluminum alloy sheet with central cracks. (t = 0.10 in.; guided.) Tests by Boeing Aircraft

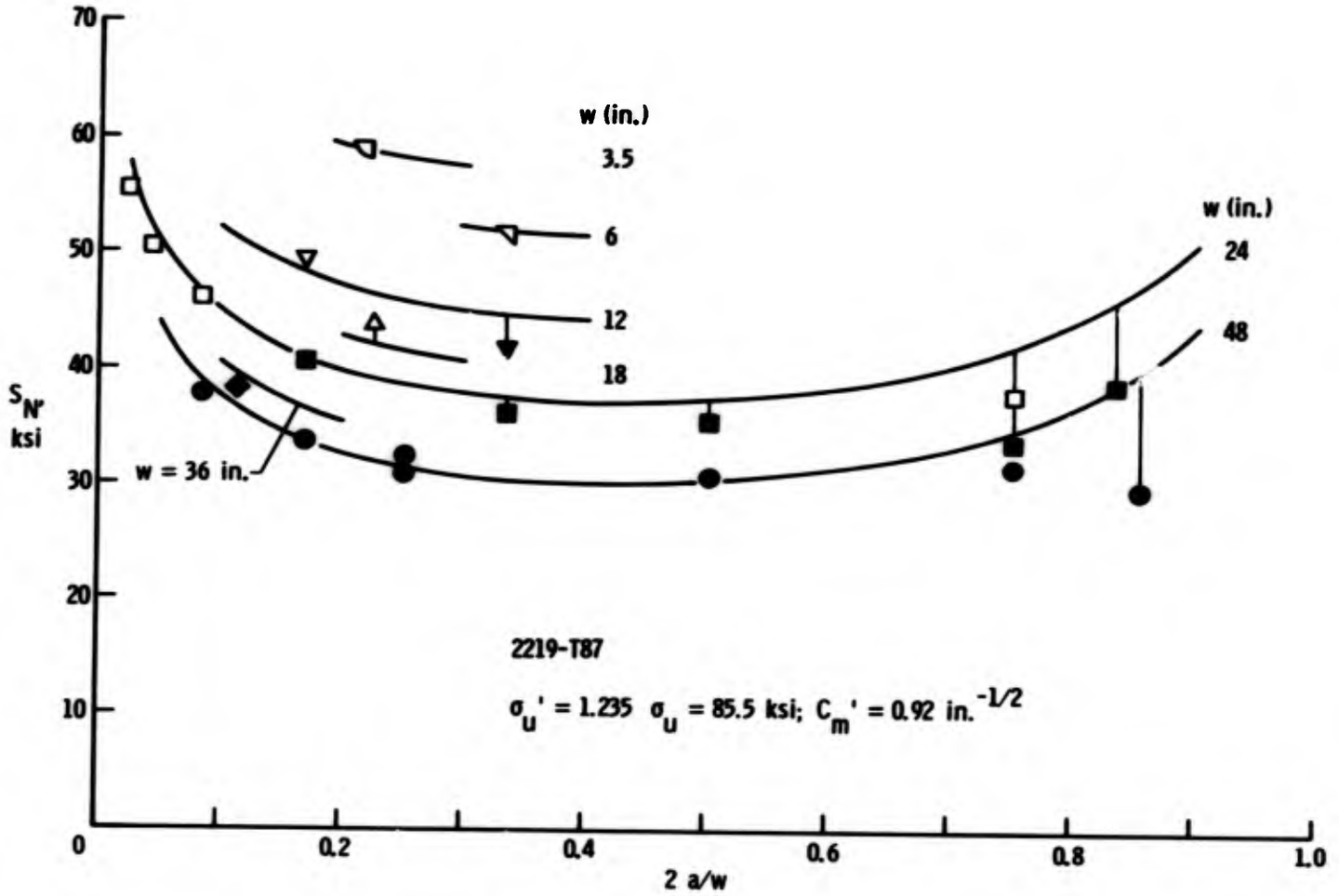

(b) Curves calculated with $\sigma_u' = 1.235$, $\sigma_u = 85.5$ ksi; $C_m' = 0.92$ in.$^{-\frac{1}{2}}$

Fig. 9 Concluded

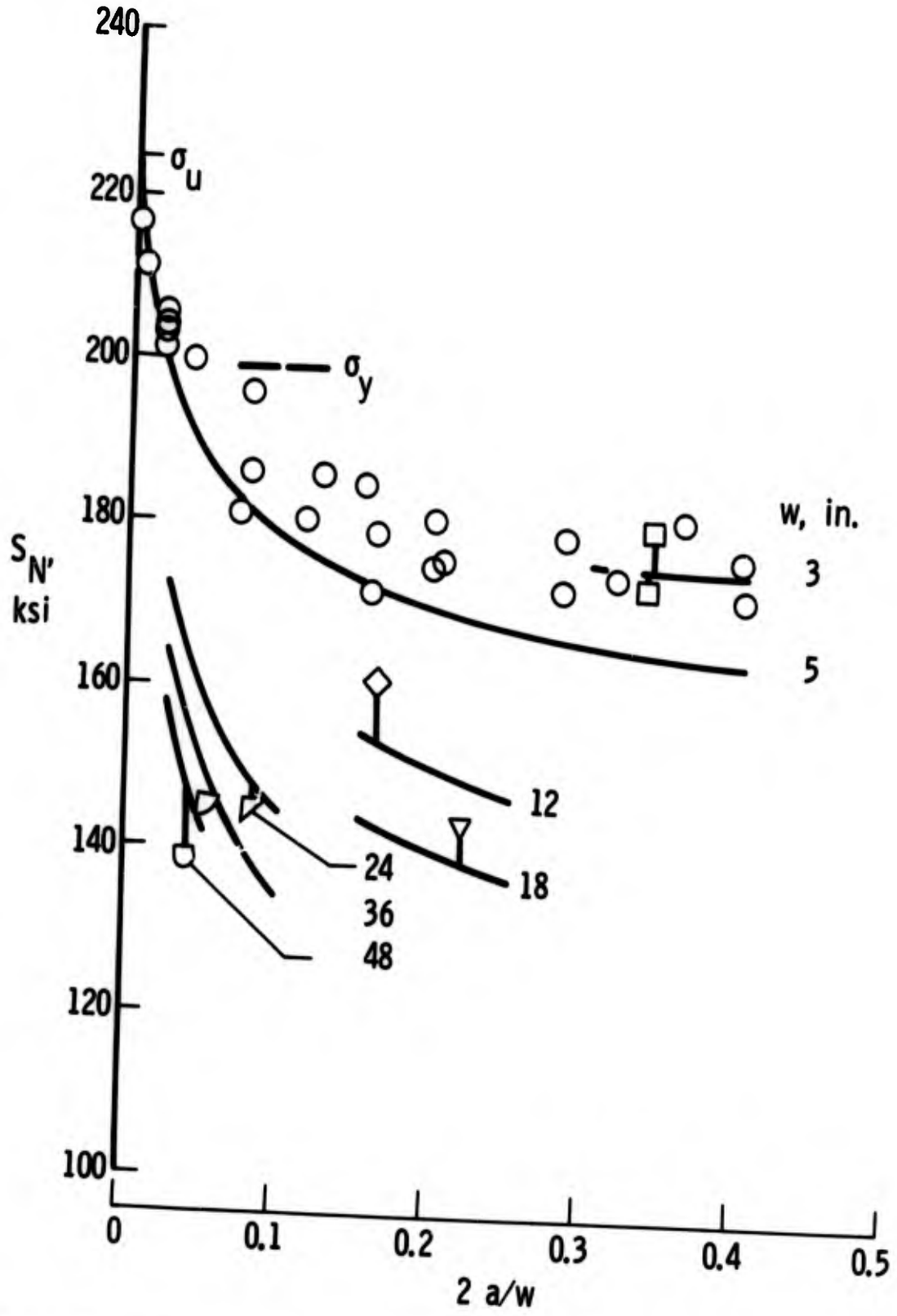

Fig. 10 Failing stresses on 4330M steel specimens with central cracks (t = 0.08 in.). Tests by Boeing Aircraft. Curves calculated with σ_u = 223 ksi; $C_m = 0.55$ in.$^{-\frac{1}{4}}$

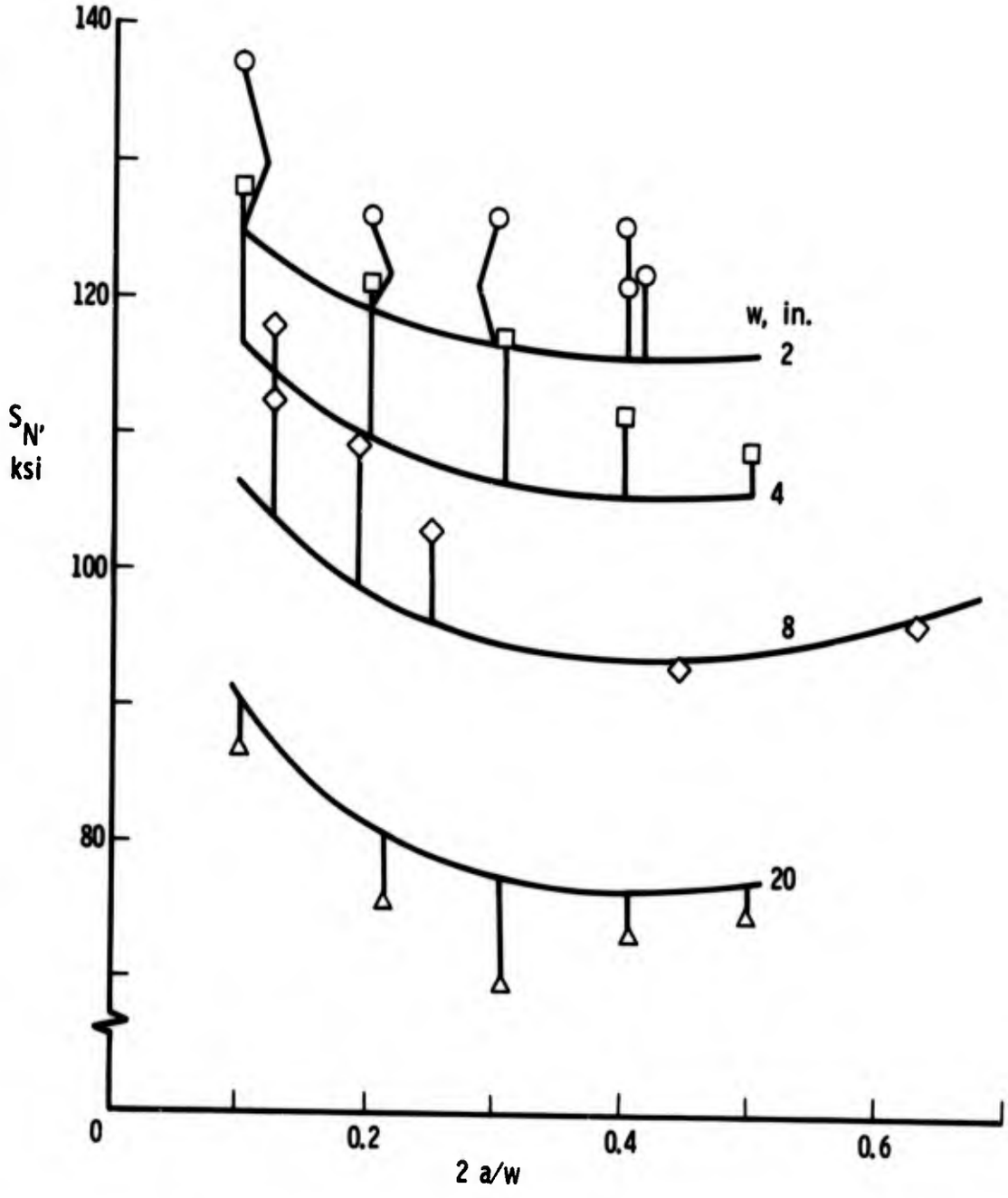

(a) Curves calculated with σ_u = 152 ksi; C_m = 0.75 in.$^{-\frac{1}{2}}$

Fig. 11 Failing stresses on Ti 8Al-1Mo-1V sheet with central cracks (duplex annealed; t = 0.050 in.; guides used). Test data from Reference 7 and unpublished data

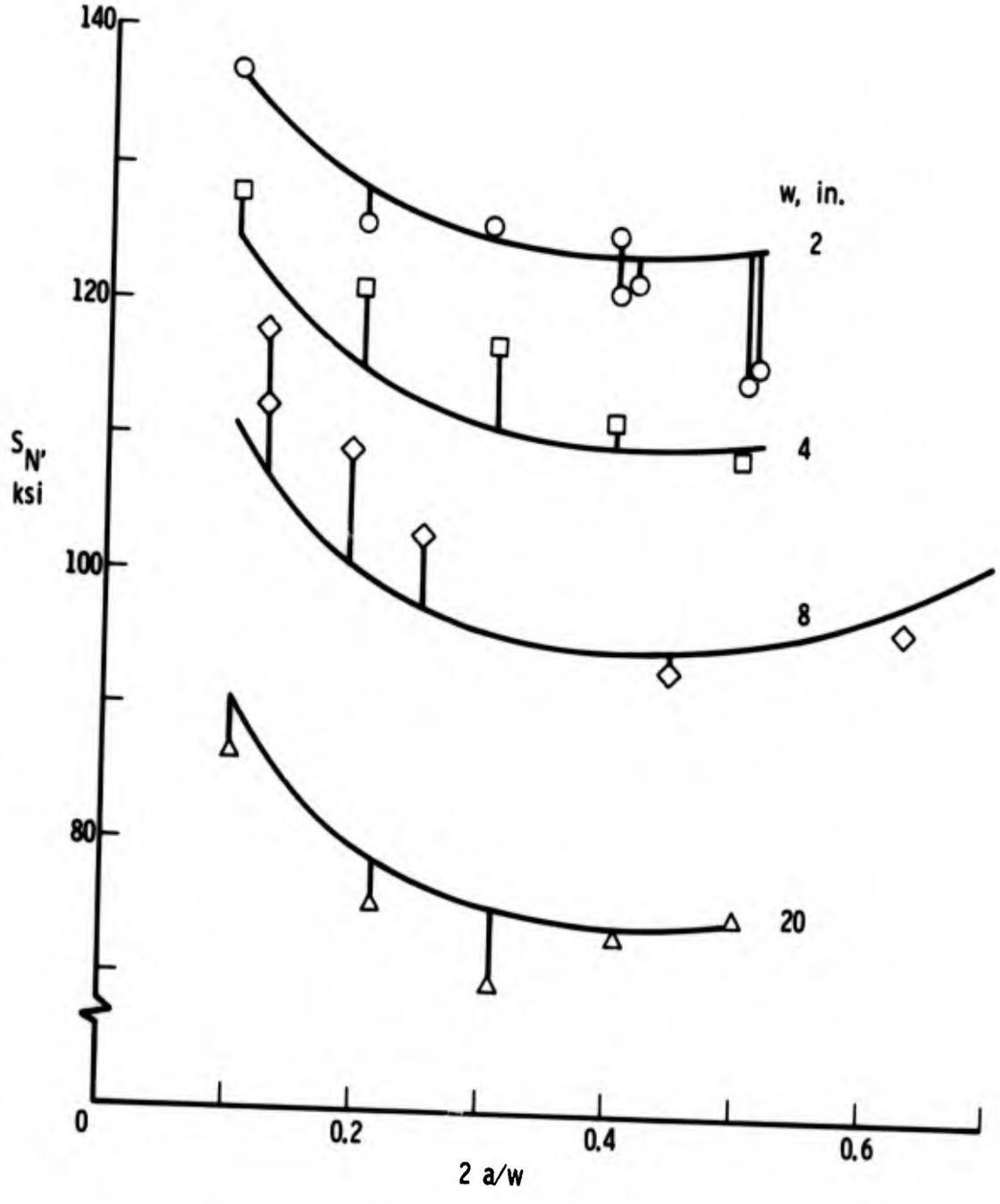

(b) Curves calculated with $\sigma_u' = 1.185$, $\sigma_u = 180$ ksi; $C_m' = 1.10$ in.$^{-\frac{1}{2}}$

Fig. 11 Concluded

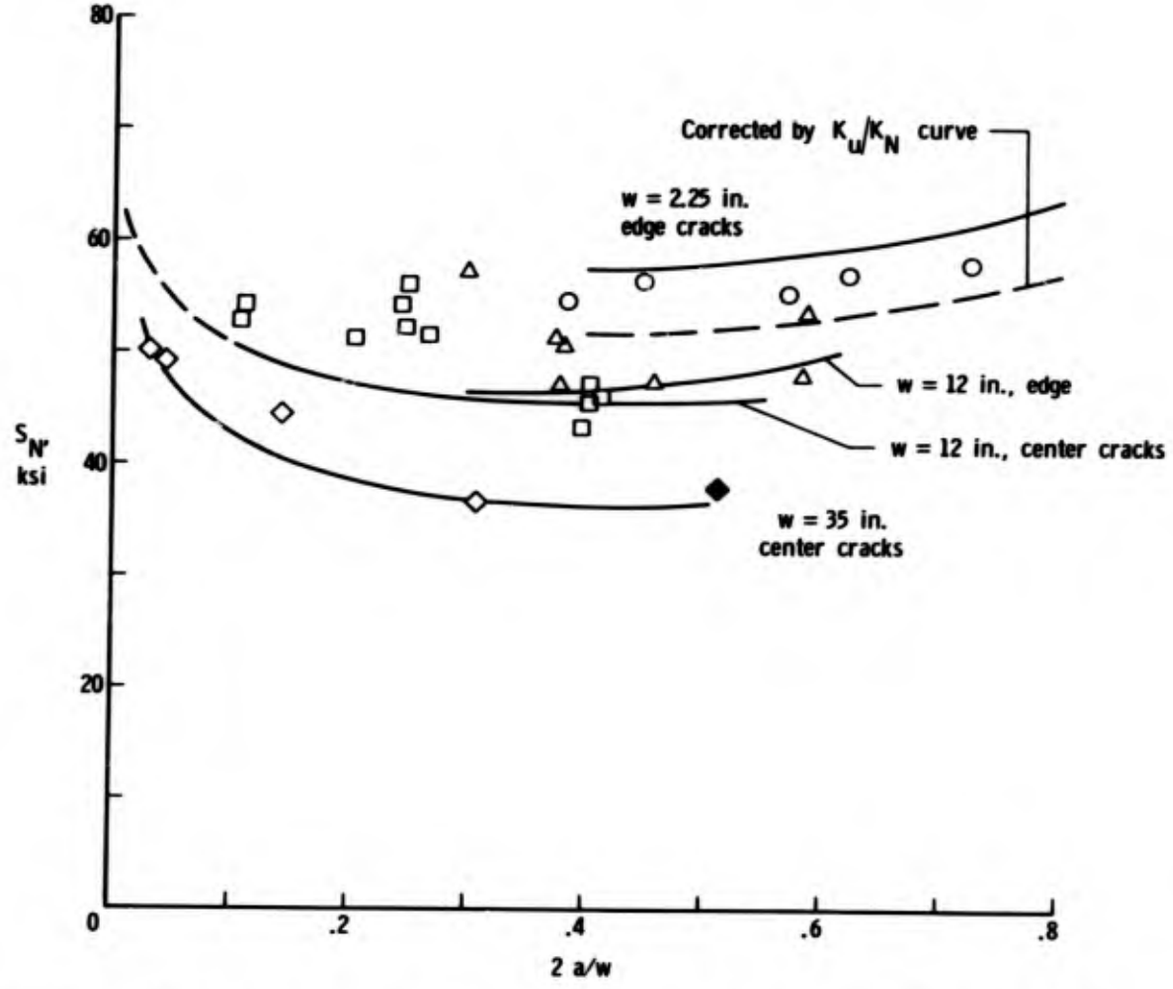

Fig. 12 Failing stresses on 2024-T3 aluminum alloy sheet with central or edge cracks (t = 0.08 to 0.10 in.; solid point guided, others corrected to guided condition by formula (16)). Test data from Reference 12. Curves calculated with σ_u = 70 ksi; C_m = 0.54 in.$^{-\frac{1}{2}}$

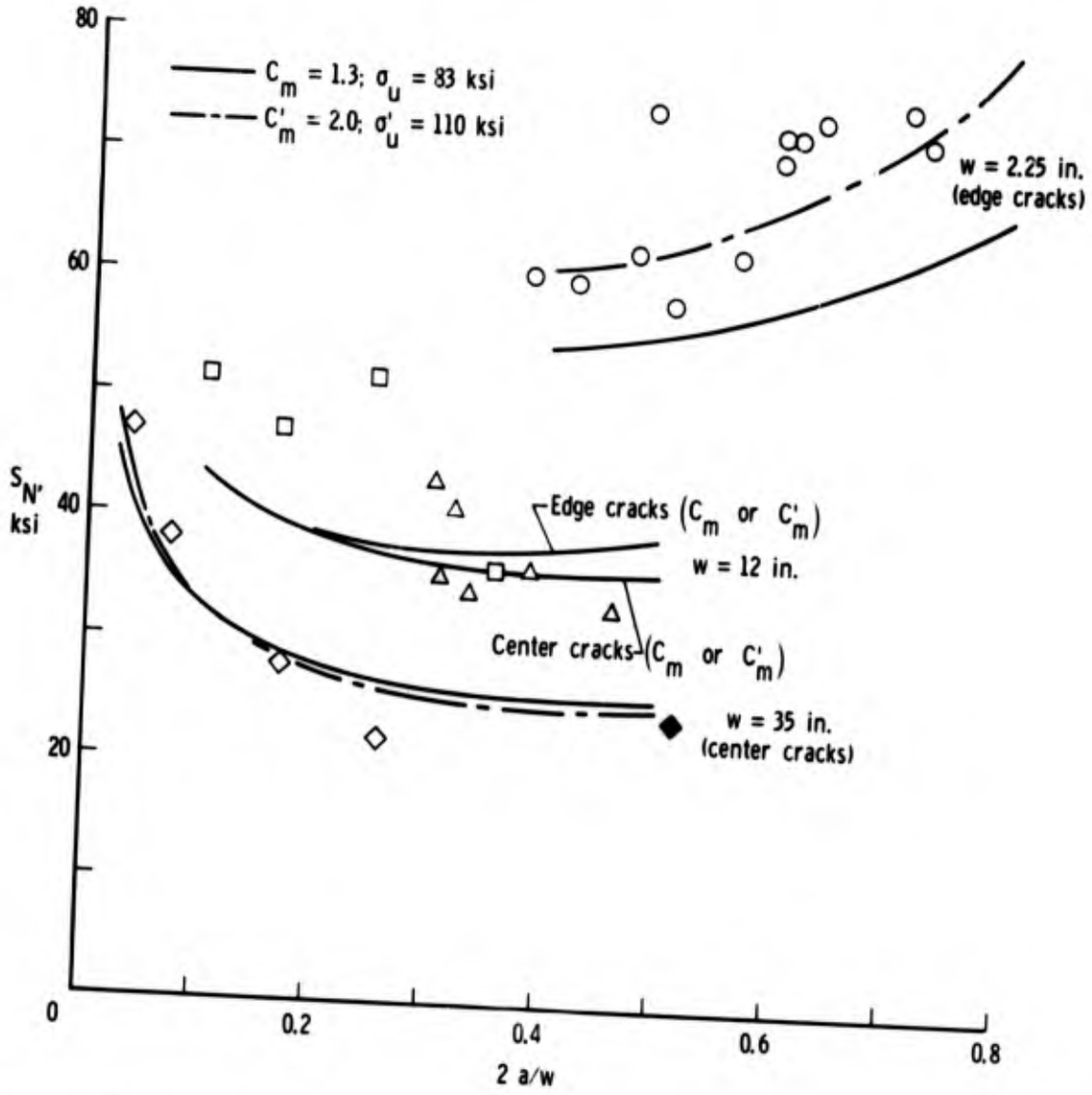

Fig. 13 Failing stresses on 7075-T6 aluminum alloy sheet with central or edge cracks (t = 0.08 to 0.10 in.; solid point guided, others corrected to guided condition by formula (16)). Test data from Reference 12

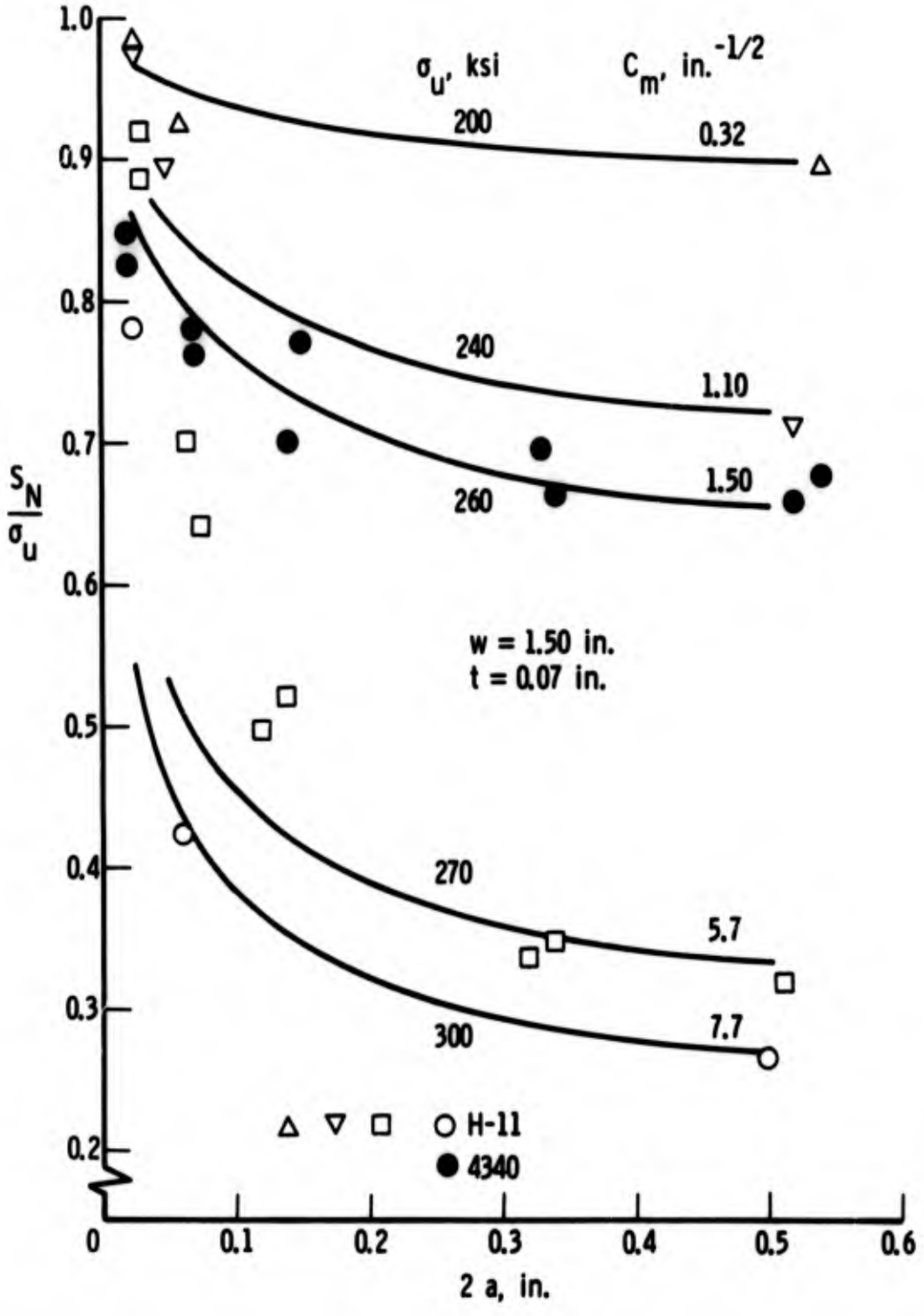

Fig. 14 Effect of short cracks on high-strength steel specimens with center fatigue cracks. Test data from Reference 13

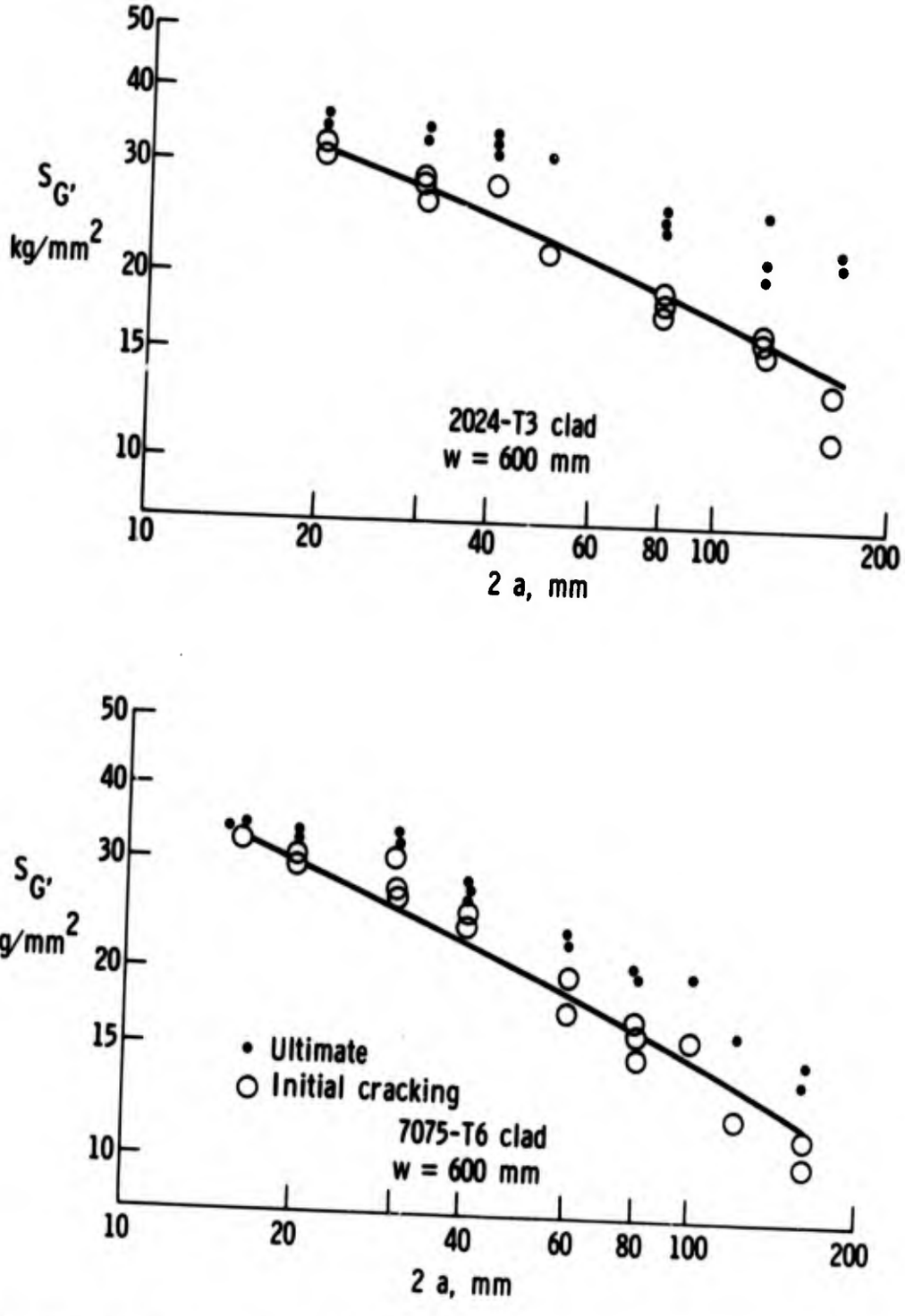

Fig. 15 Application of CSA formulas to correlation of initial cracking. Test data from Reference 14

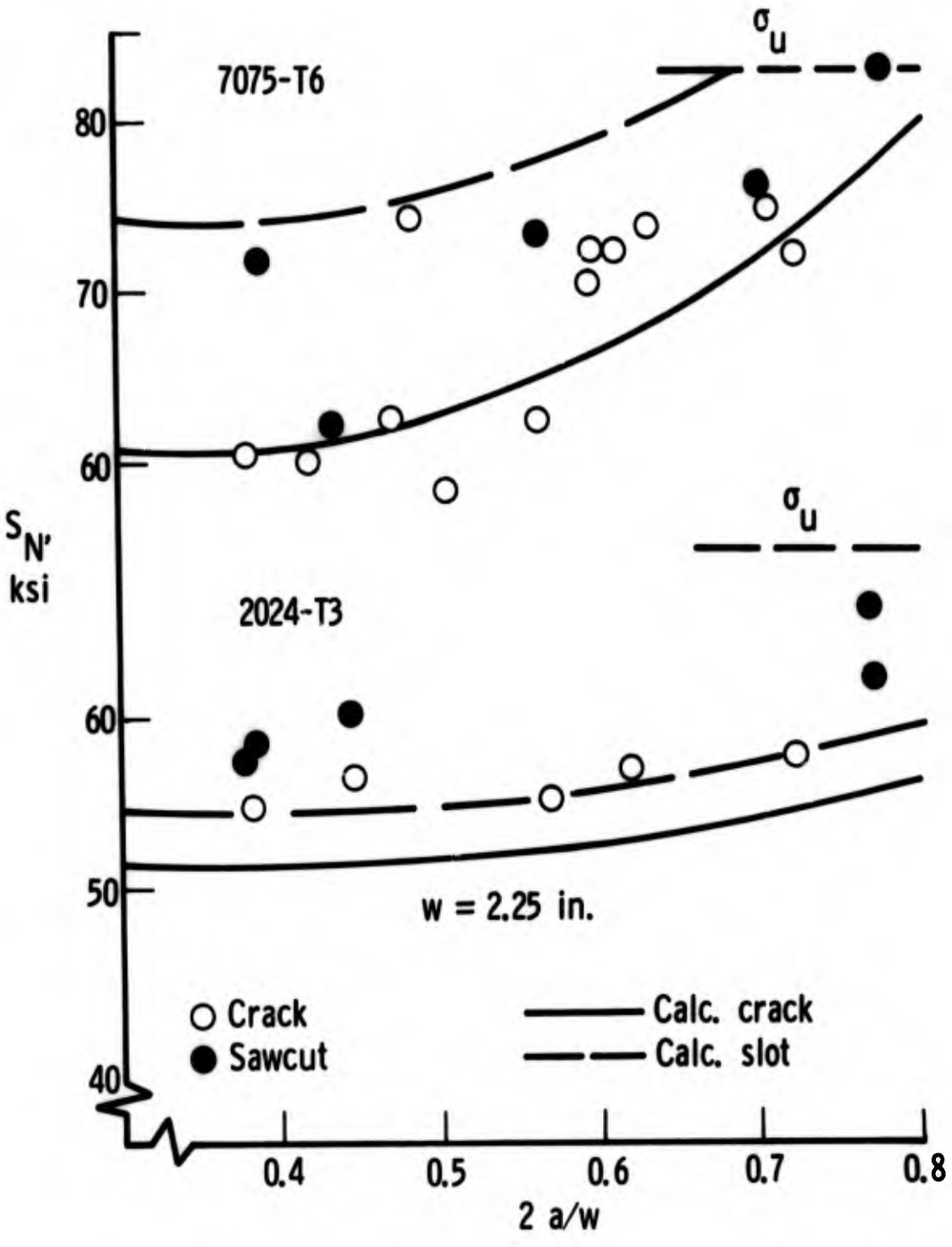

Fig. 16 Comparison between cracks and saw cuts for two aluminum alloys. (Saw cuts 0.009 in. wide)

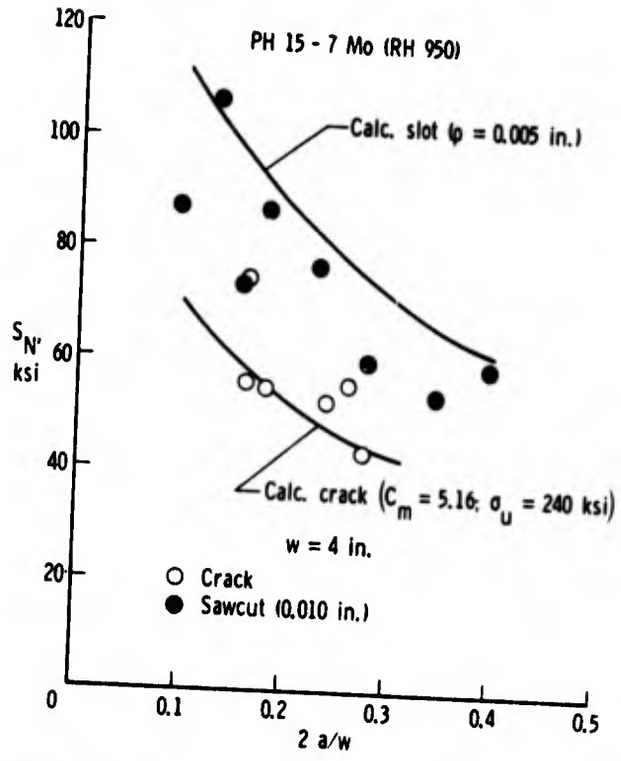

Fig. 17 Comparison between cracks and saw cuts for a steel. Test data from Reference 13

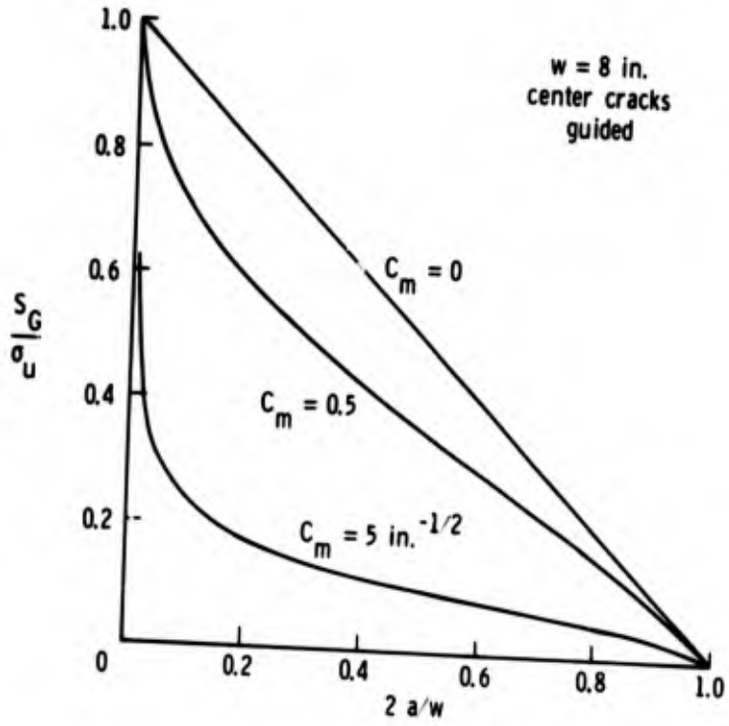

Fig. 18 Plot of S_0/σ_u versus $2a/w$ for comparing crack strengths of different materials

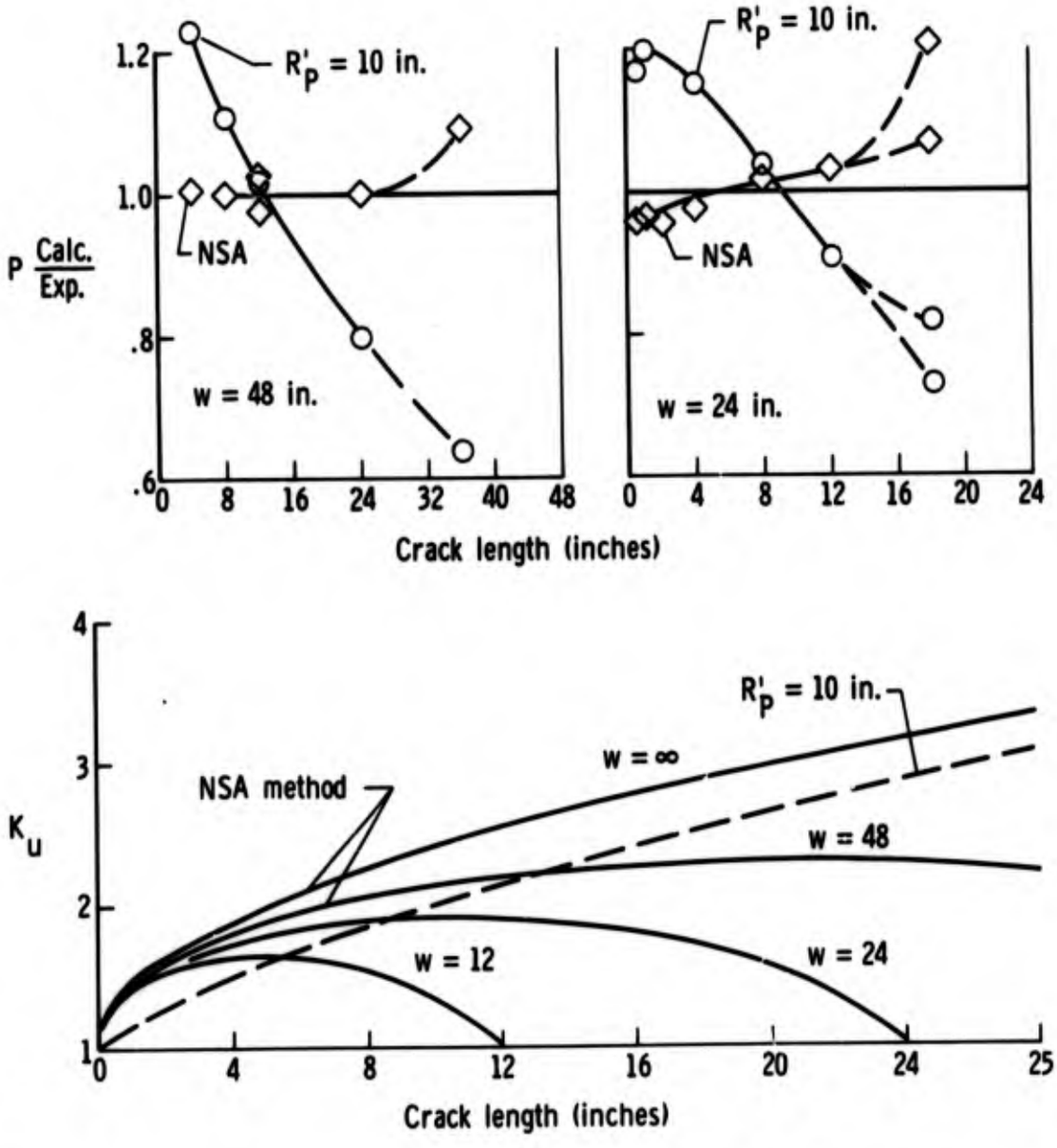

Fig. 19 Application of Denke-Christensen formula for crack strength to 2219-T87 sheet (t = 0.1 in.; guides used)

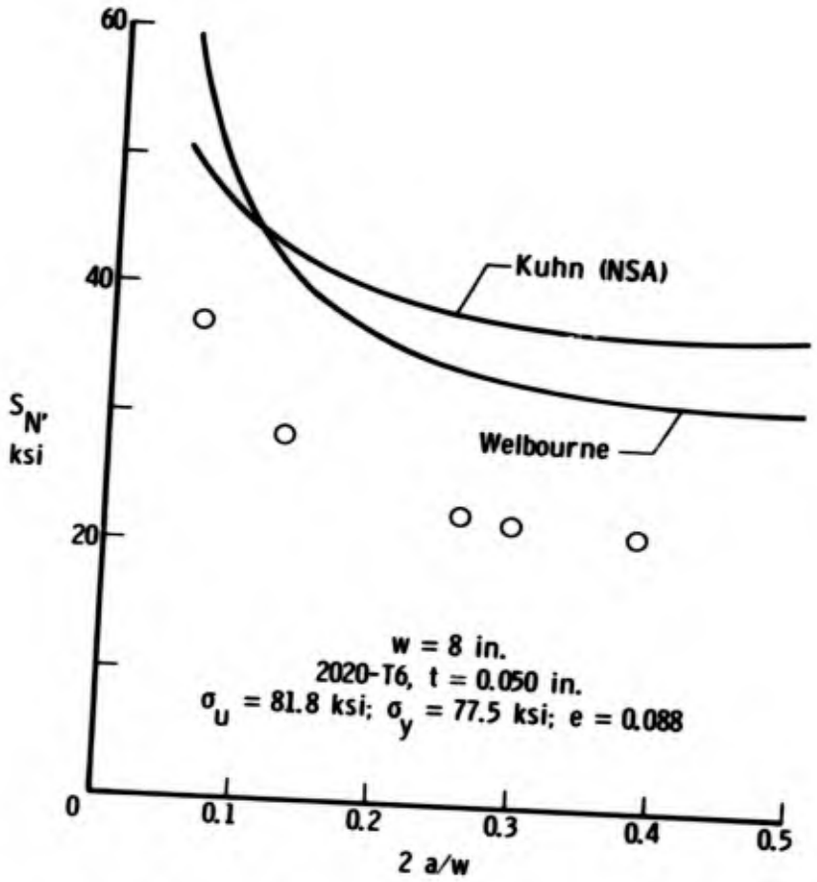

Fig. 20 Comparison between tests for 2020-T6 sheet and predictions by two methods. Test data from Reference 7; guides used

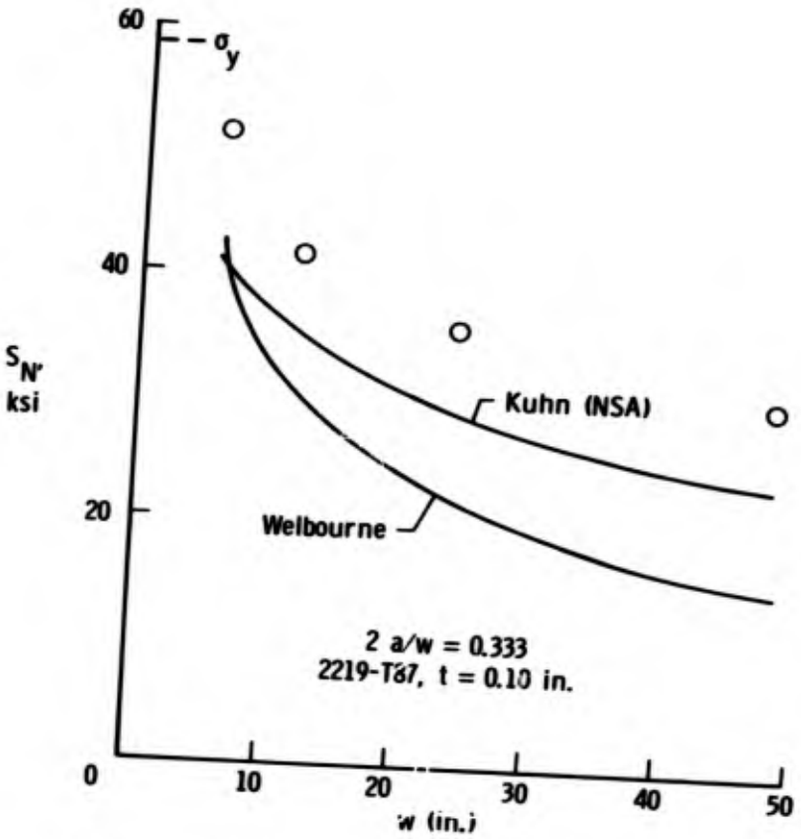

Fig. 21 Comparison between tests on 2219-T87 sheet and predictions by two methods. Guides used

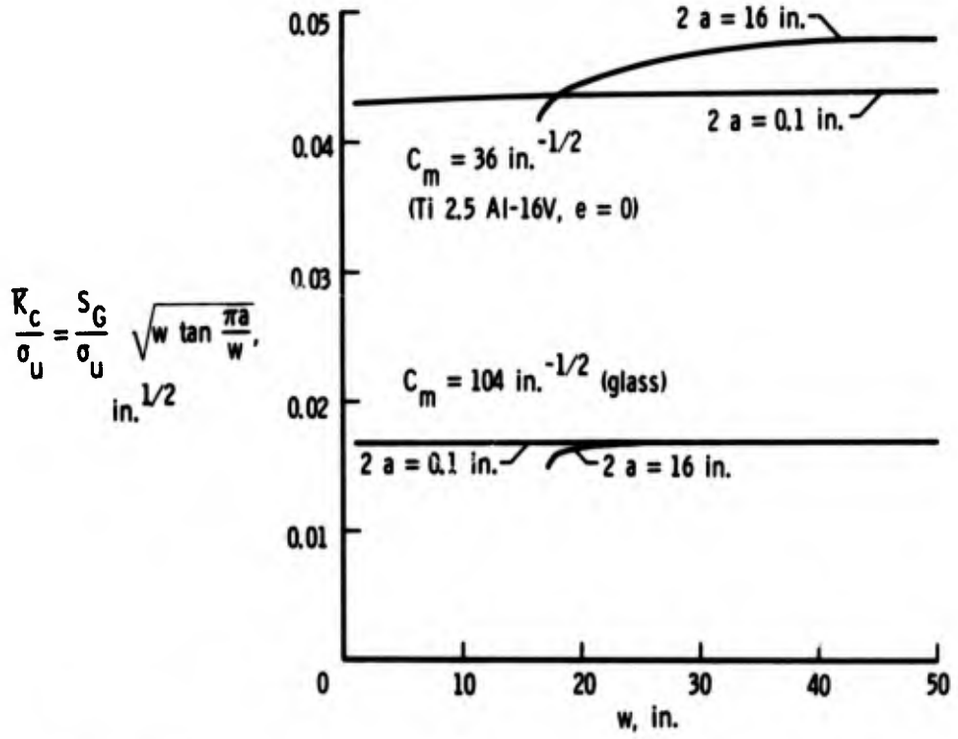

Fig. 22 Normalized notch-toughness $\bar{K}_c/\sigma_u$ for materials of high crack sensitivity

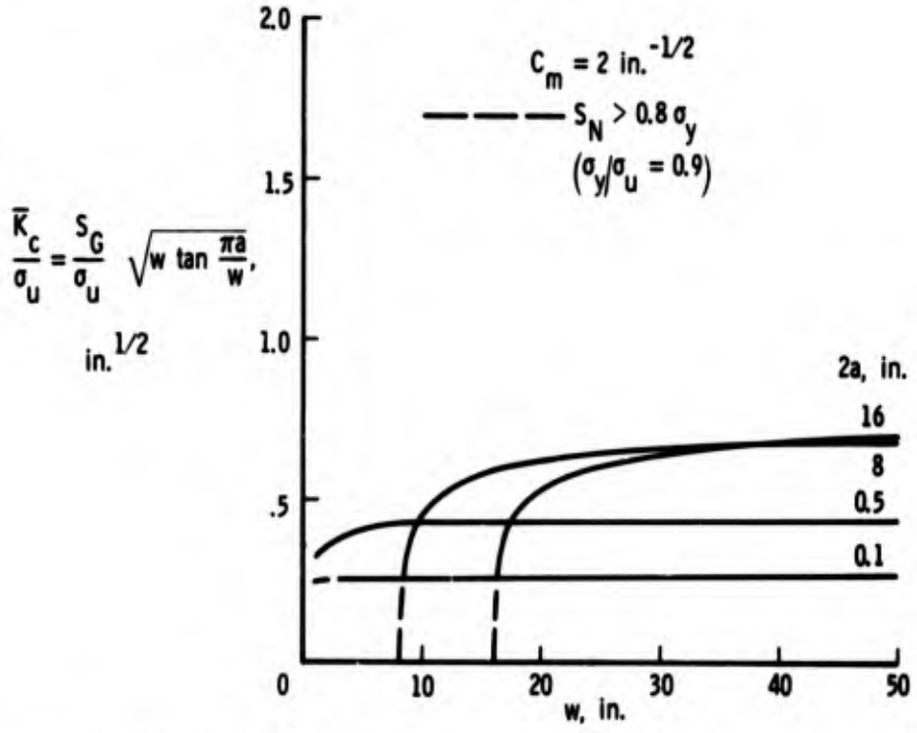

Fig. 23 Normalized notch-toughness $\bar{K}_c/\sigma_u$ for material of moderate crack sensitivity

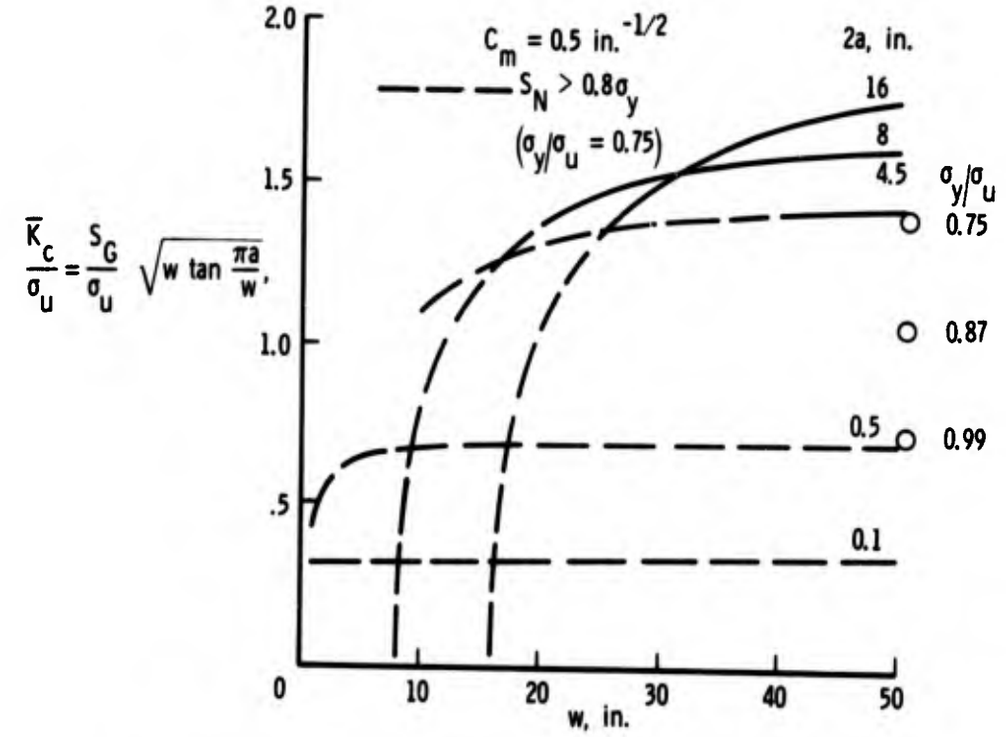

Fig. 24 Normalized notch-toughness $\bar{K}_c/\sigma_u$ for material of low crack sensitivity

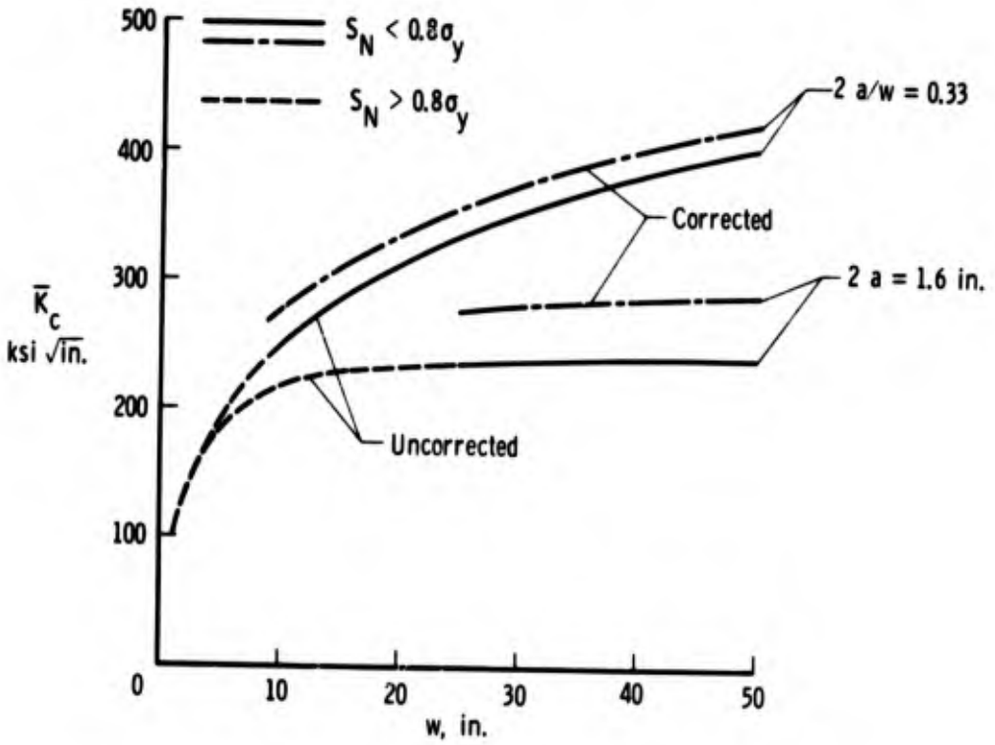

Fig. 25 Notch toughness K_c for 4330M steel without and with plastic-zone correction

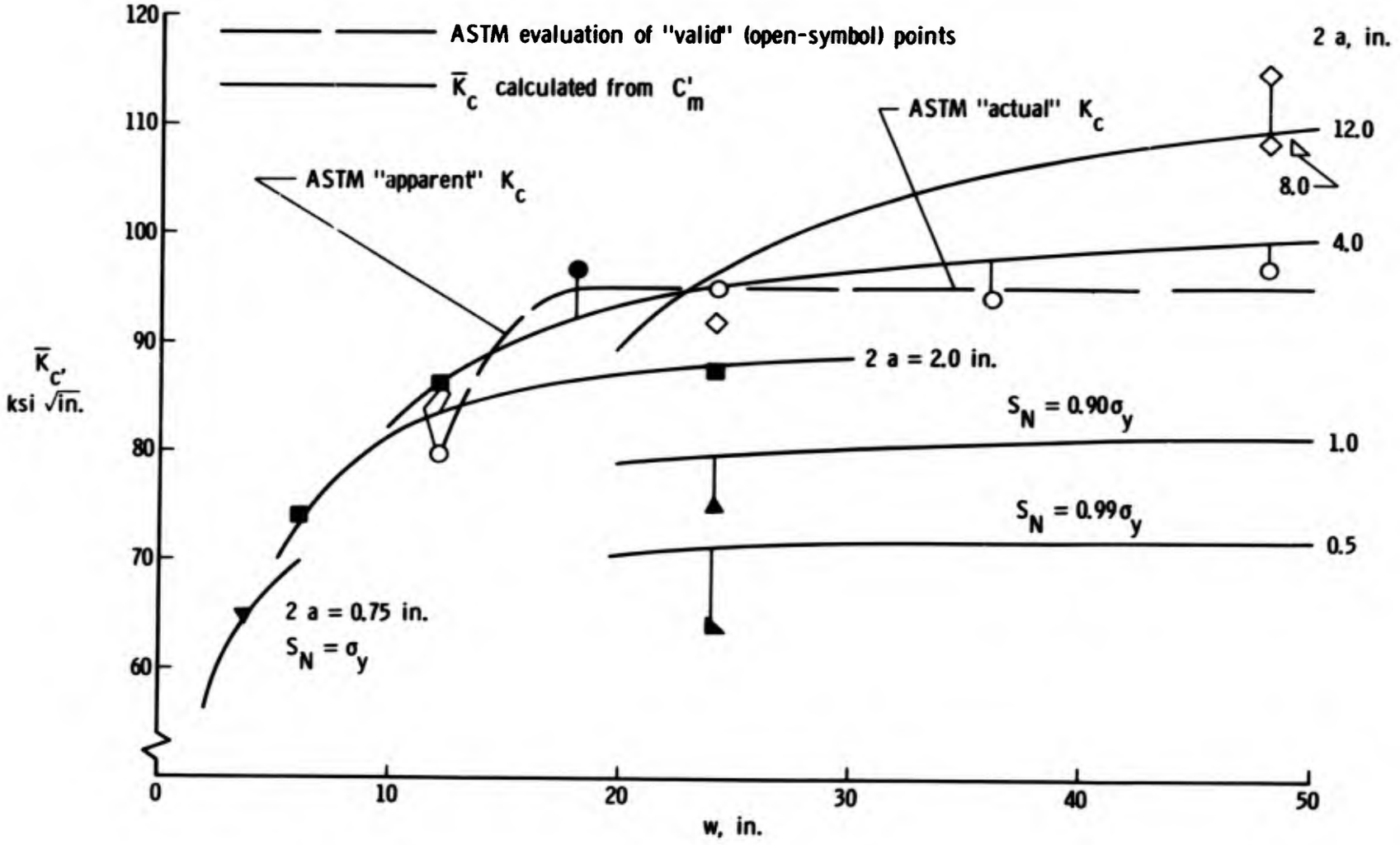

Fig. 26 Notch toughness $\bar{K}_c$ for 2219-T87 sheet as postulated by Fracture Mechanics

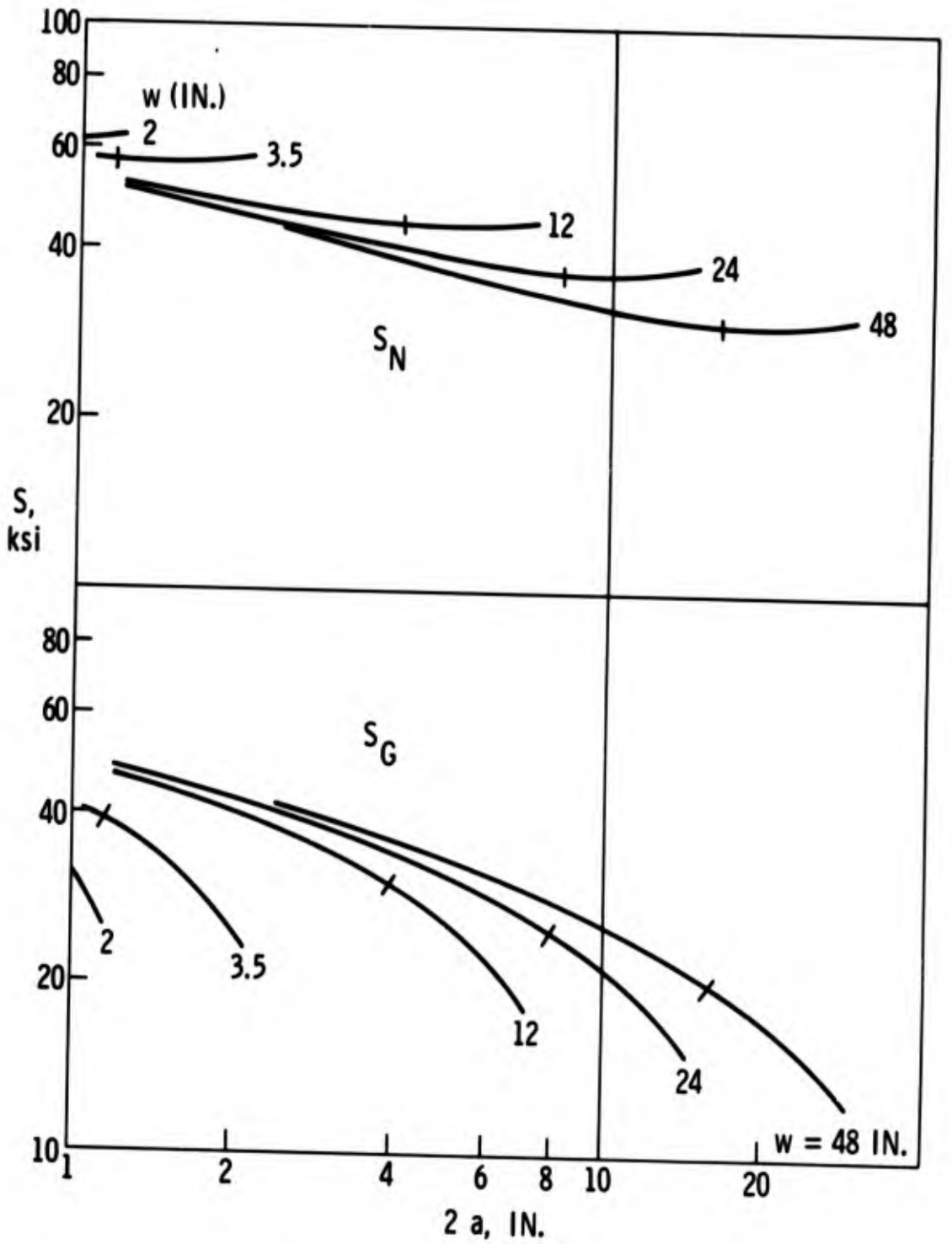

Fig. 27 Log-log plots for 2219-T87 sheet, using computed strengths from Figure 9(b)

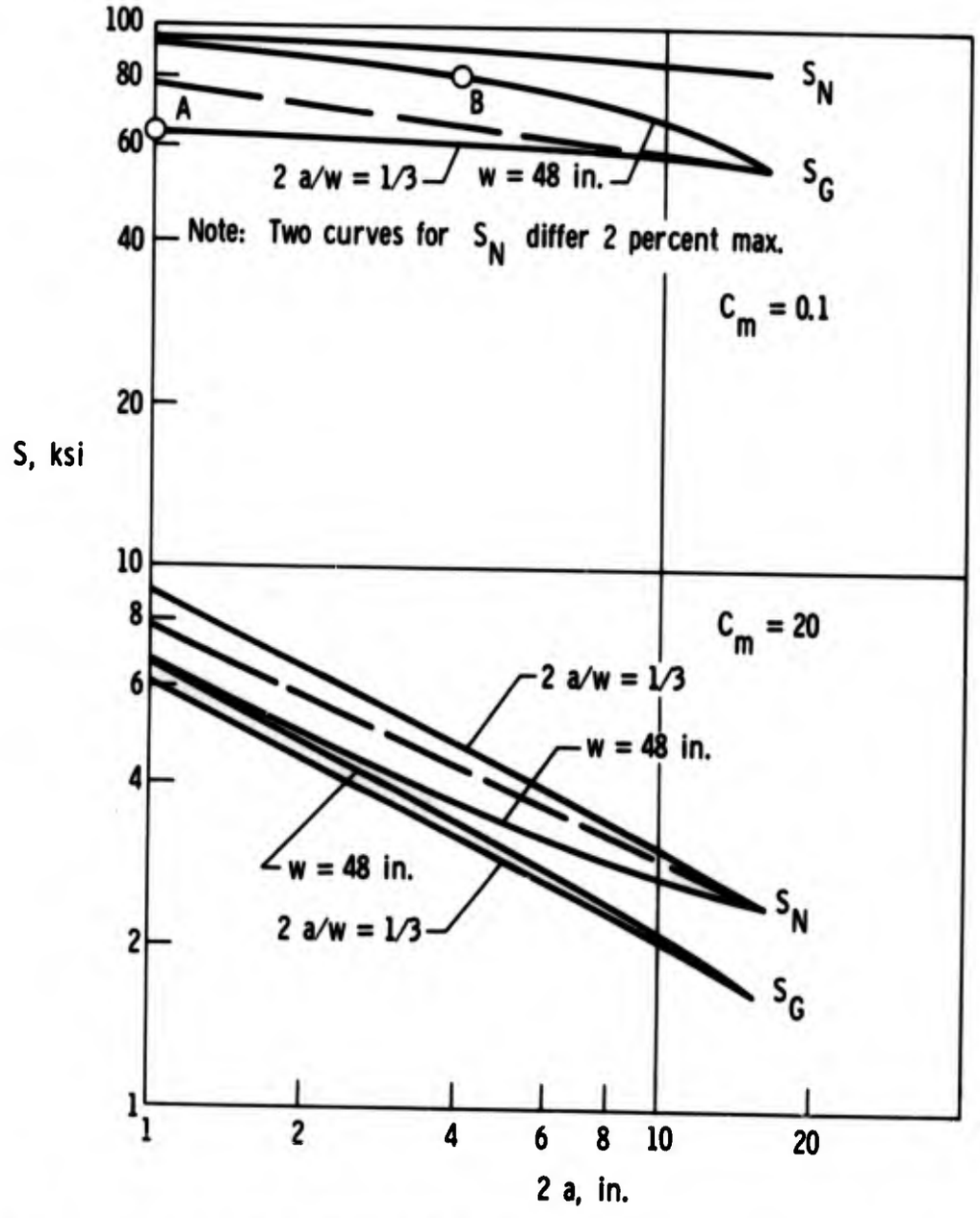

Fig. 28 Log-log plots for materials of very low and very high crack sensitivity

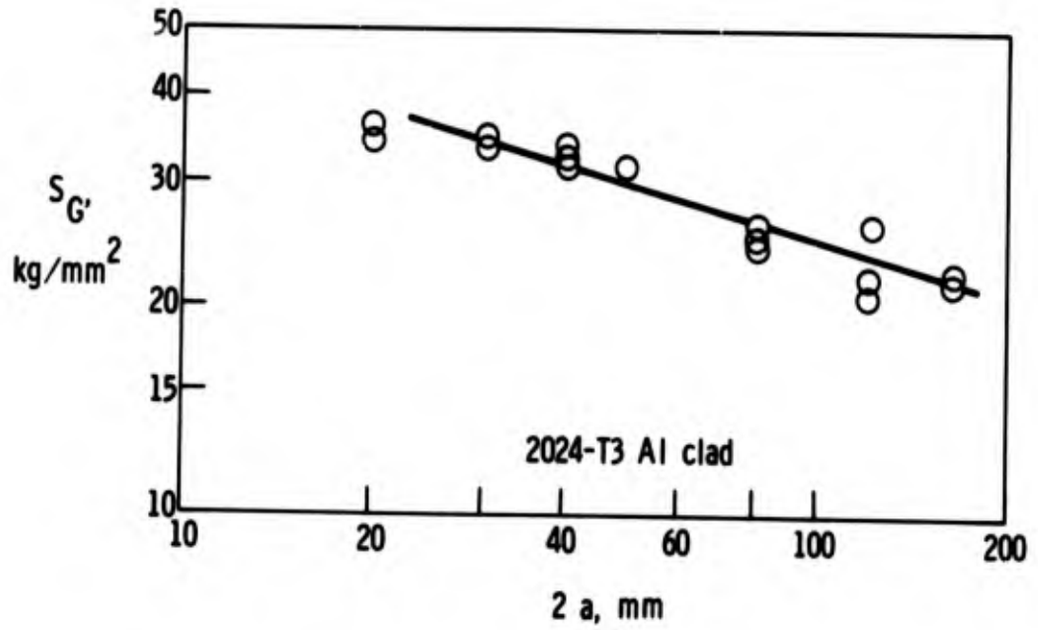

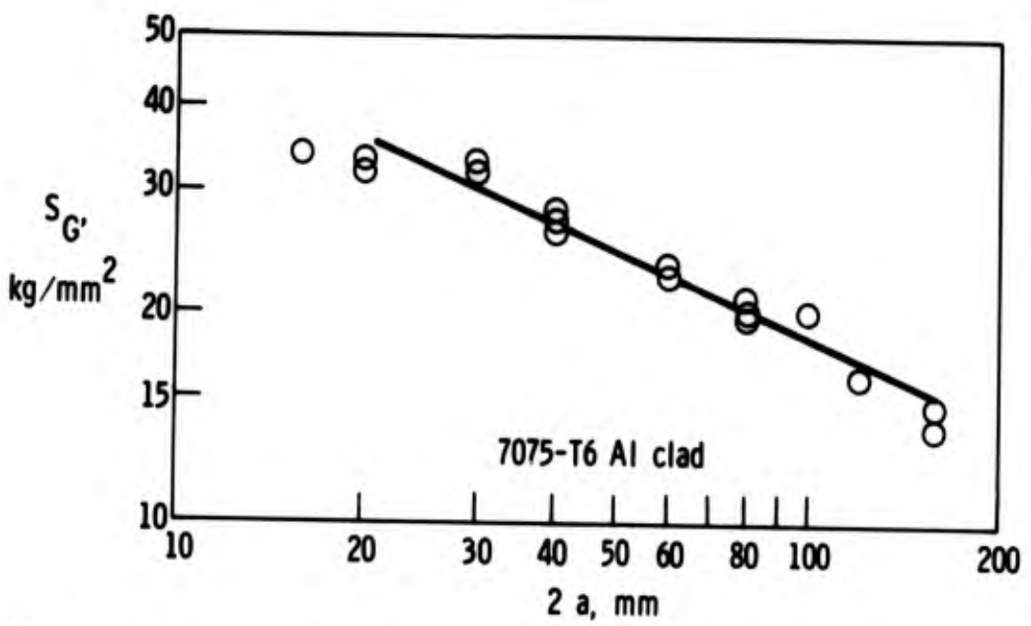

Fig. 29 Log-log plots for two aluminum alloys as given by Broek[26]

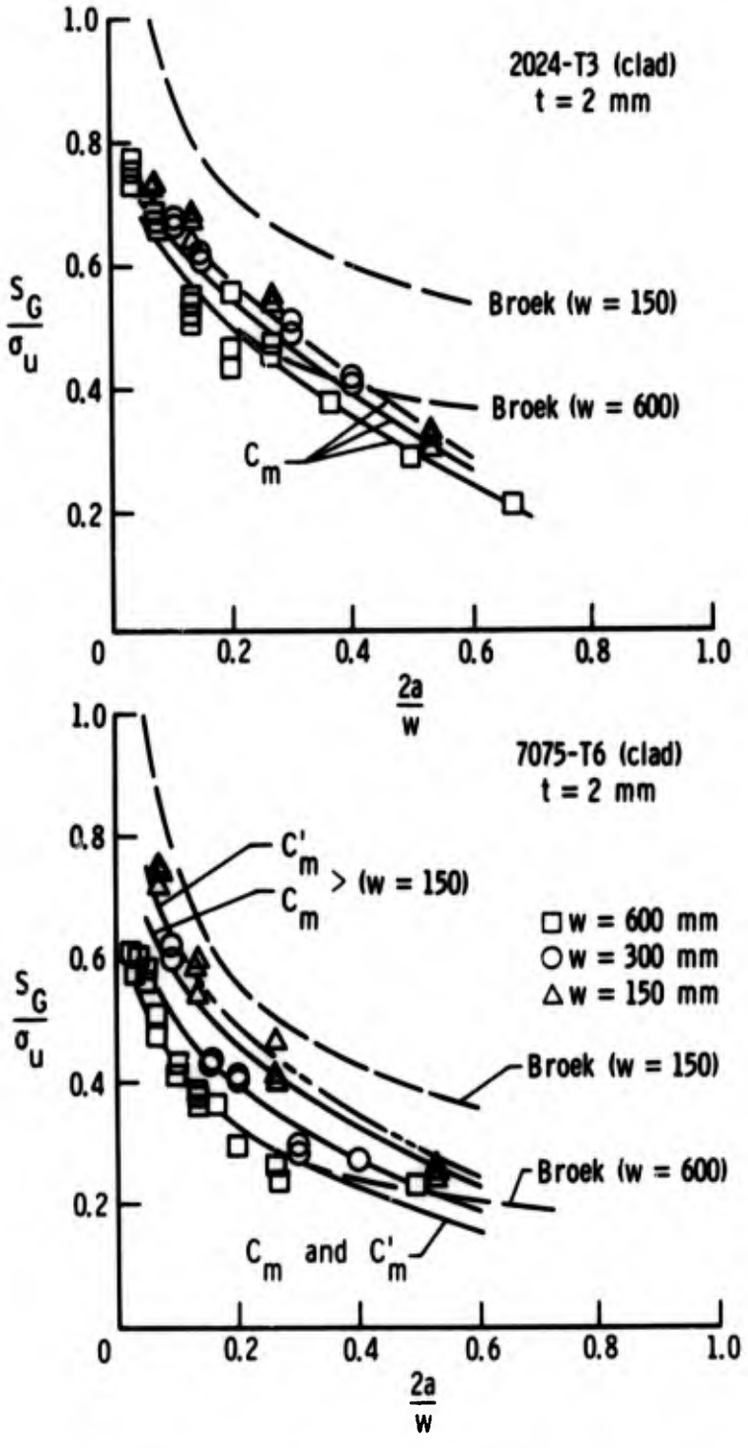

Fig. 30 Test data by Broek[26] for comparison with predictions by Broek log-log plot (Fig. 29) and predictions by CSA method. For 2024-T3 Clad: σ_u = 48 kg/mm^2; C_m = 0.096 mm$^{-\frac{1}{2}}$; K_u/K_n correction based on Figure 5. For 7075-T6 Clad: σ_u = 53.4 kg/mm^2; C_m = 0.233 mm$^{-\frac{1}{2}}$; C'_m = 0.358 mm$^{-\frac{1}{2}}$; $\sigma'_u = 1.32\,\sigma_u$

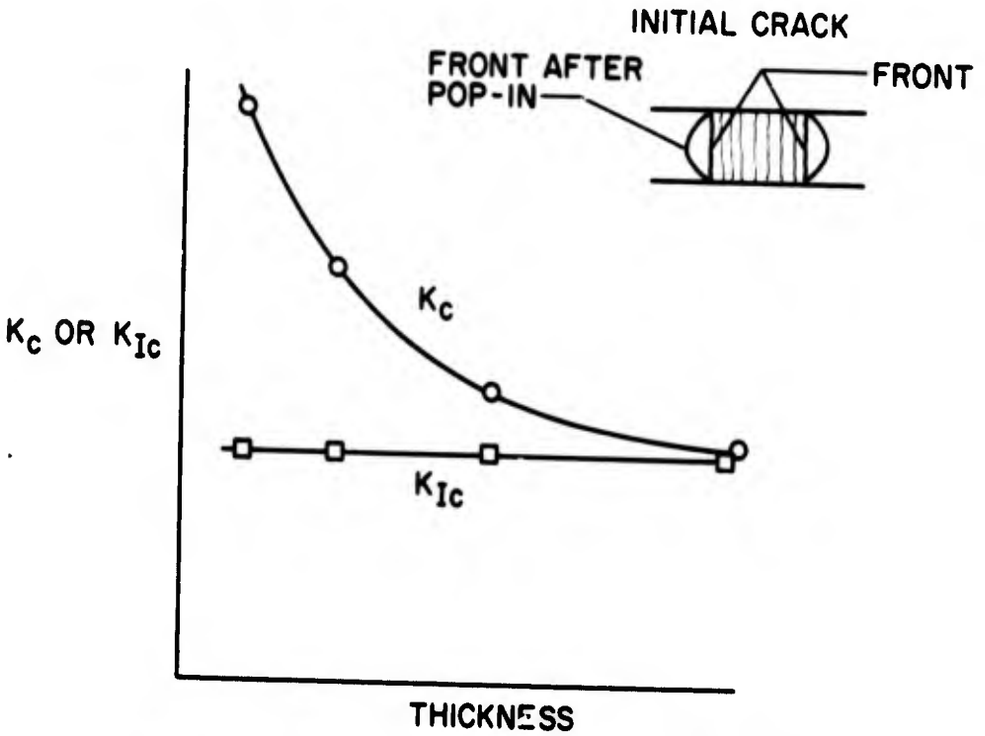

Fig. 31 Relation between K_c and K_{Ic} (schematic)

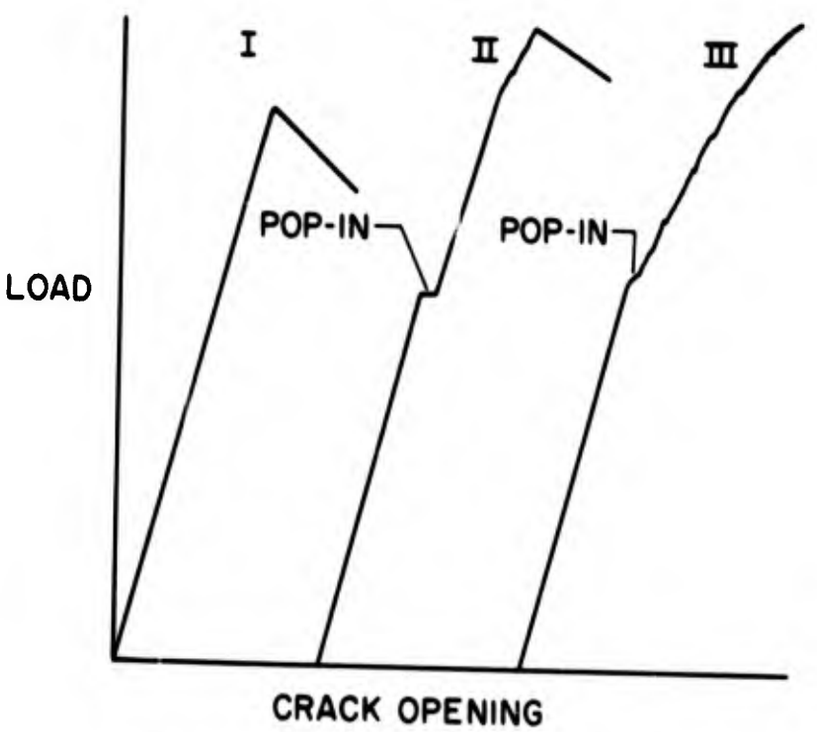

Fig. 32 Typical load-crack opening plots

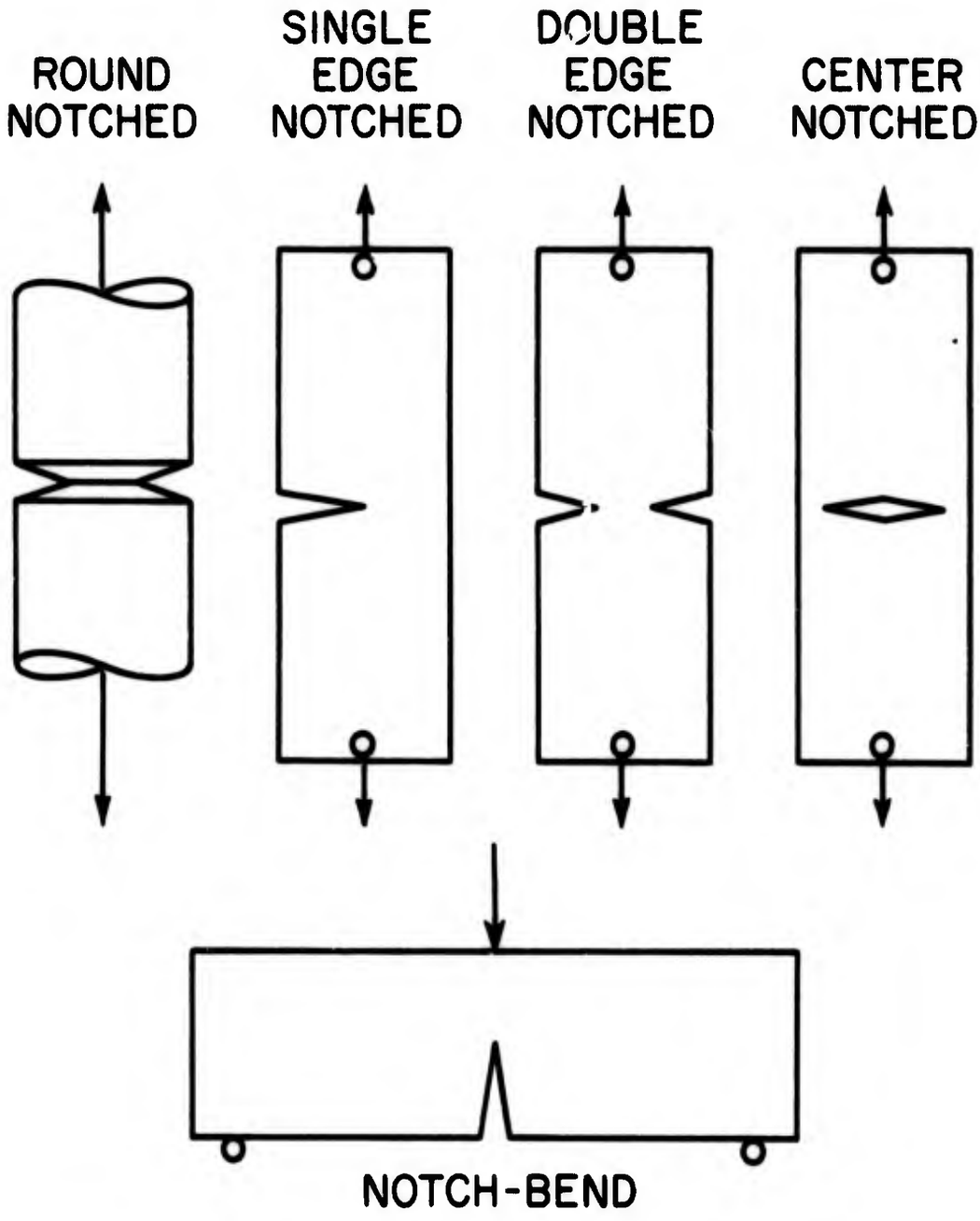

Fig. 33 Some types of specimens for K_{Ic} testing

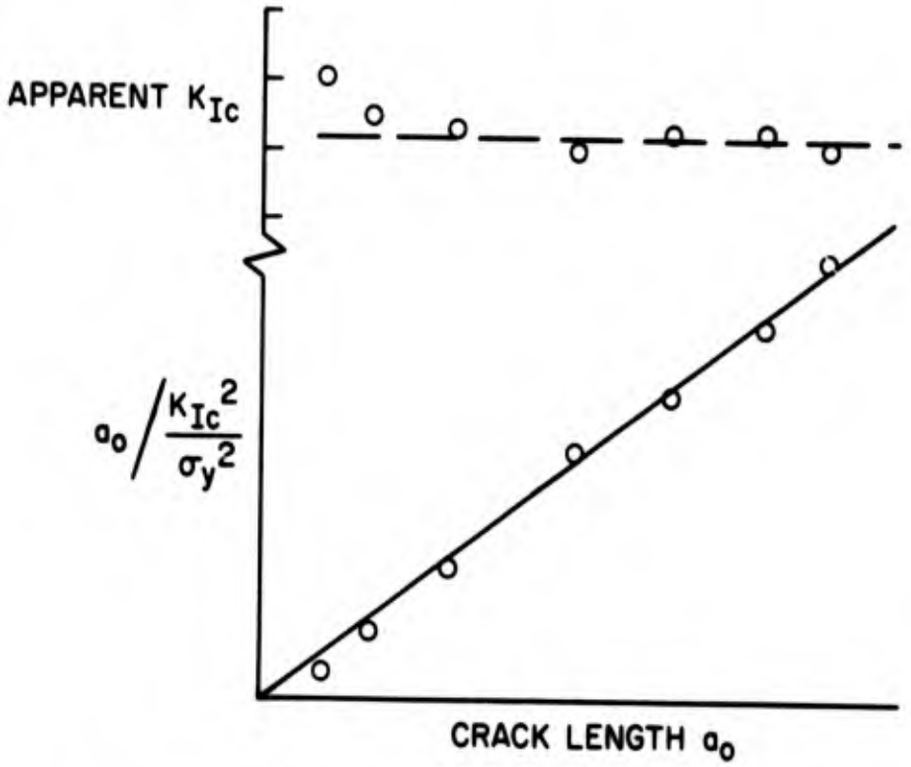

Fig. 34 Effect of crack length on apparent K_{Ic} (schematic)

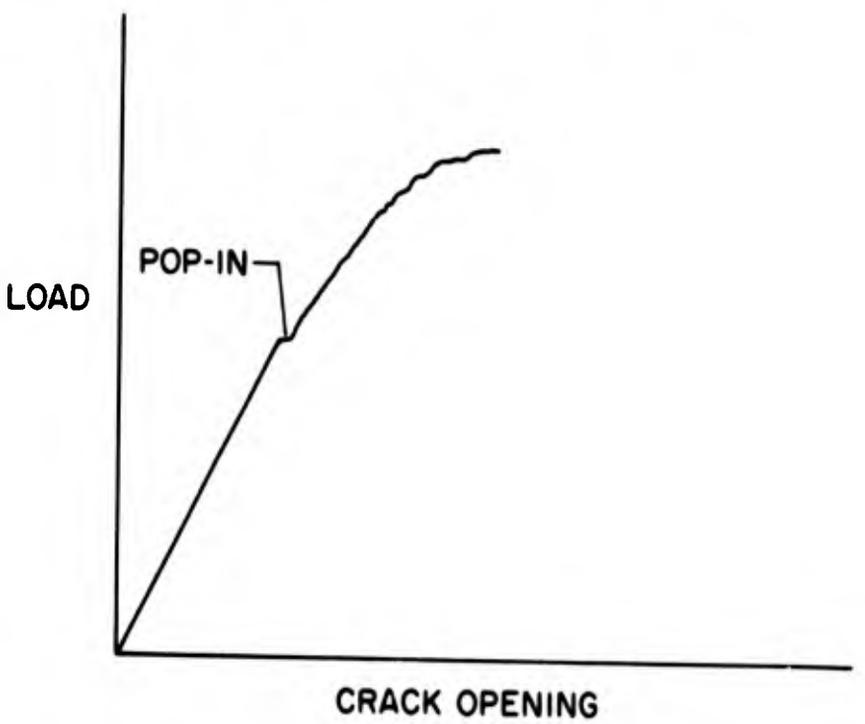

Fig. 35 Load-crack opening record for 7075-T651 plate with center notch (w = 20 in.; t = 1.00 in.; 2a = 7.00 in.; and $\rho < 0.5$ mil) from Reference 34

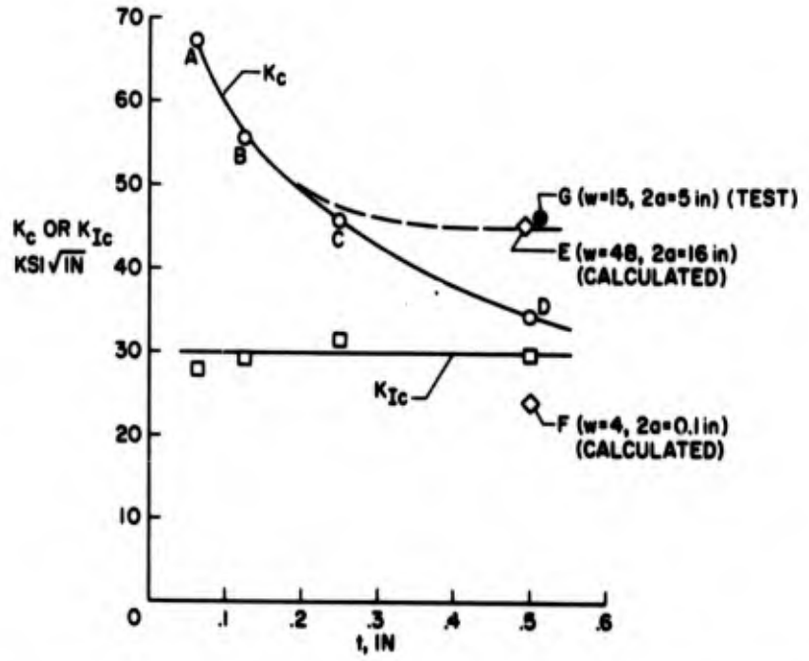

Fig. 36 K_c and K_{Ic} for 7075-T651 (transv.) aluminum alloy. Test data (except point G) from Reference 35. w = 4 in. and 2a = 1.70 in. except as noted. Each test point except G average of 2 tests

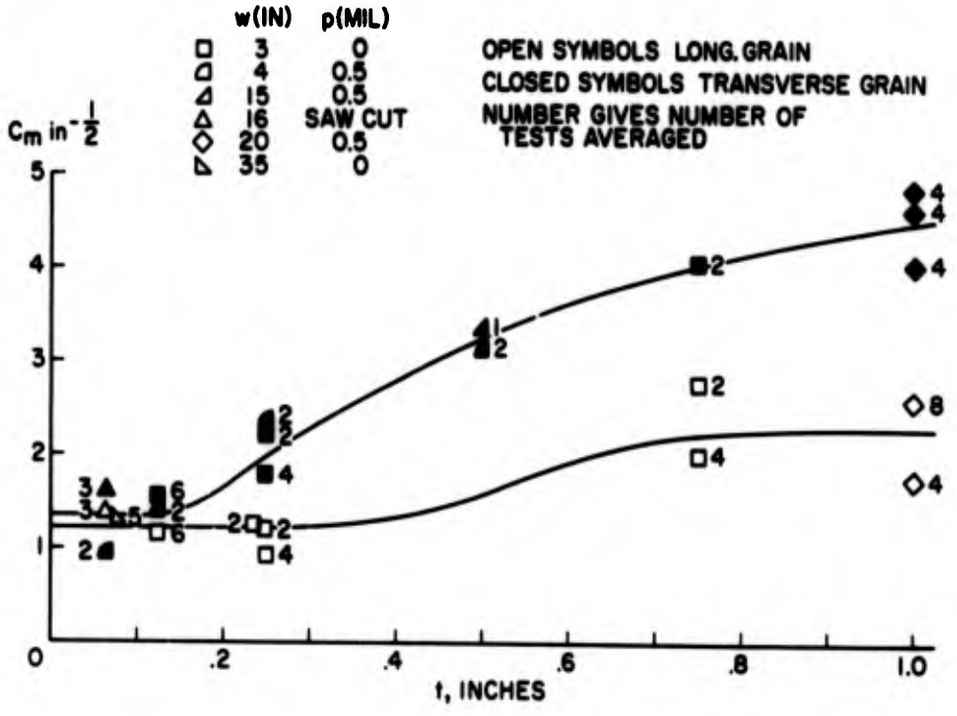

Fig. 37 Variation of C_m with thickness for 7075-T6 and -T651 aluminum alloy. Test data from References 35 and 38

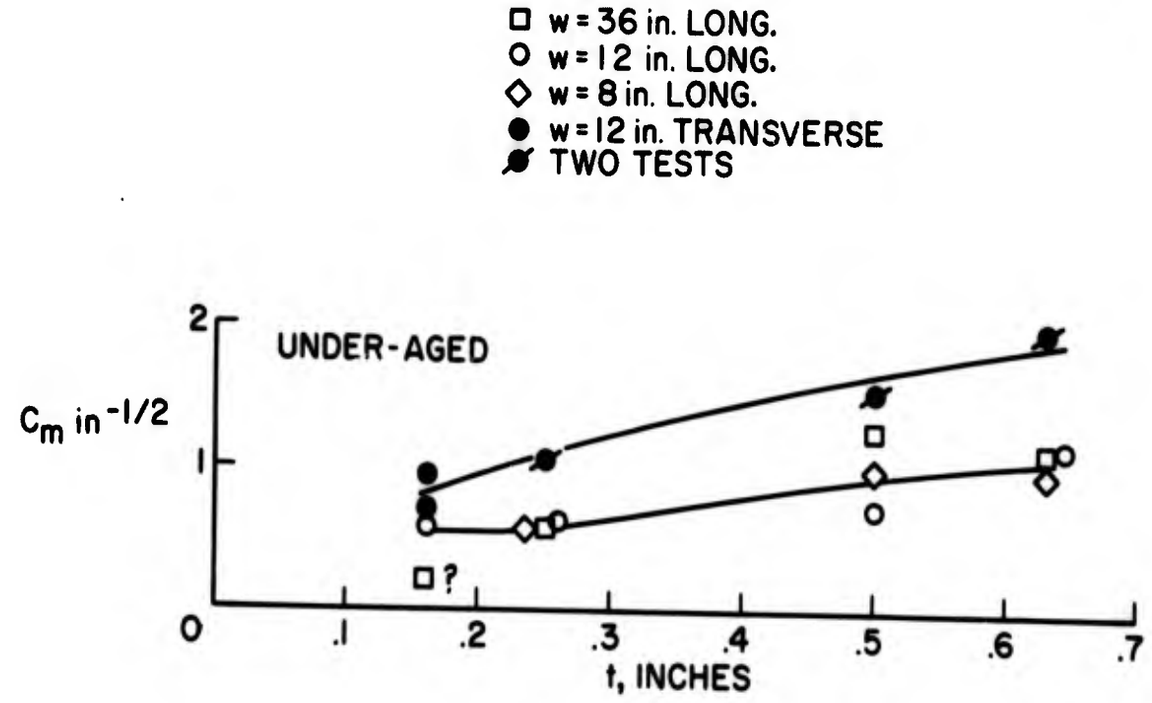

(a)

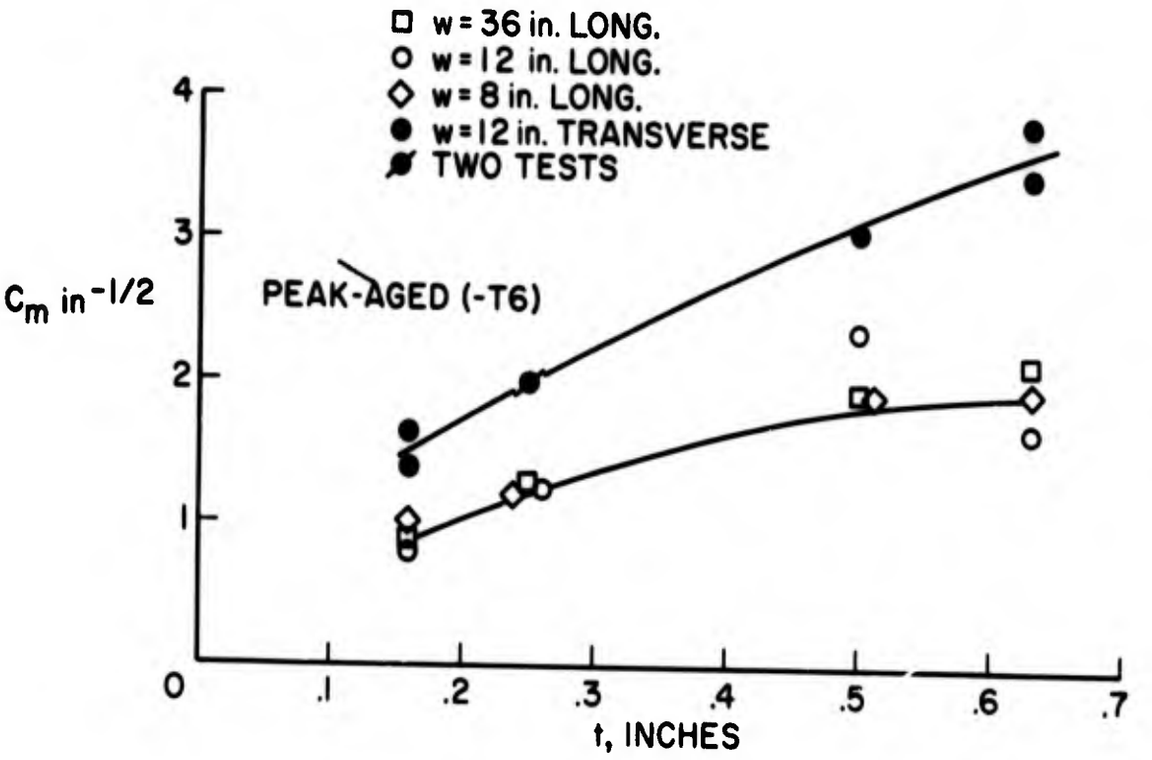

(b)

Fig. 38 Variation of C_m with thickness for 7079 aluminum alloy. (Tests by Boeing for NASA) (continued)

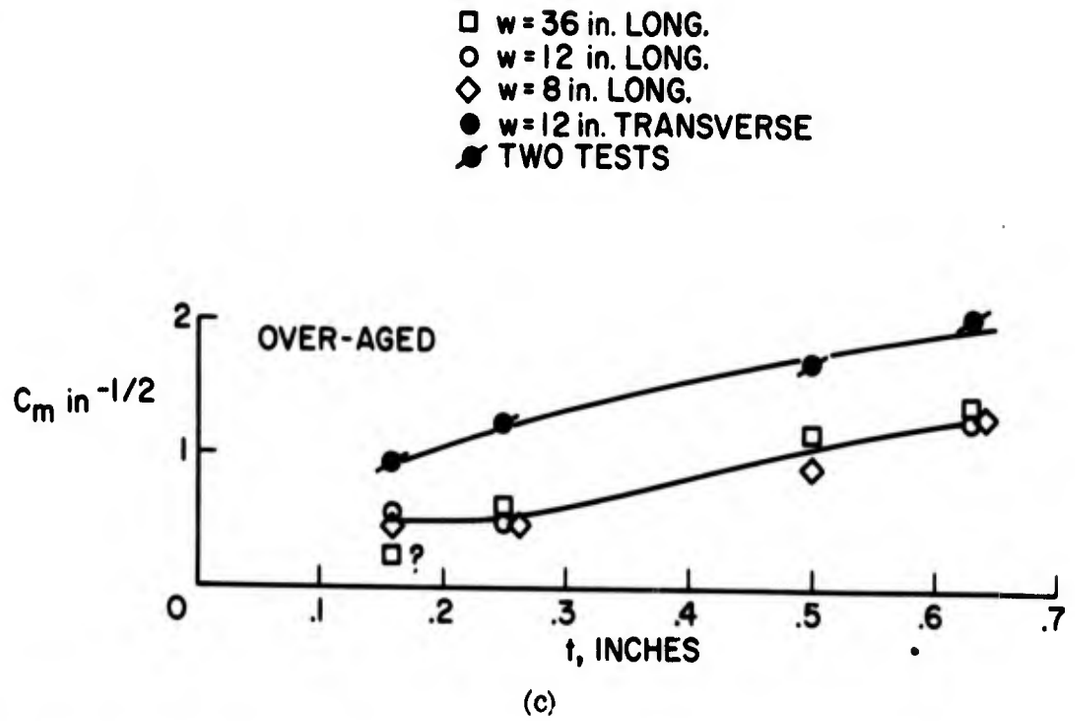

(c)

Fig. 38 Variation of C_m with thickness for 7079 aluminum alloy. (Tests by Boeing for NASA) (concluded)

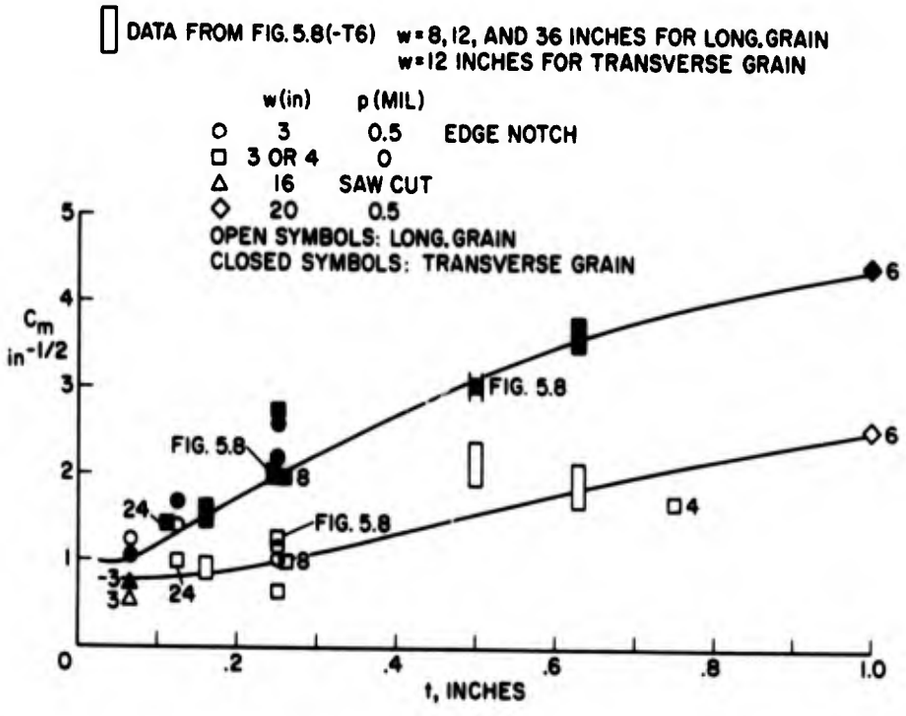

Fig. 39 Variation of C_m with thickness for 7079-T6 and -T651 aluminum alloy. (Test data from References 37 and 38, and from Figure 38)

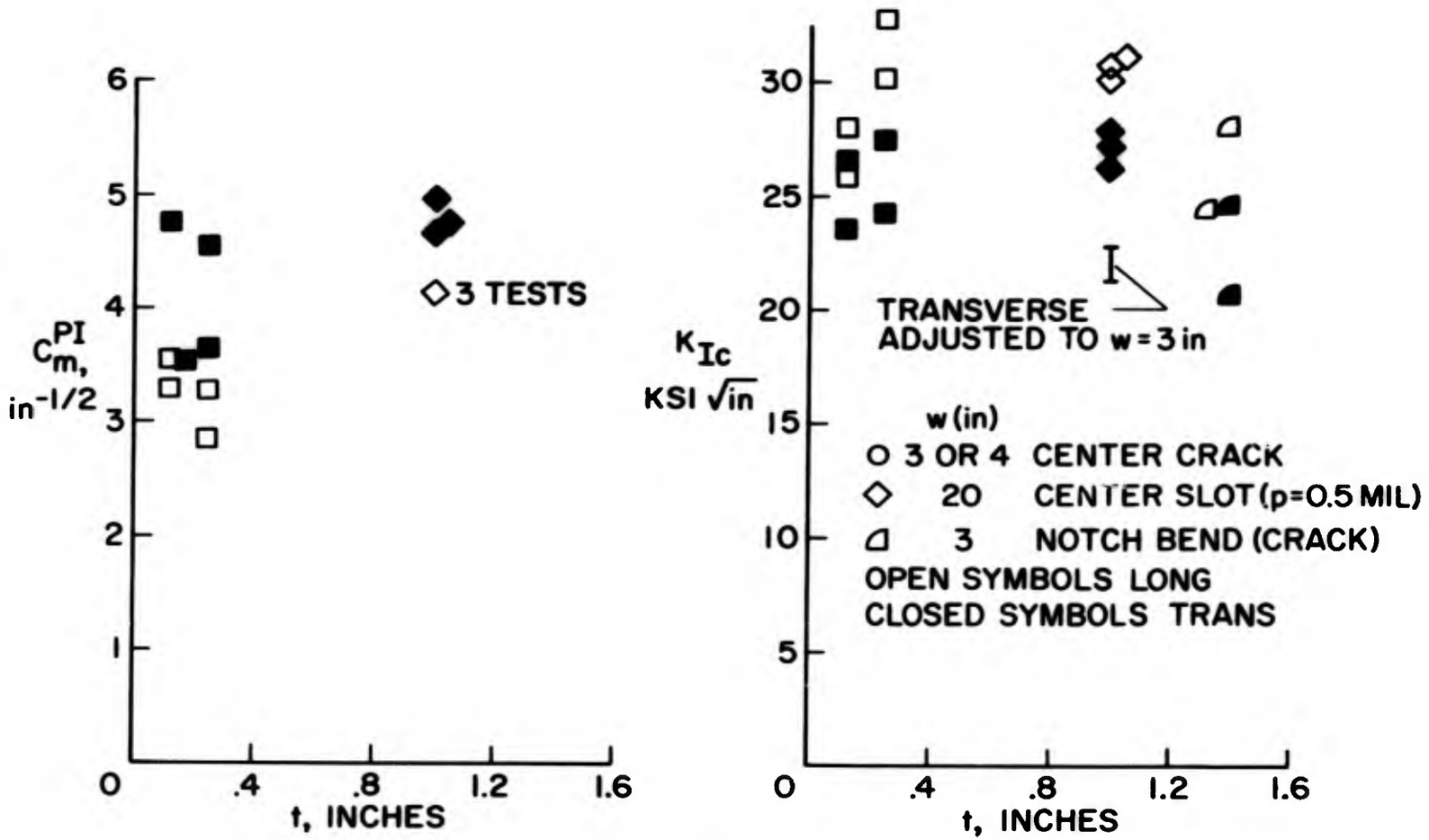

Fig. 40 Pop-in data for 7075-T651 aluminum alloy. Data from References 34 and 37. No correction for ρ made

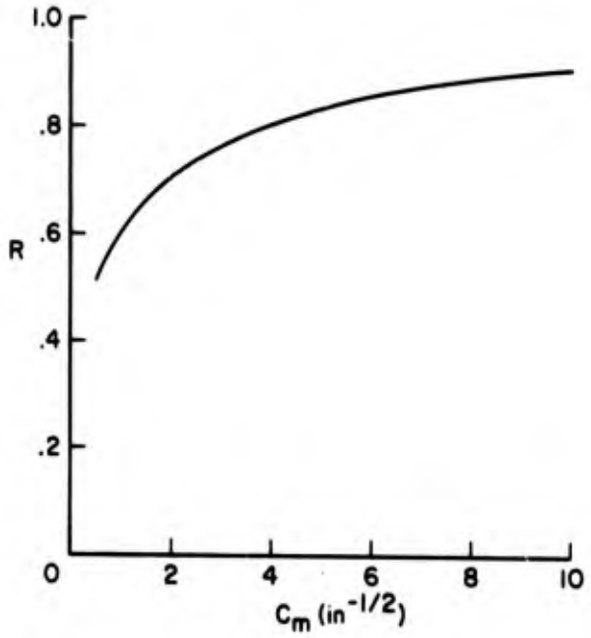

Fig. 41 Ratio $\frac{K_{Ic(w=3\ in.)}}{K_{Ic(w=20\ in.)}}$ for specimens with $2a/w = 0.33$. (Calculated by Equation (32)

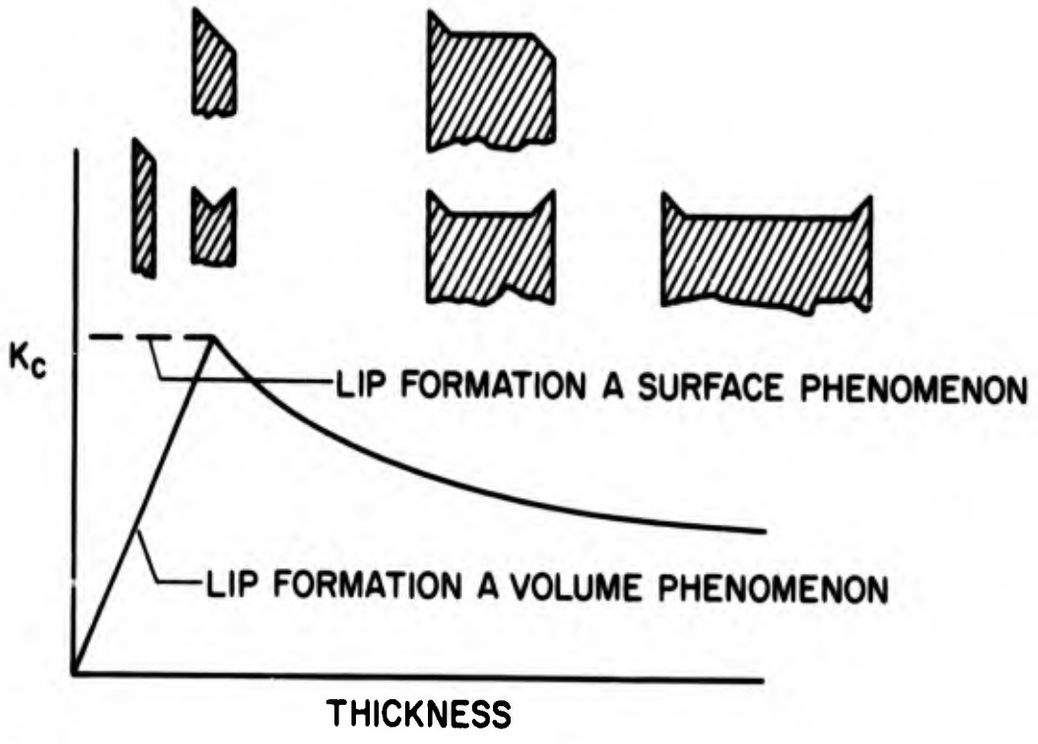

Fig. 42 "Critical" sheet thickness according to Bluhm[39]

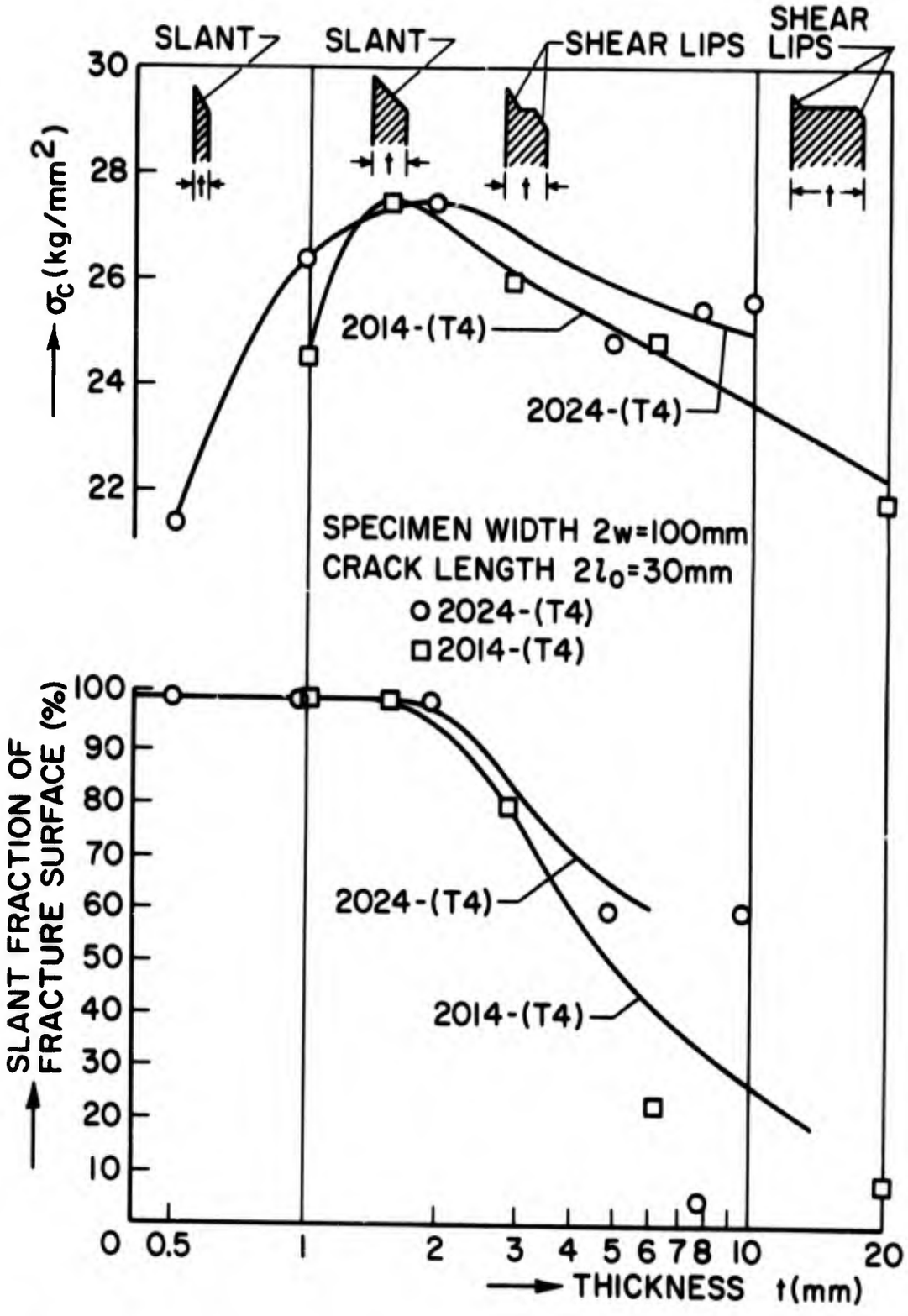

Fig. 43 Influence of thickness on residual strength and fracture mode. (From Reference 36)

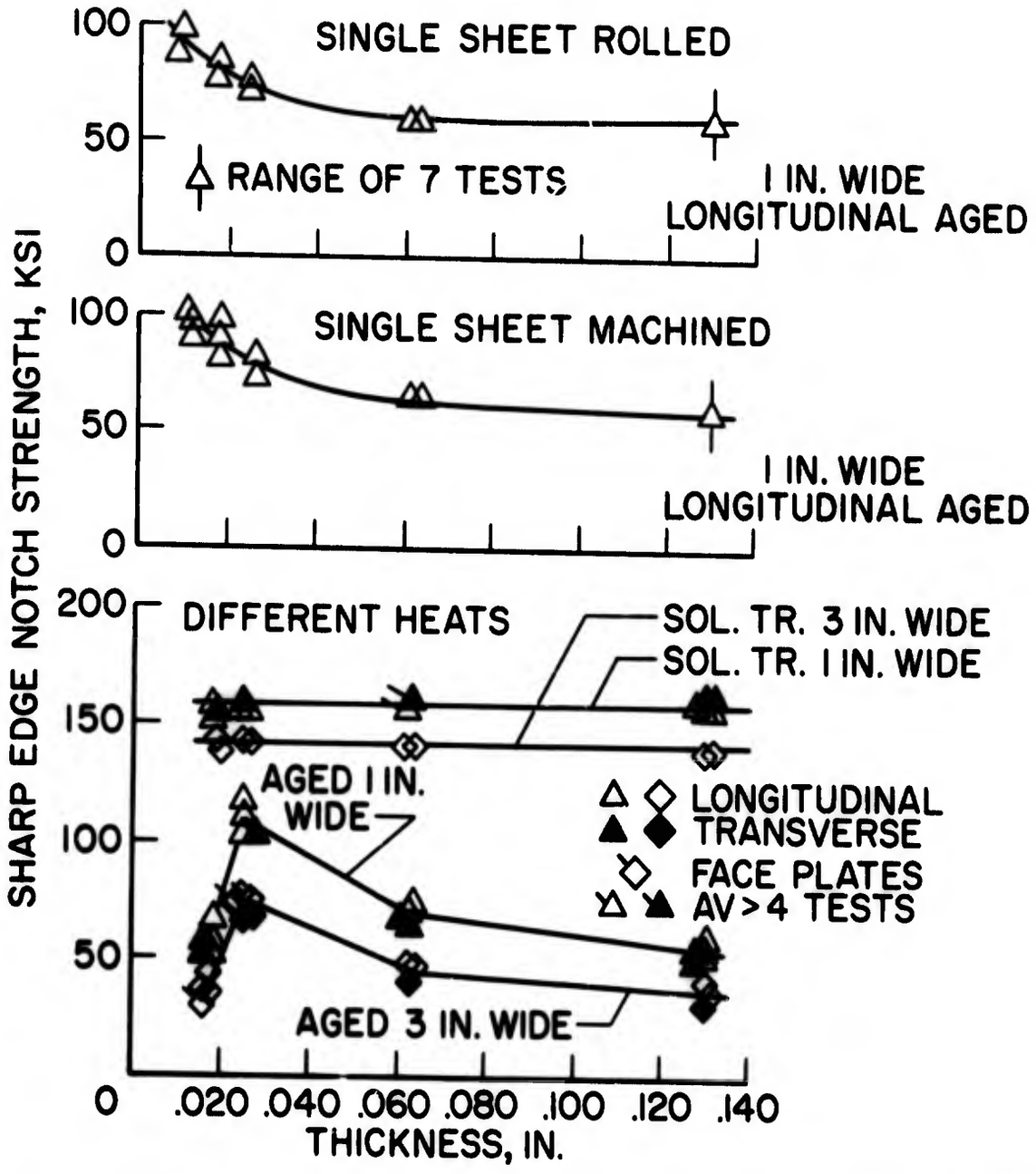

Fig. 44 Sharp edge notch strength at room temperature as a function of sheet thickness for B120VCA titanium alloy. From Reference 40

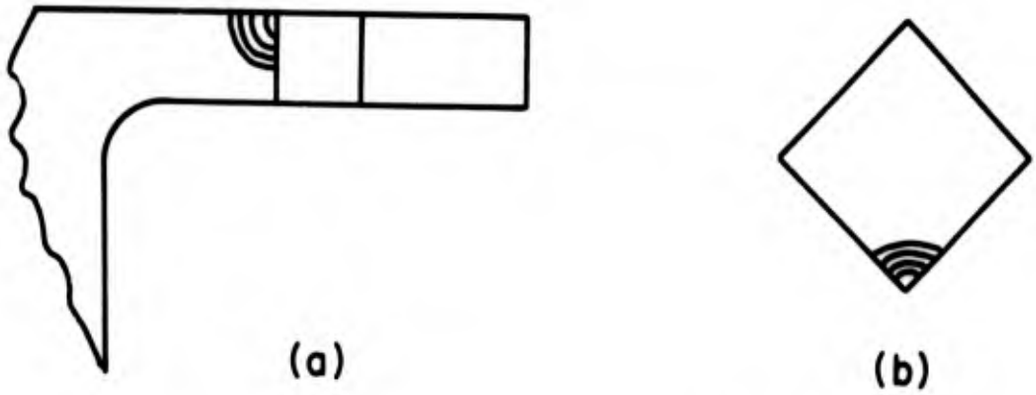

Fig. 45 Crack-bend test proposed by W. Barrois

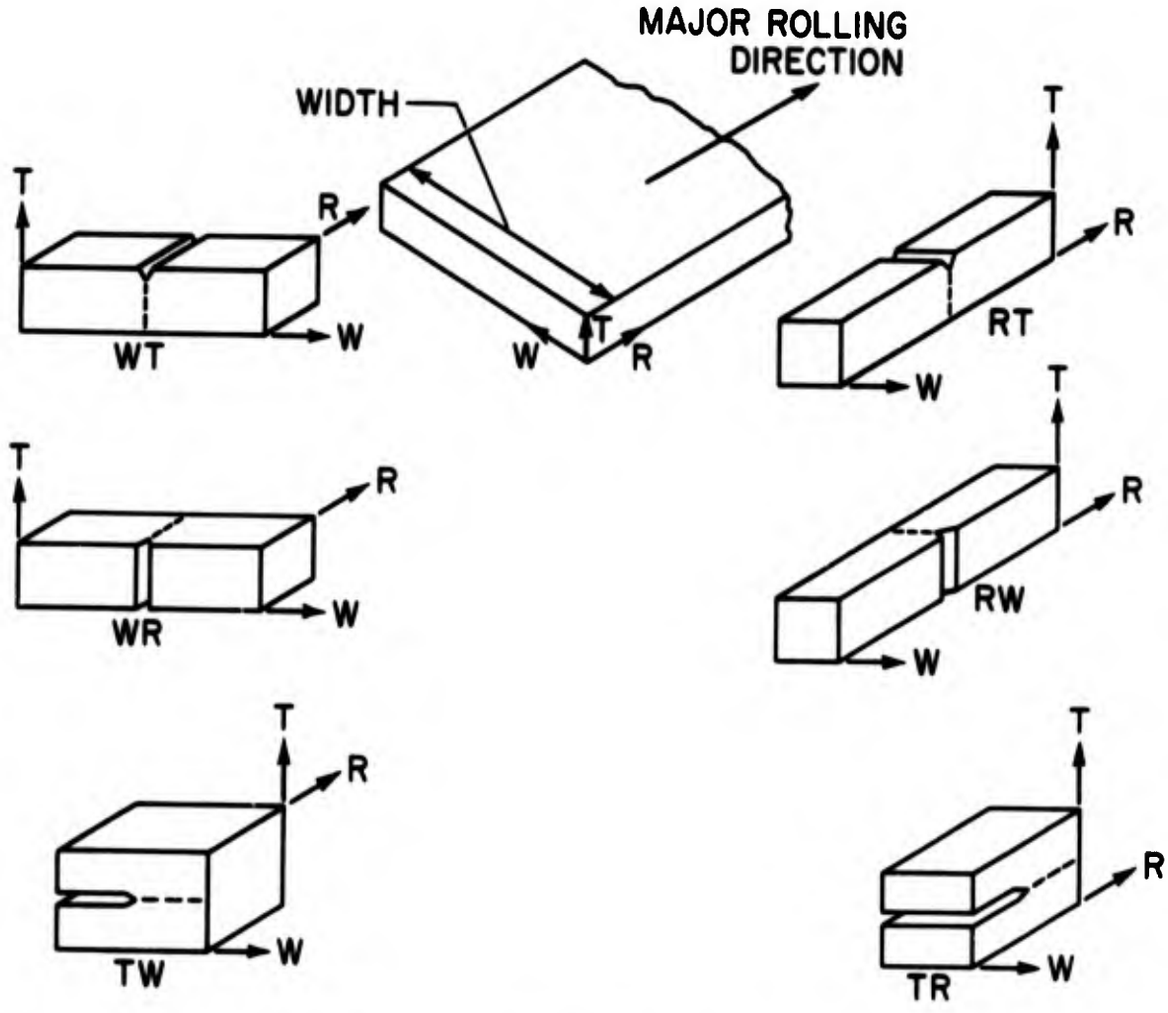

Fig. 46 Classification of plate specimens for residual strength tests